Organization and Regulation of Genes Involved in Nitrile Metabolism in Rhodococcus rhodochrous J1(Dissertation_全文)

AUTHOR(S):

Komeda, Hidenobu

(2)

Organization and Regulation of Genes Involved in Nitrile Metabolism in *Rhodococcus rhodochrous* J1

Hidenobu Komeda

1996

CONTENTS

ABBREVIATIONS

bp	Base pair(s)
CCCP	Carbonyl cyanide-*m*-chlorophenyl hydrazone
Da	Dalton
DEAE	Diethylaminoethyl-
DR	Direct repeats
DTNB	5,5'-Dithiobis(2-nitrobenzoic acid)
HEPES	*N*-2-Hydroxyethylpiperazine-*N'*-2-ethanesulfonic acid
H-NHase	High molecular mass-nitrile hydratase
HPLC	High-performance liquid chromatography
IAA	Indole-3-acetic acid
IPTG	Isopropyl-β-D-thiogalactopyranoside
IR	Inverted repeats
IS	Insertion sequence
kb	Kilobase(s)
kDa	Kilodalton
*K*m	Michaelis constant
L-NHase	Low molecular mass-nitrile hydratase
*M*r	Molecular mass
NHase	Nitrile hydratase
ORF	Open reading frame
PAGE	Polyacrylamide gel electrophoresis
PCR	Polymerase chain reaction
PTH	Phenylthiohydantoin
SDS	Sodium dodecyl sulfate
SF6847	3,5-Di-*tert*-butyl-4-hydroxybenzilidenemalononitrile
SSC	Standard saline citrate
Tris	Tris(hydroxymethyl)aminomethan
TNB	5-Thio-2-nitrobenzoate

INTRODUCTION

Nitrile compounds containing a cyano functional group such as cyanoglycosides, cyanolipids, indole-3-acetonitrile and β-cyano-L-alanine are formed by a wide range of plants (1). Nitrile compounds are also widely manufactured and extensively used by the chemical industry; acetonitrile is used as a solvent, adiponitrile is a precursor of nylon-6,6 and acrylonitrile is produced as a precursor of acrylic fibers and plastics. Nitrile herbicides such as dichlobenil (= 2,6-dichlorobenzonitrile; commercial name Casoron), bromoxynil (= 3,5-dibromo-4-hydroxybenzonitrile; commercial name Brominil), ioxynil (= 3,5-diiodo-4-hydroxybenzonitrile; commercial name Bentrol) and Buctril (= 4-(octanoyloxy)-3,5-dibromobenzonitrile) are also widely used in agriculture for rice, wheat, barley, corn and berry. These nitriles have been widely distributed in our environment in forms of industrial waste water and residual agricultural chemicals, and if their release is not controlled, finally will threaten the environment. Therefore, nitrile is an urgent target from the standpoint of environmental purification and preservation. In the author's laboratory of Kyoto University, microbial degradation of highly toxic nitriles has been studied to find that their degradation can proceed through two enzymatic pathways (2); nitrile hydratase (NHase; EC 4.2.1.84) catalyzes the hydration of a nitrile to the corresponding amide which is then converted to the acid plus ammonium by amidase (3), while nitrilase catalyzes the direct hydrolysis of a nitrile to the corresponding acid plus ammonium (4). Interest in both nitrile-converting enzymes has increasingly focused on their versatile functions: biosynthesis of the plant hormone, indole-3-acetic acid, from indole-3-acetonitrile (5-9), and enzymatic production of useful compounds from nitriles (10).

Rhodococcus rhodochrous J1, which was found in the author's laboratory, has both nitrile-degrading pathways, depending on the inducer (10). When this strain is cultured in a medium containing isovaleronitrile as an inducer, only nitrilase is induced (11). The strain also produces higher (H-NHase) (12) and lower molecular mass (L-NHase) NHases (10). Both NHases require cobalt ions and amides for their induction. They are composed of two subunits, α and β (α-subunit differs in size from β-subunit in each, and α- and β-subunits of H-NHase differ from those of L-NHase). H-NHase and L-NHase are induced by urea and cyclohexanecarboxamide, respectively. Using immobilized cells containing H-NHase, the industrial production of acrylamide from acrylonitrile was started in 1991 (30,000 tons/year). This is the first case in which biotechnology was applied in the petrochemical industry and also

the first successful example of the introduction of an industrial bioconversion process for the manufacture of a commodity chemical (10).

Both H- and L-NHase genes (*nhhBA* and *nhlBA*, respectively) have been cloned from *R. rhodochrous* J1 and sequenced (13). In each of the H- and L-NHase genes, an open reading frame (ORF) for the β-subunit (*nhhB* and *nhlB*) is located just upstream of that for the α-subunit (*nhhA* and *nhlA*). This arrangement of the coding sequences is reverse of the order found in the NHase genes of *Rhodococcus* sp. N-774 (14) and *Pseudomonas chlororaphis* B23 (15).

R. rhodochrous J1 has great catalytic potential for the hydration of nitriles to the corresponding amides (16). In this process, contamination of acrylic acid formed by amidase in the strain causes the deterioration in the quality of the manufactured acrylamide; acrylamide is expected not to be changed into acrylic acid as much as possible by the amidase. Therefore, it is important from an applied standpoint to investigate amidases coupled with NHases in this strain.

Nitrilases that utilize benzonitrile and related aromatic nitriles as substrates have been purified from *Pseudomonas* (17,18) *Nocardia* sp. NCIB 11215 (19) and NCIB 11216 (20), *Fusarium solani* (21), *Arthrobacter* sp. (22), *R. rhodochrous* J1 (23) and *Escherichia coli* transformed with a *Klebsiella ozaenae* plasmid DNA (24). Nitrilases that act on aliphatic nitriles and arylacetonitriles are also purified from *Rhodococcus rhodochrous* K22 (25) and *Alcaligenes faecalis* JM3 (26), respectively, and characterized. The nitrilases from *R. rhodochrous* J1, *R. rhodochrous* K22 and *A. faecalis* JM3 are all strongly induced by the addition of isovaleronitrile to the medium (23,25,26), making large amounts of enzyme available for application in industrial production of a wide range of useful acids from nitriles. However, the mechanisms that regulate nitrilase expression have never been understood in these strains. All nitrilases so far reported are classified as sulfhydryl enzymes since they are inactivated by thiol reagents. The *R. rhodochrous* J1 nitrilase is also inactivated by thiol reagents (23). An active cysteine residue has not yet been identified in any nitrilases.

The genus *Rhodococcus*, a member of the class Actinomycetes (27), has recently received much attention in terms of its high ability on biodegradation and biotransformation (28). However, genetic information of *Rhodococcus* has been extremely limited; research into the regulatory system of *Rhodococcus* species has so far been hampered by the lack of systems for genetic manipulation of *Rhodococcus*.

Chapter I describes the organization of the H-NHase gene cluster from *R. rhodochrous* J1. Two regulatory genes (*nhhC* and *nhhD*) required for the expression of H-NHase were identified by using a host-vector system in *Rhodococcus*. The H-NHase gene cluster was also characterized to clarify its unusual induction mechanism in *R. rhodochrous* J1. A possible insertion sequence, named IS*1164*, was fortuitously found in the intervening space between *nhhCD* and *nhhBA* and its primary structure was characterized. The distribution of IS*1164*-like element in the genomes of various *Rhodococcus* strains and other nitrile-metabolizing strains is also presented.

Chapter II describes the organization of the L-NHase gene cluster from *R. rhodochrous* J1. The author indicated the evidence of the occurrence of amidases in this strain. The author also cloned and sequenced an amidase gene (*amdA*), which is considered to be linked to the L-NHase gene. The recombinant *R. rhodochrous* J1 amidase protein in *E. coli* was also produced, purified and characterized. This chapter also describes the analyses on the mechanism of the L-NHase gene expression. In addition to *nhlBA* encoding L-NHase, two regulatory genes (*nhlC* and *nhlD*) were required for the amide-dependent induction of *nhlBA* by using the transformation system in *Rhodococcus*. *nhlC* has a sequence similarity to *nhhC*, which is involved in the H-NHase expression, and *amiC*, which is considered to be a sensor protein for inducer amides in the expression system of an aliphatic amidase in *Pseudomonas aeruginosa*, suggesting the products of both regulatory genes (NhlC and NhhC) are likely to sensor proteins for inducer amides. *nhlF*, which is situated between *nhlBA* and *amdA*, is similar to the bacterial genes encoding nickel transporters previously reported. The product of *nhlF*, NhlF transports cobalt ions into the *Rhodococcus* and *Escherichia coli* host cells. The transporter specific for cobalt ions was characterized using the transformation system in *Rhodococcus*.

Chapter III describes the analyses of the structure and induction mechanism of the nitrilase from *R. rhodochrous* J1, mainly at gene level. The nitrilase gene (*nitA*) from *R. rhodochrous* J1 was found to be similar to the bromoxynil nitrilase gene from *Klebsiella ozaenae*. An evidence that a cysteine residue (Cys-165) plays an important role in the function of the active site was also presented. A regulatory gene, *nitR*, which is situated downstream from *nitA*, was found to be responsible for the isovaleronitrile-dependent induction of *nitA* using the transformation system in *Rhodococcus*. Promoter region required for the regulation of *nitA* were also defined.

CHAPTER I Analysis of High Molecular-Mass Nitrile Hydratase (H-NHase) Gene Cluster

Section 1 Regulatory genes for the expression of catalytically active H-NHase[a]

In microorganisms that catabolyze nitriles by NHase, an interesting phenomenon is found; this enzyme, if inducible, is generally induced by amides (reaction products), not by nitriles (reaction substrates) (10). As mentioned in the introduction to this thesis, *Rhodococcus rhodochrous* J1 produces two kinds of NHases; high- and low-molecular-mass-NHases (H-NHase and L-NHase), which exhibit different physicochemical properties and substrate specificities. When this strain is cultured in a medium containing urea and cyclohexane-carboxamide in the presence of cobalt ions, H-NHase and L-NHase are selectively induced, respectively (10). Both H- and L-NHase genes were cloned from *R. rhodochrous* J1 and sequenced (13). In each of the H- and L-NHase genes, an open reading frame (ORF) for the β-subunit is located just upstream of that for the α-subunit. This arrangement of the coding sequences is reverse of the order found in the NHase genes of *Rhodococcus* sp. N-774 (14) and *P. chlororaphis* B23 (15). Expression of both H- and L-NHase genes in *E. coli* cells was examined under the control of *lac* promoter, but the level of NHase activity in the cell-free extracts is much lower than those of H- and L-NHases in *R. rhodochrous* J1 (13), suggesting that an uncharacterized regulatory gene would be present in this strain.

In this section, genes required for the expression of H-NHase have been identified by using a host-vector system in *Rhodococcus*. The H-NHase gene cluster was also characterized to clarify its unusual induction mechanism in *R. rhodochrous* J1.

MATERIALS AND METHODS

Bacterial strains and plasmids

R. rhodochrous J1 was previously isolated from soil (29). *E. coli* JM109 (30) was the host for pUC plasmids. *R. rhodochrous* ATCC12674 was the host for a *Rhodococcus-E. coli* shuttle vector plasmid pK4 (31) and its derivatives, and was used for the expression of the H-NHase gene. The plasmid pNHJ10H (13) carrying the H-NHase gene in a 6-kb *Sac*I fragment on pUC19 was used for subcloning and sequencing of genes.

Transformation of *R. rhodochrous* ATCC12674 by electroporation

A mid-exponential culture of *R. rhodochrous* ATCC12674 was centrifuged at 6,500 x *g* for 10 min at 4°C and washed three times with demineralized cold water. Cells were then concentrated 20-fold in cold water and kept on ice. Ice-cold cells (100 µl) were mixed with 1 µg DNA in 1 µl of TE buffer (10 mM-Tris/1 mM EDTA, pH 8.0) in a 1-mm-gapped electrocuvette (Bio-Rad), and subjected to a 2.0 kV electric pulse from a Gene Pulser (Bio-Rad) connected to a pulse controller (25 µF capacitor; external resistance, 400Ω). Pulsed cells were diluted immediately with 1 ml of MYP medium (31) and incubated for 2 h at 26°C. They were then spread on MYP medium containing 75 µg kanamycin ml-1.

Preparation of cell extracts and enzyme assay

R. rhodochrous ATCC12674 transformants were grown at 28°C for 48 h in MYP medium containing 0.001 g/l $CoCl_2 \cdot 6H_2O$ supplemented with urea at several concentrations, harvested by centrifugation at 4,000 x *g* at 4°C, and washed twice with 0.15 M NaCl. The washed cells were suspended in 0.1 M HEPES/KOH buffer (pH 7.2) containing 44 mM *n*-butyric acid, disrupted by sonication for 20 min (19 kHz, Insonator model 201M; Kubota, Tokyo), and centrifuged at 12,000 x *g* for 10 min at 4°C. The resulting supernatant was assayed for NHase as described previously (13). One unit of the enzyme catalyzes the formation of 1 µmol of benzamide/min from benzonitrile under the above conditions.

RNA preparation

The subculture of *R. rhodochrous* J1 was carried out as described previously (12), and 5 ml of the subculture was then inoculated into a 500-ml shaking flask containing 60 ml of a culture medium (12) with or without the following additives, *i. e.*, urea (0.75%, w/v), $CoCl_2 \cdot 6H_2O$ (0.001%, w/v), and incubated at 28°C for 48 h with aeration. Cells were collected from 60 ml of such cultures by centrifugation, and total RNA was extracted by the AGPC (Acid-Guanidium-Phenol-Chloroform) method (32).

Northern (RNA) blot hybridization

For Northern blot hybridization, each RNA sample (40 µg) was electrophoresed on a 1% agarose-formaldehyde gel and transferred to a nitrocellulose membrane filter (Schleicher & Schuell) in 20 x SSC. Prehybridization and hybridization were carried out at 42°C in a solution

consisting of 40% formamide, 5 x SSC, 0.1% SDS and 100 μg of sonicated salmon sperm DNA per ml. The DNA fragments used as probes were radiolabeled with a multiprime DNA labeling system (Amersham). Filters were washed twice at room temperature in 40% formamide, 5 x SSC, 0.1% SDS, and then washed three times at room temperature in 2 x SSC solution with 0.1% SDS.

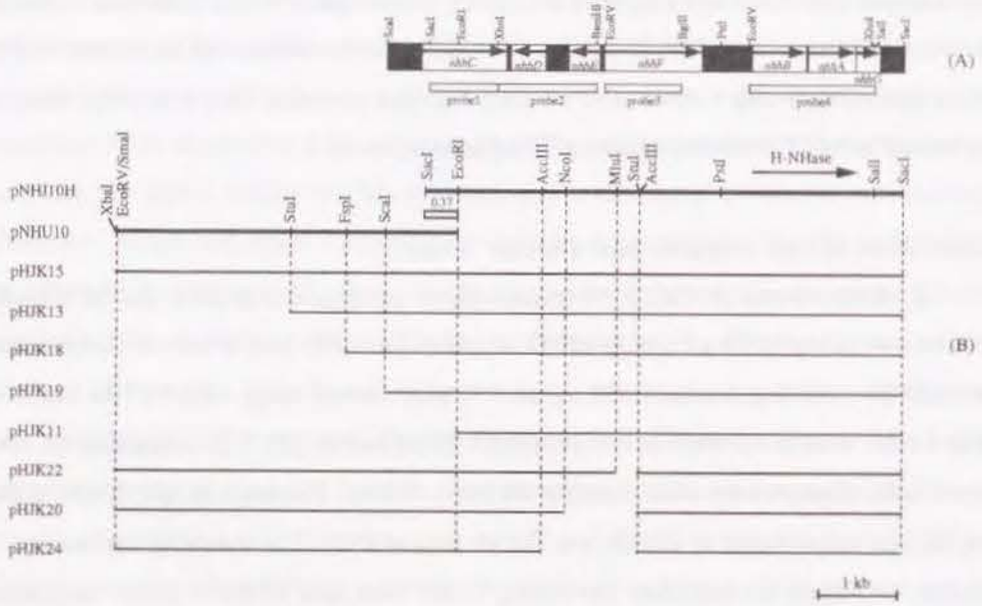

Fig. 1. Schematic view of the 6,555-bp *Sca*I-*Sac*I fragment from pHJK19 (A) and construction of a set of plasmids (B).
For clarity, only restriction sites discussed in the text are shown. The probes used in the experiment are shown (boxes). Various deletion plasmids are diagramed below the restriction maps.

RESULTS

Expression of the H-NHase gene (*nhlBA*) in *R. rhodochrous* ATCC12674

R. rhodochrous ATCC12674 harboring a plasmid containing a 6-kb insert of pNHJ10H in the blunt-ended *Eco*RI site of pK4 showed no NHase activity (data not shown). To identify the sequence elements required for the expression of the H-NHase gene (*nhhBA*), the upstream region was cloned by the DNA-probing method with a *Sac*I-*Eco*RI 0.37-kb fragment as a probe, and a plasmid pNHU10 was obtained (Fig. 1). Plasmid pHJK15 contained a 4.3-kb *Eco*RI-*Xba*I fragment from pNHU10 and a 5.66-kb *Eco*RI fragment from pNHJ10H in the *Eco*RI-*Xba*I sites of the *Rhodococcus-E. coli* shuttle vector pK4. Other plasmids (pHJK13, pHJK18 and pHJK19) shown in Fig.1 were constructed in the same manner, by inserting the

various restriction fragments from pNHU10 and the 5.66-kb *Eco*RI fragment from pNHJ10H into the *Eco*RI-blunt-ended *Xba*I sites of pK4. Plasmid pHJK11 contained only the 5.66-kb *Eco*RI fragment in the *Eco*RI site of pK4. These plasmids were used to transform *R. rhodochrous* ATCC12674 and the resulting transformants were cultured in $CoCl_2$-containing MYP medium in the presence (0.75 g/l or 3.75 g/l) or absence of urea (the best inducer of the H-NHase formation). Enzyme assay using benzonitrile as a substrate for each cell-free extract has revealed that, in addition to *nhhBA* itself, at least a 4.6-kb upstream region (from the 5' end terminus of the H-NHase gene to *Sca*I site) is required for the expression of *nhhBA* (Table 1) as in pHJK19. Nagasawa et al. (12) have already found that urea (added to the culture medium supplemented with cobalt ions) acts as a powerful inducer of H-NHase formation in *R. rhodochrous* J1. However, in the *Rhodococcus-E. coli* host-vector system used in this experiment, H-NHase was much expressed even in the absence of urea in the culture medium, and the presence of urea showed slight enhancement of H-NHase formation.

Table 1. NHase activity (units/mg·protein) in *R. rhodochrous* ATCC12674 carrying various recombinant plasmids.
Urea (0, 0.75 or 3.75 g/l) was added into the medium, and the cultivation was carried out as described in Materials and Methods.

Plasmid	Urea conc. (g/l)		
	0	0.75	3.75
pK4	N.D.	N.D.	N.D.
pHJK15	7.41	11.3	1.86
pHJK13	8.83	10.2	3.28
pHJK18	7.49	12.9	4.44
pHJK19	9.39	10.2	4.88
pHJK11	1.20	0.21	0.22
pHJK22	9.09	17.0	N.T.
pHJK20	7.09	13.3	N.T.
pHJK24	1.65	1.24	N.T.

N.D.: not detected; N.T.: not tested

H-NHase formation in the transformants was examined by SDS-PAGE (Fig. 2). The transformant carrying pHJK19 expressed larger amounts of two proteins (26 kDa and 30 kDa), independently of urea concentration in the culture medium, than the transformant with pK4 or pHJK11. Both proteins formed were found to be the α- and β-subunits of H-NHase, respectively, by determination of their N-terminal amino acid sequences on a gas-phase amino acid sequencer (Applied Biosystems, model 470A). Expression of NHase activity shown

above was dependent on the addition of cobalt ions into the medium, because the transformant harboring pHJK19 cultured in the medium without cobalt ions had no NHase activity. Moreover, none of the *E. coli* JM109 harboring pK4-derivative plasmids used in this experiment gave NHase activity, even when these transformants were cultured in the medium supplemented with urea and $CoCl_2$.

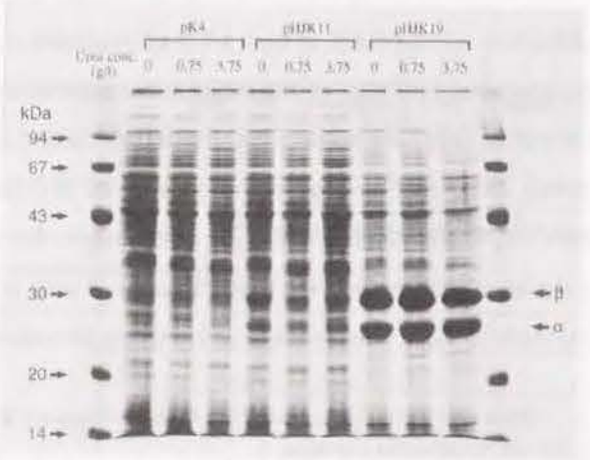

Fig. 2. Coomassie-stained SDS-PAGE showing hyperformation of the H-NHase α- and β-subunit proteins in *R. rhodochrous* ATCC12674 transformants.

Primary structure of the flanking region of the H-NHase gene

The *Pst*I-*Sal*I 1.97-kb fragment containing the H-NHase gene was sequenced previously (13). The author further sequenced the *Sca*I-*Pst*I upstream region and *Sal*I-*Sac*I downstream region required for H-NHase production. Sequence analysis revealed that this fragment consisted of 6,555 bp DNA and that five ORFs (*nhhC*, *nhhD*, *nhhE*, *nhhF* and *nhhG*) were newly found in the region in addition to *nhhBA* (Fig. 1-A).

nhhC is 1083-nucleotides long and would encode a protein of 361-amino acids (39,155 Da). A computer-aided search for protein homology revealed that the amino acid sequence deduced from *nhhC* was significantly similar to the negative regulator AmiC (33) of an aliphatic amidase gene in *Pseudomonas aeruginosa* (Fig. 3-A). *nhhD*, which is located in the opposite orientation to *nhhBA*, is 447-nucleotides long, and would encode a protein of 148-amino acids (16,457 Da). *nhhD* showed a similarity to the repressor genes *marR* (34) and *hpcR* (35) in *E. coli* (Fig. 3-B). *nhhE*, which is located in the opposite orientation to *nhhBA*, is 402-nucleotides long and would encode a protein of 133-amino acids (14578 Da). Amino acid

sequence from *nhhE* did not show significant similarity with any proteins in the NBRF data base.

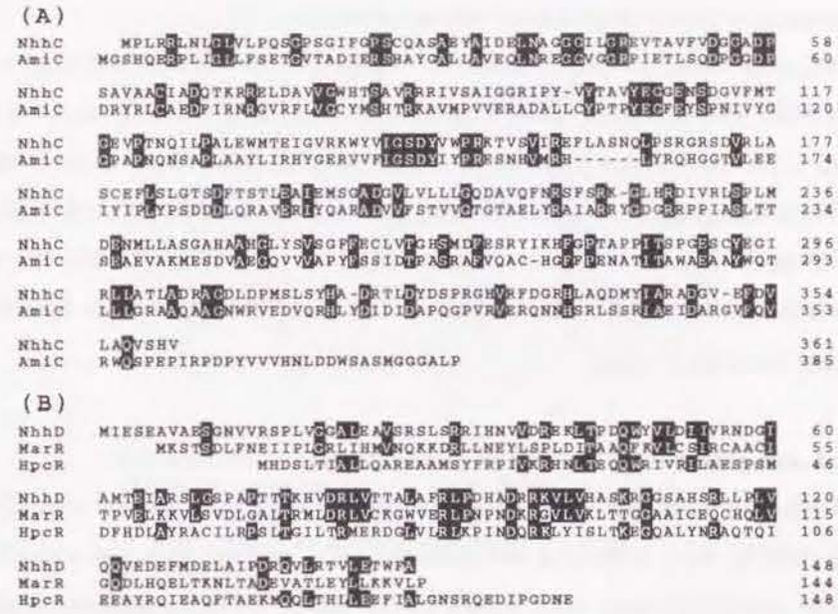

Fig. 3. Alignment of the deduced amino acid sequences of the *R. rhodochrous* J1 NhhC and NhhD with the respective homologous sequences.
Residues in black boxes indicate identical sequences; dashes denote gaps introduced to maximize alignment. Abbreviations (references); AmiC, negative regulator of aliphatic amidase from *P. aeruginosa* (33); MarR, repressor of multiple antibiotic resistant operon from *E. coli* (34); HpcR, repressor of homoprotocatechuate-degradative operon from *E. coli* (35).

nhhF is 1245-nucleotides long and would encode a protein of 414-amino acids (45,840 Da). A homology analysis revealed a strong similarity between *nhhF* and the family of transposase genes derived from IS*1081* of *Mycobacterium bovis* (36), IS*256* of *Staphylococcus aureus* (37) and IS*Rm3* of *Rhizobium meliloti* (38). Especially, there is a 78.8% match of amino acids in 413 overlapping residues between *nhhF* and the transposase gene from IS*1081*. In the flanking region of *nhhF*, 19-bp terminal inverted repeats with a 16-bp match are present 38 bp upstream from the initiation codon and 9 bp downstream from the termination codon. These findings indicate that the insertion sequence, which is composed of one ORF coding for the putative transposase and 19-bp inverted repeats, exists upstream from *nhhBA*. The designation number (IS*1164*) for this insertion sequence was assigned by the Plasmid Reference Center, Stanford University. Southern blot analysis at higher stringency using probe 3 specific for IS*1164* (see Fig. 1), against the *R. rhodochrous* J1 total DNA digested separately with several restriction enzymes, has suggested the existence of two or three

insertion element-like sequences, which are homologous to IS*1164*, in the *R. rhodochrous* J1 DNA. Although the distance between the TGA stop codon for *nhhF* and the ATG start codon for the H-NHase β-subunit is 637 bp, a search of the EMBL and Genbank databases did not show any sequences closely related to the 637 spacer region.

nhhG was found in the downstream region of *nhhA* (start and stop codons at nucleotides 5942 ATG and 6256 TGA, respectively) in the same orientation as the H-NHase gene. *nhhG* is 315-nucleotides long and would encode a protein of 104 amino acids (11,600 Da). *nhhG* is homologous to the amino terminal portion of each nhhB and nhlA, which encode β-subunit of each H- and L-NHases, respectively (11). A strong hairpin structure was observed just downstream of the termination codon for *nhhG* and may serve as a ρ-independent transcriptional termination signal.

Transcript analysis of the H-NHase gene cluster

H-NHase activities in *R. rhodochrous* J1 cultured in the medium with urea (7.5%, w/v) and $CoCl_2$ (0.01%, w/v), with urea and without $CoCl_2$, without urea and with $CoCl_2$, and without urea and $CoCl_2$ were 1.21, 0.006, 0.053, 0.002 (units/mg•protein), respectively. These findings suggest that H-NHase formation is regulated by urea and cobalt ions at the transcriptional or translational level. As described above, the *nhh* genes upstream *nhhBA* are involved in the expression of *nhhBA*. Therefore, four DNA fragments (Fig. 1) were used as probes (probe 1~4) against mRNA from *R. rhodochrous* J1 cultured in the medium in the presence or in the absence of urea and $CoCl_2$, to determine whether transcription of these ORFs and the H-NHase gene was altered by the culture conditions.

The region corresponding to probe 1 expressed one mRNA band, estimated at 1.6 kb, in the cells cultured in the medium in the absence of urea (Fig. 4). In the urea-induced cells, a mRNA band at the same size was faintly visible as well. Since the H-NHase gene was transcribed in large amounts (see below) in the urea-induced cells, the amount of RNA (corresponding to the probe 1 region) in the cells is relatively less than that in the urea-uninduced cells, suggesting that the probe 1 region, presumably *nhhC* region, expresses constitutively. Probe 2 containing *nhhD*, *nhhE* and part of *nhhC* hybridized to one major RNA band, the length of which was estimated to be 0.9 kb, only in case of the cells cultured in the medium supplemented with urea; the RNA prepared from cells grown in the absence of urea did not give the 0.9-kb band of hybridization with probe 2. No hybridization signals with probe 3 were detected, suggesting that little or no *nhhF* is expressed. Probe 4 containing *nhhBA* and

nhhG hybridized to one dense RNA band, the lengh of which was estimated at 1.8 kb, when the RNA was prepared from the urea-induced cells.

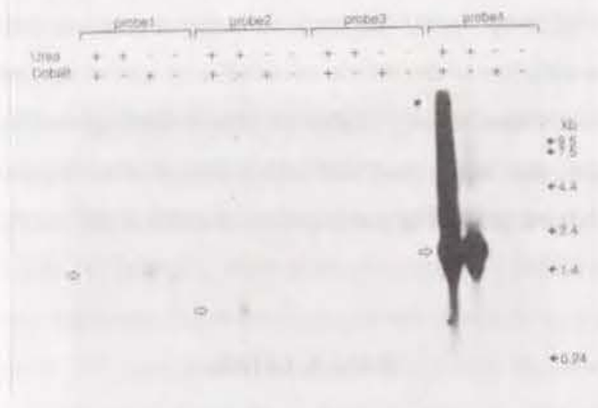

Fig. 4. Northern blots of RNA from *R. rhodochrous* J1 cultured in the medium in the presence (+) or in the absence (-) of urea and $CoCl_2$ and hybridized with probes 1~4 in Fig. 1. Open arrows point to prominent transcripts; those in the probe 1, probe 2 and probe 4 regions correspond to 1.6, 0.9 and 1.8 kb, respectively.

Nagasawa *et al.* (29) have previously reported that the addition of cobalt ions to the culture medium is indispensable not only for catalytic activity but also for NHase formation in *R. rhodochrous* J1; and the enzyme is induced by cobalt ions. In the author's study, the addition of cobalt ions to the medium is required for the expression of H-NHase activity in the *R. rhodochrous* ATCC12674 transformants. However, Northern blot hybridization analysis has shown that the H-NHase gene is transcribed in a large amount by urea as an inducer, irrespective of the addition of cobalt ions to the medium. These findings confirm the previous suggestion (13) that the expression of H-NHase activity rather than the expression of the H-NHase gene depends on the presence of cobalt ions, and these ions appear to play an important role in enhancing the folding or the stabilization of the subunit polypeptides of the enzyme.

The need of the three genes for the expression of *nhhBA*

To examine the need of *nhhD*, *nhhE* and *nhhF* for the expression of the *nhhBA*, three deletion plasmids (pHJK22, pHJK20 and pHJK24) were constructed (Fig. 1). Enzyme assays using benzonitrile as a substrate for each transformant revealed that *nhhD* was essential for the expression of the H-NHase gene, but *nhhE* and *nhhF* (IS*1164*) were not. This can be explained as follows. The transformants harboring pHJK22 or pHJK20, which excludes the

284-bp *Mlu*I-*Stu*I region corresponding to the internal portion of *nhhF* or the 928-bp *Nco*I-*Stu*I region covering the whole of *nhhE* and an amino terminal portion of *nhhF*, respectively, exhibited NHase activity (Table 1). On the other hand, the transformant harboring pHJK24, which excludes the 1228-bp *Acc*III fragment covering the amino terminal 10 amino acid residues of *nhhD* in addition to the whole of *nhhE* and amino terminal portion of *nhhF*, significantly decreased NHase activity (Table 1). These findings and the above experiments using pHJK11 suggest that both *nhhC* and *nhhD* are positive regulators involved in the expression of the H-NHase gene. The participation of *nhhG* in the *nhhBA* expression remains to be determined.

DISCUSSION

Five ORFs (*nhhC*, *nhhD*, *nhhE*, *nhhF* and *nhhG*) that flank the *nhhBA* in *R. rhodochrous* J1 have been characterized. This gene organization is distinct from that of each NHase gene which has already been reported (10). Of these genes, *nhhC* and *nhhD* are indispensable for the intracellular formation of an active recombinant H-NHase in *R. rhodochrous* ATCC12674, whereas *nhhE* and *nhhF* (IS*1164*) have been found to have no influence on the expression of the H-NHase gene. *nhhC*, which was shown to express constitutively in *R. rhodochrous* J1 by Northern blot analysis, has significant similarity of the amino acid sequence to the negative regulator AmiC of the *P. aeruginosa* aliphatic amidase, which is induced by some low-molecular-mass amides such as acetamide and propionamide (39). Induction of the *P. aeruginosa* amidase is regulated by AmiC which is considered to respond to the presence of amides as a sensor protein (40).

H-NHase of *R. rhodochrous* J1 is also induced by amide compounds, i.e., acetamide, propionamide, acrylamide, methacrylamide and urea, which are products of the nitrile hydration reaction catalyzed by NHase. The sequence analysis and the mapping experiment for the transcriptional initiation site of the H-NHase gene have demonstrated that no sequence homologous to amidase sequence exists in the upstream region of the H-NHase gene and that the transcription initiates at 71 and 48 bp upstream from the ATG initiation codon of *nhhB* (data not shown); *nhhBA* and the downstream region, *nhhG*, are transcribed in a single mRNA, and are not part of a larger operon including the amidase gene. The finding that the AmiC-homologue (*nhhC*) region is responsible for the expression of *nhhBA* which is not linked to any amidase gene, is noteworthy, while similarity of the amino acid sequence is not observed

among amide-degrading enzymes; AmiE (the *Pseudomonas* amidase) does not show any similarity to amidases coupled with the Rhodococcus sp. N-774 NHase (14) and the *P. chlororaphis* B23 NHase (15). Assuming that NhhC as well as AmiC functions as a sensor protein sensitive to amide compounds, it is suggested that NhhC will be involved in the induction of H-NHase synthesis in some way, leading to occurrence of unusual induction mechanism in which NHase is formed by amides (the NHase reaction products).

Another ORF (*nhhD*) which shares a homology of amino acid sequence with putative repressor genes, *marR* and *hpcR*, from *E. coli*, is also required for the expression of *nhhBA* in *R. rhodochrous* ATCC12674 (Table 1). Both of the *mar* (multiple antibiotic resistance) operon and the *hpc* (homoprotocatechuate)-degradative operon are shown to be negatively regulated by the *marR* (34) and *hpcR* (35) gene products, respectively. On the other hand, the author's findings that deletion of the amino terminal portion of *nhhD* significantly decreased NHase activity in the *R. rhodochrous* ATCC12674 transformant and that the transcription was stimulated by urea in the culture medium in *R. rhodochrous* J1 have indicated the necessity of *nhhD* as a positive regulator in the process of H-NHase formation.

While the sequences homologous to IS*1164* were observed in *R. rhodochrous* J1 DNA, whether IS*1164* functions as a mobile element in *R. rhodochrous* J1 remains to be determined. However, by the Southern hybridization method, we have already found the distribution of IS*1164* in some *Rhodococcus* species. The existence of IS*1164* upstream of *nhhB* and the existence of the transcriptional terminator located just downstream of *nhhG* support the finding in our Northern blot analysis that the H-NHase gene and its downstream region *nhhG* constitute a single transcriptional unit; both genes are cotranscribed in a single polycistronic mRNA in the presence of urea irrespectively of the presence of cobalt ions. This is in contrast with the organization of gene clusters for NHases from *Rhodococcus* sp. N-774 (14, 41), *Rhodococcus* sp. (42), *Rhodococcus erythropolis* (43), *P. chlororaphis* B23 (15) and *Brevibacterium* sp. R312 (44), in which an amidase gene is located just upstream of each NHase gene with the same orientation. In the case of *R. rhodochrous* J1, the putative insertion sequence (IS*1164*) instead of an amidase gene is located in the upstream region from *nhhBA*, suggesting the rearrangement of the H-NHase gene cluster by IS*1164* in the course of evolution.

The role of nitrile-converting enzymes in biosynthesis of the phytohormone, indole-3-acetic acid, is recently attracting increasing attention. cDNAs of nitrilase, which catalyzes the hydrolysis of indole-3-acetonitrile to indole-3-acetic acid plus ammonia, from a plant

Arabidopsis thaliana have been cloned (6-8). The occurrence of a biosynthetic pathway for indole-3-acetic acid from indole-3-acetonitrile via indole-3-acetamide by the combined action of NHase and amidase are also reported in phytopathogenic bacteria *Agrobacterium tumefaciens* and in leguminous bacteria *Rhizobium* (9). The existence of IS*1164* [homologous to the *Rhizobium* IS*Rm3* which is a component of reiterated sequence IV of the nod megaplasmid (38)] in the upstream region of *nhhBA* may be related with such biosynthesis of indole-3-acetic acid from indole-3-acetonitrile. Studies on nitrile metabolism in *Rhodococcus* at both protein and gene levels could provide information about biosynthesis of indole-3-acetic acid in plant-associated bacteria and plants, and the evolutionary relationships of the former to the latter organisms.

SUMMARY

The 4.6-kb region 5'-upstream from the gene encoding a cobalt-containing and amide-induced high molecular-mass nitrile hydratase (H-NHase) from *Rhodococcus rhodochrous* J1 was found to be required for the expression of the H-NHase gene (*nhhBA*) with a host-vector system in a *Rhodococcus* strain. Sequence analysis has revealed that there are at least five open reading frames (*nhhC*, *nhhD*, *nhhE*, *nhhF* and *nhhG*) in addition to *nhhBA*. Deletion of *nhhC*, and *nhhD* resulted in decrease of NHase activity, suggesting a positive regulatory role of both genes in the expression of the *nhhBA*. *nhhC* showed significant similarity to a regulatory protein, AmiC, which is involved in regulation of amidase expression by binding an inducer amide in *Pseudomonas aeruginosa*. *nhhF*, which has been found to be uninvolved in regulation of H-NHase expression by enzyme assay for its deletion transformant and Northern blot analysis for *R. rhodochrous* J1, showed high similarity to transposases from insertion sequences of several bacteria. Determination of H-NHase activity and H-NHase mRNA levels in *R. rhodochrous* J1 has indicated that the expression of the H-NHase gene is regulated by an amide at the transcriptional level. These findings suggest the participation of *nhhF* (IS*1164*) in the organization of the H-NHase gene cluster and the involvement of *nhhC* in unusual induction mechanism, in which H-NHase is formed by amides (the products in the NHase reaction), but not by nitriles (the substrates).

Section 2 Insertion sequence IS*1164* in the H-NHase gene cluster[b]

An insertion sequence (IS) is a mobile genetic element which is able to transpose to numerous sites on plasmids and chromosomes of microorganisms or plants, usually to give rise to their copies (45); however, only two studies have so far been reported on IS from *Rhodococcus* strains. IS*1166* and IS*1295* have recently been identified on a plasmid present in *Rhodococcus* sp. IGTS8 (46), whereas IS-*Rf* is isolated from *Rhodococcus fascians* using the *Bacillus subtilis sacB* gene as a selection marker (47).

As described in the previous chapter, studies on *nhhBA* regulation in *R. rhodochrous* J1 revealed the existence of five ORFs (*nhhC*, *nhhD*, *nhhE*, *nhhF* and *nhhG*) in addition to *nhhBA* in the H-NHase gene cluster. Two ORFs (*nhhC* and *nhhD*) were found to play positive regulatory roles in the process of the H-NHase formation; the intervening space between *nhhBA* and *nhhCD* was about 2.6 kb. The author has fortuitously found a possible IS in this region.

In this section, the author examined IS*1164* (including *nhhF*) from *R. rhodochrous* J1. In addition, The author compared the structure of IS*1164* and IS*1081*, which shows the highest similarity to IS*1164*, and found two pairs of terminal inverted repeats flanking their probable transposases. The distribution of IS*1164*-like elements in the genomes of various *Rhodococcus* strains and other nitrile-metabolizing strains is also presented.

MATERIALS AND METHODS

Strains, culture conditions and plasmids

Table 1 shows the microbial strains used in this chapter. For the preparation of total DNAs, *Rhodococcus* strains were cultured in a medium consisting of 5 g Tryptone (Difco), 5 g yeast extract (Oriental Yeast, Tokyo, Japan), 1 g glucose and 1 g K_2HPO_4/l distilled water (pH 7.0), and the other strains were cultured as described previously (9,26,48). The plasmid pNHJ10H (13) carrying *nhhBA* of *R. rhodochrous* J1 in the 6-kb *Sac*I fragment on pUC19 was used for subcloning of gene.

Enzymes and chemicals

Restriction endonuclease was purchased from Takara Shuzo Co, Ltd. (Kyoto, Japan) or Toyobo Co. Ltd. (Osaka, Japan). [α-^{32}P]dCTP (110 TBq/mmol) was from Amersham

(Tokyo, Japan). All other chemicals used were from commercial sources and were reagent-grade.

DNA manipulation

Total DNA of *R. rhodochrous* J1 and the other strains were isolated and purified as described by Saito and Miura (49). DNA manipulation was performed essentially as described by Sambrook *et al.* (30).

Southern hybridization

Southern blots against the restriction endonuclease-digested total DNA were prepared as described by Sambrook *et al.* (30). The 967-bp *Eco*RV-*Bgl*II fragment in IS*1164* was purified from a low-melting agarose gel, labelled with α-[^{32}P]dCTP using a Multiprime DNA labelling system (Amersham) and used to probe the Southern blots. Prehybridization and hybridization were performed at a higher stringency using a solution consisting of 50% (v/v) formamide, 2 x SSC (1 x SSC = 0.15 M NaCl, 15 mM sodium citrate), 1% (w/v) SDS and 10% (w/v) dextran sulfate at 42°C; the blots were then washed twice in 2 x SSC for 5 min at room temperature, twice in 2 x SSC containing 1% SDS for 20 min at 42°C and twice in 0.2 x SSC containing 1% SDS for 20 min at 42°C.

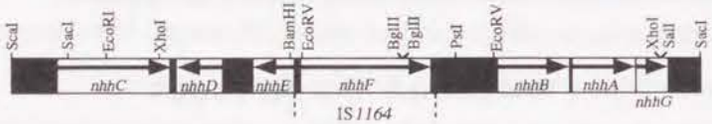

Fig. 1. Genetic organization of the H-NHase gene cluster.
nhhB and *nhhA* are genes encoding H-NHase β- and α- subunit proteins, respectively (13). *nhhC* and *nhhD* have recently been found to be required for the H-NHase expression. *nhhE* and *nhhF* are not involved in the H-NHase expression.

RESULTS

Occurrence of IS*1164* in the H-NHase gene cluster

The author has identified the sequence elements (*nhhC* and *nhhD*) required for the expression of *nhhBA* encoding H-NHase (Fig. 1). Between their elements and *nhhBA*, there is *nhhF* encoding the putative transposase that had high similarities to the transposases from IS elements previously reported *i.e.*, *Mycobacterium bovis* IS*1081* (78.8% identity) (36), *Staphylococcus aureus* IS*256* (36.4% identity) (37) and *Pseudomonas cepacia* IS*406*(36.0% identity) (50). In the flanking region of *nhhF*, two pairs of terminal inverted repeats (IR), 27-bp sequence with 18-bp matches for IR-1 and 19-bp sequence with 16-bp matches for IR-2 were observed; IR-1 are flanked by 9-bp direct repeats (DR). These findings suggest that *nhhF* encodes a presumed transposase and constitutes an insertion sequence, accompanied with the flanking direct and inverted repeats. The G + C content (66.9%) of IS*1164* resembled that of the *Rhodococcus rhodochrous* genome (67-73%, ref. 28).

Comparison of the ends of IS*1164* and IS*1081*

IS*1164* from *R. rhodochrous* J1 has the structural features shared by transposable elements as described above. Furthermore, it is noteworthy that IS*1164* has two pairs of IR that are accompanied with the intervening space of 47-bp between IR-1 (Left) and IR-2 (Left) and with 1-bp between IR-1 (Right) and IR-2 (Right) (Fig. 2). The alignment of extremities of IS*1164* and IS*1081* showed marked similarity between them (Fig. 2), indicating that IS*1081* also contains two pairs of IR flanked by 8-bp DR. To the author's knowledge, existence of two pairs of IR in the flanking region of transposase gene has not been previously reported. The two pairs of IR are highly conserved between both ISs, suggesting the functional role for these IR sequences. On the contrary, DR corresponding to the possible target-site duplications show little sequence similarity.

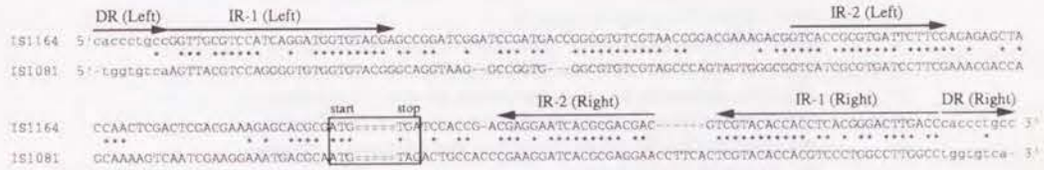

Fig. 2. Comparison of the DNA sequences around the ends of IS*1164* and IS*1081*.
The putative target-site duplications (9-bp for IS*1164* and 8-bp for IS*1081*) are in lower-case letters. DNA regions encoding the presumed transposases are boxed.

Determination of copy number of IS*1164* in *R. rhodochrous* J1

To determine how many copies of the insertion sequence (IS*1164*) are present in *R. rhodochrous* J1 genome, Southern blot hybridization was carried out. Southern blots against the *R. rhodochrous* J1 total DNA that had been digested separately with restriction enzymes *Eco*RI, *Pst*I, *Sac*I, *Eco*RI plus *Sac*I, and *Pst*I plus *Bam*HI, which do not have their sites within IS*1164*, were exposed to the IS*1164* internal probe of a 967-bp *Eco*RV-*Bgl*II fragment. Southern blot analysis at a higher stringency revealed that, in all cases, the probe hybridized

with a single bold band and two or three thin bands (Fig. 3). The bold band at all lanes was found to correspond to the DNA fragment containing IS*1164* judging from the size of these fragments. This suggests that two or three insertion element-like sequences, which are homologous to IS*1164* to some extent, are present and that IS*1164* is a repeated sequence in the *R. rhodochrous* J1 genome.

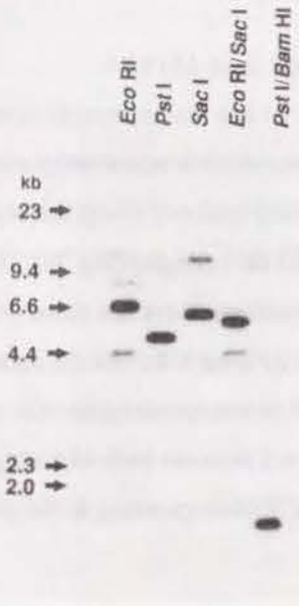

Fig. 3. Determination of the copy number of IS*1164* in total DNA of *R. rhodochrous* J1.
Total DNA (4 μg) from *R. rhodochrous* J1 was digested with several endonucleases indicated (sites not present in IS*1164*), separated by electrophoresis on a 0.7% agarose gel, transferred to a nylon membrane and hybridized with the labelled IS*1164* probe (Materials and Methods). Sizes are shown in kilobase pairs.

Distribution of IS*1164*-like elements in other *Rhodococcus* and nitrile-metabolizing strains

To investigate the distribution of an IS*1164*-like element in other *Rhodococcus* and nittile-metabolizing strains, we carried out Southern blot analysis against their *Eco*RI-digested total DNAs by using the 967-bp *Eco*RV-*Bgl*II fragment in IS*1164* as a probe (Fig. 4). Difference in the intensity of the bands could correspond to multiple copies for one band or to less sequence similarity between the target DNA and the probe used. Eleven out of 16 *Rhodococcus* strains (lanes 2~17 in Fig. 4) were found to contain an IS*1164*-like element. In

particular, *R. rhodochrous* NCIB9703 and *R. rhodochrous* NCIB11277 contained the element at a relatively higher copy number, at least 6 and 7 copies per genome, respectively. However, *P. chlororaphis* B23 (48), *Alcaligenes faecalis* JM3 (26) and *Agrobacterium tumefaciens* IAM B-261 (9), which are found to contain the enzymes involved in nitrile metabolism, just like *R. rhodochrous* J1, contained no DNA sequence showing similarity to IS*1164* from *R. rhodochrous* J1.

Fig. 4. Distribution of IS*1164* among various *Rhodococcus* and other nitrile degrading strains.
Total DNA (8 μg) from *R. rhodochrous* J1 (lane 1), *R. rhodochrous* K22 (lane 2), *R. rhodochrous* ATCC9356 (lane 3), *R. rhodochrous* ATCC19140 (lane 4), *R. rhodochrous* ATCC19149 (lane 5), *R. rhodochrous* JCM2157 (lane 6), *R. rhodochrous* JCM3202 (lane 7), *R. rhodochrous* NCIB9703 (lane 8), *R. rhodochrous* NCIB11277 (lane 9), *R. erythropolis* IFO12539 (lane10), *R. erythropolis* IFO12682 (lane 11), *R. erythropolis* JCM2892 (lane 12), *R. erythropolis* JCM6823 (lane 13), *R. rubropertinctus* JCM3204 (lane 14), *Rhodococcus* sp. N-774 (lane 15), *Rhodococcus* sp. NCIB11215 (lane 16), *Rhodococcus* sp. NCIB11216 (lane 17), *P. chlororaphis* B23 (lane 18), *A. faecalis* JM3 (lane 19), *A. tumefaciens* IAM B-261 (lane 20) was digested with *Eco*RI (site not present in IS*1164*), separated by electrophoresis on a 0.7% agarose gel, transferred to a nylon membrane and hybridized with the labelled IS*1164* probe (Materials and Methods). Sizes are shown in kilobase pairs.

DISCUSSION

Transposable elements are characterized by the presence of terminal inverted repeat sequences that are essential for transposition and the presence of direct repeat sequences that are probably duplicated upon insertion. *nhhF* encoding possible transposase has several features found in the known IS elements in its flanking region: terminal inverted repeats and target-site duplications. These structural features have been used to identify IS elements such as IS*1081* from *Mycobacterium bovis* (36), IS*1201* from *Lactobacillus helveticus* (51), IS*T2* from *Thiobacillus ferrooxidans* (52) without providing direct evidence for transposition. Sequence

comparisons of the putative transposase encoded by *nhhF* with those of other IS elements suggest that IS*1164* is a new member of an IS family including IS*1081* (36), IS*256* (37), IS*406* (50), *Lactococcus lactis* IS*905* (53), *Rhizobium meliloti* IS*Rm3* (38), IS*1201* (51), *Mycobacterium smegmatis* IS*6120* (54), *Rhodococcus* sp. IGTS8 IS*1166* (46) and IS*T2* (52). Of these members, IS*406*, IS*905*, IS*Rm3*, IS*6120* and IS*1166* have been previously shown to have ability to transpose. IS*1164* and IS*1081* share a high degree of identity (78.8%), suggesting that these IS elements had a recent common ancestry. However, a search of the EMBL and Genbank databases did not show any homologous sequences in *Streptomyces* to IS*1164*, although *Rhodococcus* belongs to Actinomycete (27) including *Streptomyces*; Furthermore, *Rhodococcus* has significantly high G+C content as well as *Strepytomyces* does.

IS*1164* is located between *nhhBA* encoding H-NHase and *nhhCD* encoding positive regulators for *nhhBA* expression in *R. rhodochrous* J1 DNA. It seems reasonable to suppose that IS*1164* has been inserted individually between *nhhCD* and *nhhBA* because IS*1164* is bracketed by possible target site duplications. Southern hybridization revealed that IS*1164*-like elements are widely distributed among *Rhodococcus*: 11 out of 16 *Rhodococcus* strains tested showed positive hybridization signals. However, except for the case of *R. erythropolis* JCM2892 (43) (lane 12 in Fig. 4), no signal was detected in *R. erythropolis* JCM6823 (43), *Rhodococcus* sp. N-774 (14) or *P. chlororaphis* B23 (15), which possess NHase genes with significant similarities to *nhhBA*. On the other hand, IS-like elements have been detected even in *R. rhodochrous* K22 (25), *R. erythropolis* IFO12682, *Rhodococcus* sp. NCIB11215 (19) and NCIB11216 (20), which produce nitrilase. *R. rhodochrous* ATCC19149, *R. rhodochrous* NCIB9703 and *R. rhodochrous* NCIB11277, which gave hybridization signals, oxidize alkylbenzenes, oxidize hydrocarbons and utilize hydrocarbons, respectively. Recently, a mechanism has been proposed by which *tcbAB* on Tn*5280* can be mobilized and joined with *tcbCDE* to form a novel catabolic pathway degrading chlorobenzenes (55). Moreover, five copies of IS*6100* have also been identified on plasmid pOAD2, which carries genes encoding nylon oligomer-degrading enzymes (56). Although it is still unclear whether IS*1164*-like elements found in *Rhodococcus* by Southern hybridization method are involved in acquirement of ability that degrades recalcitrant highly toxic nitriles containing a cyano functional group and other aromatic compounds in *Rhodococcus*, the presence of these IS*1164*-like elements suggests such a possibility.

The genus *Rhodococcus* has been poorly characterized genetically. Only three kinds of ISs are so far known in *Rhodococcus*: IS*1166* and IS*1295* from *Rhodococcus* sp. strain

IGTS8 (46) and IS-*Rf* from *R. fascians* DSM20131 (47). In terms of similarity, IS*1164* and IS*1166* appear to belong to the same family. On the other hand, IS*1295* is dissimilar to IS*1164*. We could not compare IS-*Rf* with IS*1164* because only IR of IS-*Rf* have been reported. Whether IS*1164* functions as a mobile element in *R. rhodochrous* J1 remains to be determined. However, we have found IS*1164*-like elements in some *Rhodococcus* species including *R. rhodochrous*, *R. erythropolis* and *R. rubropertinctus*, indicating that these elements show a broad host range. Further investigations on IS*1164* are needed to clarify whether IS*1164* can be useful for genetic manipulation of the genomes of *Rhodococcus*, which are expected to be useful in various fields.

SUMMARY

An insertion sequence (IS*1164*) from *Rhodococcus rhodochrous* J1 has been identified by its nucleotide sequence. This 1430 bp-long IS has two pairs of imperfect terminal inverted repeats (IR-1 and IR-2) flanked by nine base pair direct repeats (DR), and contains an open reading frame encoding a putative transposase with similarities to those found in IS*1081* from *Mycobacterium bovis*, IS*256* from *Staphylococcus aureus* and IS*406* from *Pseudomonas cepacia*. Structures of the terminal region containing inverted repeats were found to be highly conserved both in IS*1164* and in IS*1081*. Hybridization analyses against total DNA from *R. rhodochrous* J1, 16 *Rhodococcus* strains and 3 other bacteria catabolizing nitriles as well as *R. rhodochrous* J1, using an internal DNA fragment within IS*1164* as a probe, showed that *R. rhodochrous* J1 had three other IS*1164*-like elements and 11 out of 16 *Rhodococcus* strains contained IS*1164*-like elements varying in copy number from one to at least seven. Their elements are present not only in *Rhodococcus* producing recalcitrant nitriles-degrading enzymes (nitrile hydratase and nitrilase) but also in *Rhodococcus* utilizing alkylbenzenes and hydrocarbons.

CHAPTER II Analysis of Low Molecular-Mass Nitrile Hydratase (L-NHase) Gene Cluster

Section 1 Occurrence of amidases in *Rhodococcus rhodochrous* J1[c]

Rhodococcus rhodochrous J1 has great catalytic potential for the hydration of nitriles to the corresponding amides (16). This strain produces two kinds of cobalt-containing nitrile hydratases (NHases); one is a high *M*r-NHase (H-NHase) and the other is a low *M*r-NHase (L-NHase) (10). When *R. rhodochrous* J1 was cultured in the medium containing urea or cyclohexanecarboxamide in the presence of cobalt ions, the H-NHase and L-NHase were inducibly formed selectively. In fact, the industrial production of acrylamide from acrylonitrile using the *R. rhodochrous* J1 H-NHase was started in 1991 (30,000 tons per year). This is the first successful example of using a biotransformation process to produce a commodity chemical. In the nitrile-degrading pathway by NHase, amidase is essential for the growth of the strain, when the strain is cultured in a medium containing a nitrile as a sole source of carbon/nitrogen, because the amide formed by NHase has to be converted into the corresponding acid and ammonia (3). In this process, contamination of acrylic acid formed by amidase in the strain causes the deterioration in the quality of the manufactured acrylamide; acrylamide is required not to be changed into acrylic acid as much as possible by the amidase. Therefore, it is important from an applied standpoint to investigate amidases coupled with NHase. In this section, The author presents the evidence that at least two amidases exist in *R. rhodochrous* J1.

MATERIALS AND METHODS

Strain and culture conditions

R. rhodochrous J1 (29) was subcultured at 26.5°C for 24 h in 8 ml of a basal medium consisting of 10 g of glycerol, 0.5 g of KH_2PO_4, 0.5 g of K_2HPO_4, 0.1 g of $MgSO_4 \cdot 7H_2O$, 1 g of yeast extract (Oriental Yeast, Tokyo), and 5 g of Polypeptone (Daigo, Osaka)/liter of distilled water (pH 7.2). This subculture was inoculated into a 2-liter shaking flask containing 500 ml of the basal medium with one of the amides listed on the Table in the presence or absence of $CoCl_2 \cdot 6H_2O$ (0.001%, mass/vol).

Assay for amidase activity

After 48 h of cultivation, cells were harvested from each culture by centrifugation, washed with 0.01 M potassium phosphate buffer (pH 7.5), and then suspended in 0.1 M of the same buffer. Amidase activity was assayed in a reaction mixture (2 ml) containing 50 mM potassium phosphate buffer (pH 7.5), 10 mM benzamide or 100 mM propionamide, and an appropriate amount of the cel suspension. The reaction was done at 25°C for 15-100 min and stopped by the addition of 0.2 ml of 1 M HCl. The benzoic acid formed in the reaction mixture was measured as described previously (23). The propionic acid formed in the reaction mixture was measured by gas chromatography under the same conditions as the acrylamide detection (48). Cell growth of *R. rhodochrous* J1 was estimated turbidimetrically by a dry cell calibration curve of the absorbance at 610 nm: 0.44mg dry cell mass/ml was equivalent to 1.0 unit of OD_{610}.

Table. Effects of various amides on the amidase formation.
Various amides (0.1%; mass/vol) were added to the basal medium in the absence (left panel) or in the presence (right panel) of cobalt ions.

-Co	Specific activity (U/mg dry cell mass)			+Co	Specific activity (U/mg dry cell mass)		
Compound	Propionamide propionic acid (P)	Benzamide benzoic acid (B)	P/B	Compound	Propionamide propionic acid (P)	Benzamide benzoic acid (B)	P/B
None	1.01	0		None	0.207	0	
Acetamide	1.66	0		Acetamide	0.635	0	
Propionamide	2.98	0		Propionamide	0.838	0	
N-Methylpropionamide	2.83	0.184	15.4	*N*-Methylpropionamide	0.280	0.0361	7.8
N,N-Dimethylpropionamide	1.65	0.127	13.0	*N,N*-Dimethylpropionamide	0.333	0.212	1.6
Butylamide	0.505	0.0093	54.3	Butylamide	0.327	0.0042	77.9
Crotonamide	0.767	0.0113	67.9	Crotonamide	0.235	0.018	13.1
Methacrylamide	1.60	0.0912	17.5	Methacrylamide	1.09	0.137	8.0
Lactamide	0.922	0		Lactamide	0.059	0	
Benzamide	0.602	0.0182	33.1	Benzamide	0.134	0.0358	3.7
Cyclohexanecarboxamide	1.08	0.0407	26.5	Cyclohexanecarboxamide	0.247	0.0052	47.5
ε-Caprolactam	1.78	0.0204	87.3	ε-Caprolactam	0.864	0.0198	43.6
N-Methyl-ε-caprolactam	0.804	0.145	5.5	*N*-Methyl-ε-caprolactam	0.640	0.212	3.0
Urea	2.23	0		Urea	0.787	0	

RESULTS AND DISCUSSION

As shown in the Table, whether cobalt ions are added to the basal medium or not, *R. rhodochrous* J1 cells cultured with each amide added to the culture medium showed amidase activity for propionamide as a substrate. Even when amide was not added to the basal medium, the activity degrading propionamide was found, but cells cultured in a synthetic medium consisting of glycerol, KH_2PO_4, K_2HPO_4, $MgSO_4$, NH_4Cl, NaCl and vitamin mixture (11) did not have any amidase activities; amidase activity may be induced by some amide-like compounds in the basal medium. When H-NHase was induced by urea, *R. rhodochrous* J1

cells were not able to hydrolyze benzamide as a substrate at all. On the other hand, when L-NHase was induced by cyclohexanecarboxamide, the cells could hydrolyze not only benzamide but also propionamide as substrates. The ratio of propionamide-degradation to benzamide-degradation (P/B) was not constant under each condition. The similar observation applied to the cell-free extract obtained from each cell suspension by sonication for 20 min with an insonator model 201M (Kubota, Tokyo). These findings demonstrate that there are at least two kinds of amidases in *R. rhodochrous* J1; they provided information leading to the manufacture of pure acrylamide to be established.

R. rhodochrous J1 cells cultured with L-NHase induced by cyclohexane-carboxamide did not attack acrylamide at all, but the cells containing H-NHase supplied in the industrial production just acted on acrylamide (0.967 U/mg dry cell mass) at 25°C, and had barely any activity at low temperatures in the reaction mixture. To prevent the formation of the by-product acrylic acid, the practical reaction has been done at a low temperature (2-4°C), because this reduces the amidase activity and the H-NHase is not easily inactivated even at this temperature. Acrylamide was also a good inducer for the formation of NHase in this strain. However, growth of the strain and NHase activity in this occasion were lower than those when H-NHase was induced. Thus, urea was selected instead of acrylamide has been used in the form of a polymer as an immobilizer of *R. rhodochrous* J1.

The addition of cobalt ions to the culture medium was indispensable for NHase activity both in *R. rhodochrous* J1 and in the *Escherichia coli* transformant containing H- or L-NHase gene. (13) On the contrary, in general, the cobalt addition lowered amidase activity for propionamide by 20-90% (Table). When amides such as *N*,*N*-dimethylpropionamide, crotonamide, methacrylamide, benzamide, and *N*-methyl-ε-caprolactam were used as inducers, the addition of cobalt ions enhanced amidase activity for benzamide only 1.5-2.0 times, while NHase activity was strongly enhanced more than 60-times (data not shown) by the cobalt addition into the medium containing each amide. These findings indicate that amidases do not seem to require cobalt ions for their activity.

In *Rhodococcus* sp. N-774 (14), *Pseudomonas chlororaphis* B23 (15), and *Rhodococcus* sp. (42), each amidase gene is found in the same orientation and just upstream from each NHase gene, which is significantly similar to the *nhhBA* and *nhlBA*. Judging from the gene arrangement of both enzymes and the sequential nitrile degradation route through the combination of NHase and amidase, there might be amidases that are induced together with H- and L-NHase by urea and cyclohexanecarboxamide, respectively, and cobalt ions.

Amidase itself as well as NHase might be useful in the production of higher-value acids from the corresponding nitriles or amides in cooperation with an NHase. We have never isolated an amidase gene that is coupled with an H-NHase gene. Cloning of this amidase and overexpression of the amidase gene coupled with L-NHase gene from *R. rhodochrous* J1 in *Escherichia coli* are now being studied.

SUMMARY

R. rhodochrous J1, of which the high-*M*r nitrile hydratase has been used for the industrial manufacture of acrylamide from acryronitrile, produced at least two amidases differing in substrate specificity, judging from the effects of various amides on amidase activity in this strain. These amidases seemed to be inducible enzymes depending on amide compounds.

Section 2 Amidase coupled with L-NHase : Sequencing and expression of the gene and purification and characterization of the gene product[d]

The microbial degradation of nitriles proceeds through two enzymatic pathways. One is the nitrilase pathway, in which nitrilase hydrolyzes nitriles directly to the corresponding carboxylic acids and ammonia. The other pathway is a combination of nitrile hydratase (NHase) and amidase. Firstly, nitriles are hydrated into the corresponding amides by NHase. Secondly, amides are hydrolyzed into the corresponding carboxylic acids and ammonia by amidase. *Rhodococcus rhodochrous* J1 has both nitrile-degrading pathways, depending on the inducer (10). When this strain is cultured in medium containing isovaleronitrile as an inducer, only nitrilase is induced (11). The strain also produces higher (H-NHase) and lower molecular mass (L-NHase) NHases (10). Both require cobalt ions and amides for their induction. They are composed of two subunits, α and β (The α-subunit differs in size from the β-subunit in each, and the α- and β-subunits of H-NHase differ from those of L-NHase.). H-NHase and L-NHase are induced by urea and cyclohexanecarboxamide, respectively. In fact, the use of H-NHase in *R. rhodochrous* J1 as the third-generation strain for the industrial production (30,000 tons per year) of the important chemical commodity acrylamide from acrylonitrile was recently pioneered in Japan (10).

When the strain was cultured in the optimum medium, the amount of H-NHase in the cell-free extracts corresponded to more than 50% of the total soluble protein. However, the *R. rhodochrous* J1 amidase, along with amidases from *Rhodococcus* sp. N-774 (14,57) and *P. chlororaphis* B23 (15), which were used as 1st- and 2nd-generation strains respectively in the industrial manufacture of acrylamide, have never been investigated in form of protein, because of the low activity in these strains. Functional analysis of the amidase in *R. rhodochrous* J1 will certainly help to elucidate the hyperproduction of NHase and hypoproduction of amidase and subsequently allow the manufacture of pure acrylamide to be established. In the previous section, the author showed the evidence that at least two amidases, which are induced coordinately with H-NHase or L-NHase in *R. rhodochrous* J1. In this section, the author cloned and sequenced the amidase gene, which is considered to be linked to the L-NHase gene (*nhlBA*) (13). The recombinant *R. rhodochrous* J1 amidase protein in *Escherichia coli* was also produced, purified and characterized.

MATERIALS & METHODS

Bacterial strain and plasmids

Escherichia coli JM109 was the host for pUC18/19 plasmid transformation and phage M13 mp18/19 propagation (30). The plasmid pNHJ20L, carrying the L-NHase gene (*nhlBA*) of *R. rhodochrous* J1 in the 9.4 kb *Sac*I fragment on pUC19 (13), was used for subcloning and sequencing the gene.

Materials, enzymes and chemicals

DEAE-Sephacel, Mono-Q^{TM}HR 5/5, Superose^{TM}12 and a low-molecular-mass standard kit were obtained from Pharmacia (Uppsala, Sweden). Marker proteins for molecular mass determination by HPLC were purchased from the Oriental Yeast Co. (Tokyo, Japan). All other chemicals used were from commercial sources and of reagent grade.

DNA sequencing

DNA fragments containing the amidase gene were cloned into M13 vectors and sequenced by dideoxy chain-termination (58) using Sequenase version 2.0 (United States Biochemical Corp., Cleveland, USA) and a *Tth* (*Thermus thermophilus*) Sequence Kit (Toyobo, Osaka, Japan).

Preparation of crude extracts from *Escherichia coli* transformants

Recombinant *E. coli* JM109 was cultured aerobically to full growth in 10 ml of 2 x YT medium containing 80 μg/ml ampicillin in 100 ml test tube at 37°C, and then transferred to 100 ml of the same medium in a 500-ml shaking flask with isopropyl-β-D-galactopyranoside (IPTG) added to a final concentration of 1 mM to induce the *lac* promoter. After a further 7- or 12-h cultivation, cells were harvested by centrifugation, suspended in 5 ml 0.1 M potassium phosphate buffer (pH 7.5) containing 1 mM dithiothreitol, disrupted by sonication for 10 min (19 kHz; Insonator Model 201M, Kubota, Tokyo, Japan) and centrifuged at 12,000 x *g* for 30 min. The resulting supernatants were dialyzed for 5 h against 2 l 0.02 M potassium phosphate buffer (pH 7.5) containing 1 mM dithiothreitol, and 0.05 M potassium phosphate buffer (pH 7.5) containing 1 mM dithiothreitol and 45% (mass/vol.) glycerol for 10 h. The resulting dialysates were assayed for the enzyme.

Enzyme assay

The standard reaction mixture (1 ml) for assaying the amidase activity contained 10 mmol potassium phosphate buffer (pH 7.5), 10 mmol benzamide and an appropriate amount of the enzyme. The reaction was performed at 30°C for 30 min and stopped by adding 0.1 ml 1 M HCl. The amount of benzoic acid formed in the reaction mixture was determined by HPLC under the same conditions as described previously (13) with the exception that the ratio of KH_2PO_4-H_3PO_4 to acetonitrile was 1 : 1 (by vol.). One unit of the enzyme was defined as the amount catalyzing the formation of 1 µmol benzoic acid/min from benzamide under the above conditions. Protein was determined by the Coomassie brilliant blue G-250 dye-binding method of Bradford (59) using bovine serum albumin as a standard protein.

PCR amplification

A modified DNA fragment coding for the amidase was obtained by means of polymerase chain reaction (PCR). DNA was amplified using a thermal cycler (Perkin-Elmer/Cetus, USA). The reaction mixture contained 150 ng of template DNA, 100 pmol of each oligonucleotide pool, and *Tth* (*Thermus thermophilus*) DNA polymerase (Toyobo, Osaka, Japan) in a volume of 100 ml. One thermal cycle consisted of 95°C for 1 min, 42°C for 1 min, and 75°C for 3 min. A total of 30 cycles was performed. The PCR-synthesized DNA was purified from an agarose gel.

Purification of the amidase from *Escherichia coli* transformant

E. coli JM109 harboring pALJ30 was subcultured at 37°C for 12 h in a 100 ml test tube containing 10 ml of 2 x YT medium with 80 µg/ml ampicillin. One milliliter of the subculture was then inoculated into a 500 ml shaking flask containing 100 ml of the above medium. After a 4 h incubation at 37°C with reciprocal shaking, IPTG was added to the medium to a final concentration of 0.3 mM to induce the *lac* promoter, followed by a further incubation at 28°C for 4 h. Eight hours from the start, the cells were harvested by centrifugation for 10 min at 9,000 x *g* at 4°C, and washed with 10 mM potassium phosphate buffer (pH 7.5) containing 1 mM dithiothreitol. All purification steps were performed at 0 to 4°C using potassium phosphate buffer (pH 7.5) containing 1 mM dithiothreitol and 20% (mass/vol.) glycerol unless otherwise specified. Centrifugation was carried out for 30 min at 100,000 x *g*.

Step 1. Preparation of cell-free extracts. Washed cells from 2.4 liters of culture were suspended in 50 ml 0.1 M buffer and disrupted by sonication at 19 kHz or 20 min with an

insonator model 201M (Kubota). The cell debris was removed by centrifugation. The resulting supernatant was used as the cell-free extract.

Step 2. DEAE-Sephacel column chromatography. The solution from step 1 was applied to a DEAE-Sephacel column (3.5 by 60 cm) equilibrated with 10 mM buffer. After the column was washed thoroughly with 10 mM buffer, followed by the same buffer containing 0.1 M KCl and 0.2 M KCl, the enzyme was eluted with 1.5 liters 10 mM buffer containing 0.3 M KCl. The active fractions were pooled.

Step 3. Ammonium sulfate fraction. Solid ammonium sulfate was added to the resulting enzyme solution to give 45% (mass/vol.) saturation. The pH was maintained at 7.5 with ammonia. After stirring for 4 h or more, the precipitate was removed by centrifugation, and ammonium sulfate was added to the supernatant to give 60% (mass/vol.) saturation. The suspension was then centrifuged, and the pellet was dissolved in 0.1 M buffer, followed by dialysis for 24 h against three changes of 2 liters 10 mM buffer.

Step 4. FPLC Mono-Q™ column chromatography. The enzyme solution from step 3 was applied to a Mono-Q™ HR 5/5 column equilibrated with 10 mM buffer, which was attached to a FPLC system (GP-250, Pharmacia, Sweden). After the column was washed with the same buffer, the enzyme was eluted by increasing the ionic strength of KCl in a linear fashion from 0 to 1 M in the same buffer, at a flow rate of 0.5 ml/min. The active fractions were pooled.

Step 5. FPLC Superose™12 column chromatography. The enzyme solution from step 4 was applied to a Superose™ 12 gel filtration column (1 cm x 30 cm) equilibrated with 0.1 M buffer. The rate of column elution was 0.5 ml/min using the FPLC system. The active fractions were combined.

Analytical measurements

SDS-PAGE was performed by the method of Laemmli (60). In order to estimate the molecular mass of the enzyme, the sample (20 µg) was applied to HPLC (Toyo Soda CO-8000 system; Tokyo, Japan) on a TSK G-3000SW column (0.75 x 60 cm; Toyo Soda, Japan), at a flow rate of 0.6 ml/min, with 0.1 M sodium phosphate buffer (pH 7.2) containing 0.1 M Na_2SO_4 at room temperature. The absorbance of the eluate was recorded at 280 nm. The molecular mass of the enzyme was then calculated from the relative mobility compared to those of the standard proteins, glutamate dehydrogenase (290 kDa), lactate dehydrogenase (140kDa), enolase (67 kDa), adenylate kinase (32 kDa) and cytochrome *c* (12.4 kDa) (products of Oriental

Yeast Co.). The purified amidase (1 mg in 1 mM potassium phosphate buffer, pH 7.5) was used directly for NH_2-terminal sequencing by automated Edman degradation with a Shimadzu protein sequencer PSQ-1 system equipped with a Wakosil phenylthiohydantoin column (4.6 x 250 mm; Wako Pure Chemical).

Substrate specificity

The standard reaction mixture (1 ml) was composed of 10 µmol potassium phoshate buffer (pH 7.5), 10 mmol amide and appropriate amount of the enzyme. The reaction proceeded at 30°C for 10-30 min, and was stopped by adding 0.1 ml 1 M HCl to the reaction mixture. The amount of NH_3 produced in the reaction mixture was colorimetrically estimated by the phenol/hypochlorite (61) method using a Conway micro-diffusion apparatus (62).

Stereoselectivity

The amounts of 2-phenylpropionic acid and 2-phenylpropionamide were assayed by HPLC under the same conditions as those used for the determination of benzoic acid with the exception that 205 nm instead of 230 nm was used as the detection wavelength. Diastereoisomeric amide derivatives of 2-phenylpropionic acid were determined at 254 nm. The configuration of 2-phenylpropionic acid was determined by a modificatioin of the method of Hutt et al. (63). The solution (0.2 ml) containing no more than 2 µmol 2-phenylpropionic acid was mixed with 0.1 ml 1 M HCl and 0.75 ml CH_2Cl_2. After shaking and brief centrifugation, the water phase was evacuated and the remaining CH_2Cl_2 portion was reacted for 2 h at room temperature in a freshly prepared mixture (1 ml) with the following composition : *S*-(-)-1-(1-naphthyl)-ethylamine, 0.5 mg/ml; 1-ethyl-3-(3-dimethylaminopropyl)-carbodiimide hydrochloride, 0.5 mg/ml; and 1-hydroxybenzotriazole anhydrous, 0.1 mg/ml. The sample was then dried in a rotary evaporator and resuspended in 0.2 ml of the above HPLC solvent. The retention times of the resultant diastereoisomeric amides of *S*-(+)- and *R*-(-)-2-phenylpropionic acids were 11.4 and 12.7 min, respectively.

Acyl transferase activity

The transferase activity was measured by estimating the amount of acylhydroxamate formed from hydroxylamine and an acyl donor. Amide, acid or ester was used as the acyl donor substrate. The standard reaction mixture (1 ml) was composed of 100 µmol potassium phosphate buffer (pH 7.5), 10 µmol of the acyl donor and 1 mmol hydroxylamine•HCl and an

appropriate amount of the enzyme. The reaction proceeded at 30°C for 10-30 min and was stopped by adding 2 ml of $FeCl_3$ (8%, mass/vol.) in HCl (2%, mass/vol.). The extinction was read at 500 nm with a Shimadzu UV-240 spectrophotometer and related to the amount of hydroxamate formed in the reaction by comparison with a standard curve.

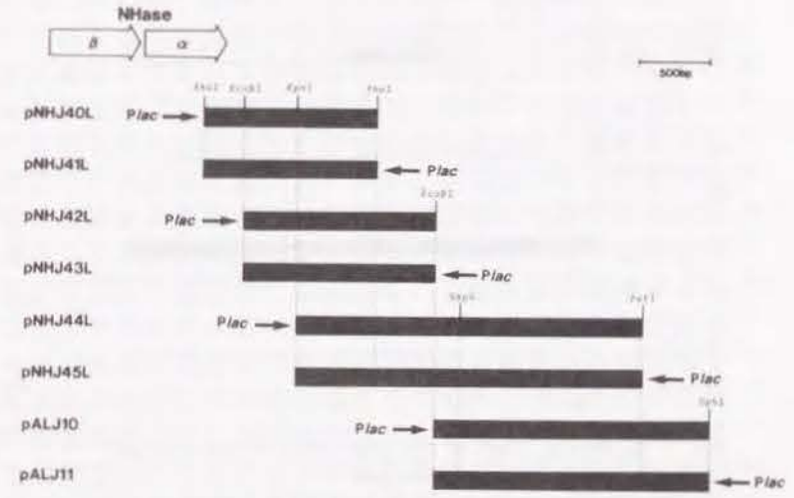

Fig. 1. Construction of a set of plasmids for subcloning of the amidase gene.
All of the restriction fragments were inserted at appropriate positions in pUC18/19.
The location and direction of the *lac* promoter are indicated.

RESULTS

Locating the amidase gene by subcloning the downstream region of the L-NHase gene

DNA fragments were prepared by digesting the cloned 9.4-kb insert of plasmid pNHJ20L (13) and inserted into pUC18 or pUC19 (Fig. 1). The ligated mixture was introduced by transformation into *E. coli* JM109 and ampicillin-resistant transformants were selected on 2 x YT agar medium containing 80 µg/ml ampicillin. These transformants were cultured and cell-free extracts were prepared as described in Materials and Methods. Enzyme assays using propionamide and benzamide as substrates for each cell-free extract showed that only the recombinant *E. coli* harboring pALJ10 had amidase activity and the transformants harboring the other plasmids had none. However, *E. coli* harboring pALJ10 and other subclones including pNHJ20L had no amidase activity in the presence of natural inducers (cobalt and cyclohexanecarboxamide) instead of IPTG. This finding suggested that a 1.96-kb *Eco*RI-*Sph*I

region located 1.9 kb downstream of *nhlA* encoding the L-NHase α-subunit was essential for the expression of amidase activity in the presence of IPTG.

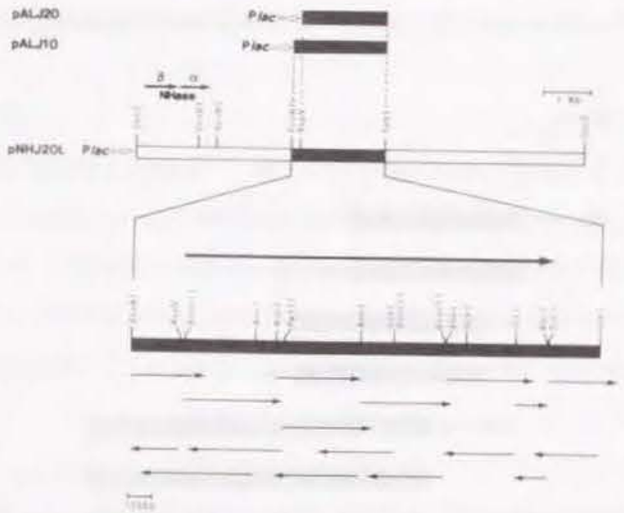

Fig. 2. Restriction maps of the insert DNA of pALJ10 and sequencing strategy of the amidase gene.
Plasmid pALJ10 contains a 1.96-kb *Eco*RI-*Sph*I fragment at the corresponding sites of pUC18. Plasmid pALJ20 contains a 1.76-kb *Nsp*V-*Sph*I fragment at the *Acc*I-*Sph*I sites of pUC18. Arrows indicate the direction and extent of sequence determination. The nucleotide sequence was determined between the *Eco*RI and *Sph*I sites. The upper arrow indicates the direction and length of structural gene of the amidase (*amdA*).

Nucleotide sequence of the amidase gene (*amdA*)

The sequencing strategy is shown in Fig. 2 and Fig. 3 shows the 1958-bp nucleotide sequence. The *Eco*RI-*Sph*I fragment of pALJ10 contained an open reading frame encoding 515 amino acids (*M*r = 54,626 Da) which started with ATG (methionine) and terminated with TAA. A typical Shine-Dalgarno sequence (64) was present 8 bp upstream from the initiation codon, but no consensus promoter sequences found in other prokaryotes (65) were observed in the upstream region. A strong hairpin structure (ΔG = -174 kJ/mol) just downstream of the termination codon of the open reading frame may serve as a ρ-independent transcriptional termination signal. The predicted amino acid sequence of the open reading frame was compared with those of amidases from *Rhodococcus* sp. N-774 (14), *P. chlororaphis* B23 (15), *Rhodococcus* sp. (42) and indole-3-acetamide hydrolase from *Pseudomomonas savastanoi* (66) (Fig. 4). There was a 60.6% match of amino acids in 513 overlapping residues

between *R. rhodochrous* J1 and *Rhodococcus* sp. N-774 whose nucleotide sequence was identical with that of *Brevibacterium* R312 (44).

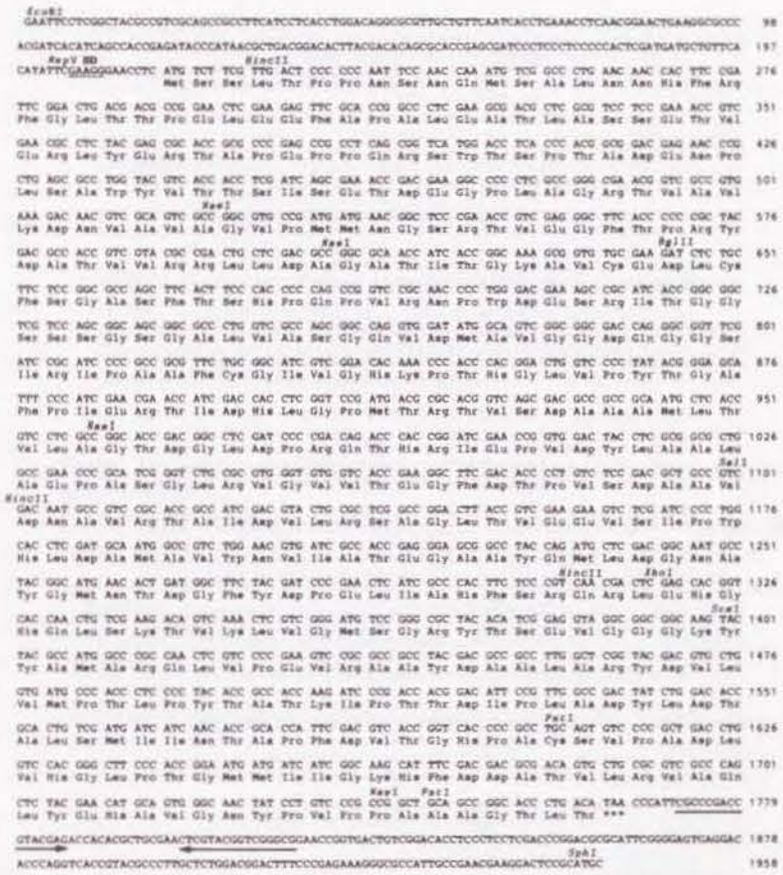

Fig. 3. Nucleotide and amino acid sequences of the amidase gene (*amdA*).
Potential ribosome-binding sequence are indicated by SD, and a relevant stop codon is indicated by asterisks. An inverted repeat sequence downstream from the amidase gene (*amdA*) is indicated by opposing arrows.

Production of the amidase protein in *E. coli*

To produce the amidase in *E. coli*, a 1.7-kb *Nsp*V-*Sph*I fragment was inserted between the *Acc*I and *Sph*I sites of pUC18, resulting in pALJ20 (Fig. 2). In this construction, the amidase gene (*amdA*)was under the control of the *lac* promoter. When *E. coli* harboring pALJ20 was cultivated in the presence of IPTG at 28°C or 37°C, amidase activity was detected in the supernatant of the sonicated cell-free extracts obtained at 12,000 x *g*. Culture condition of 12-h incubation at 28°C gave the highest activity [2.43 nmol•min^{-1}•(mg protein)$^{-1}$].

However, this amidase activity was even lower than that of *R. rhodochrous* J1 cultured in the presence of cyclohexanecarboxamide and cobalt [13.5 nmol•min^{-1}•(mg protein)$^{-1}$].

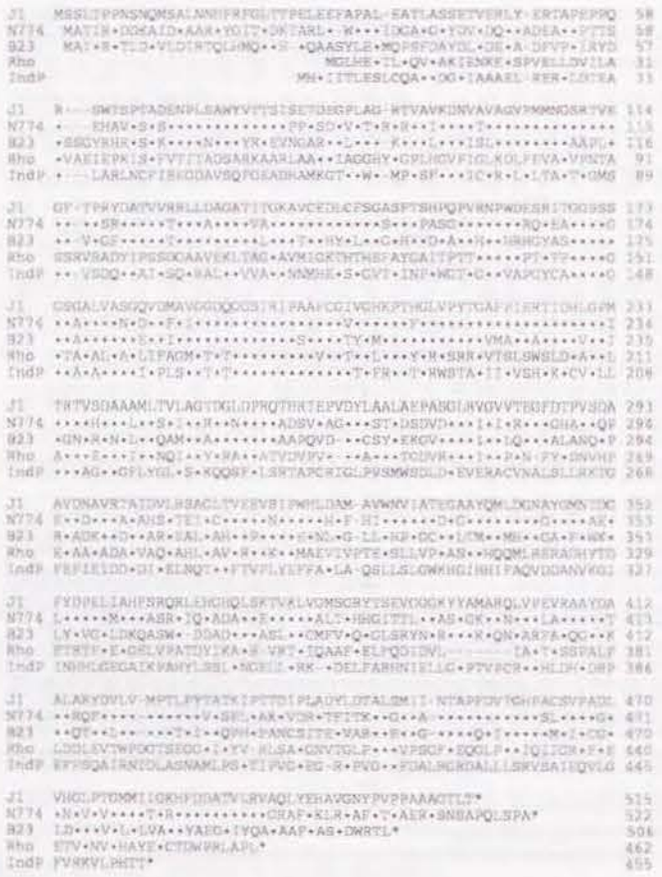

Fig. 4. Comparison of the deduced amino acid sequences of amidases from various strains.
Amino acid sequences of amidases from *R. rhodochrous* J1 (J1), *Rhodococcus* sp. N774 (N774), *P. chlororaphis* B23 (B23) and *Rhodococcus* sp. (Rho) and of indole-3-acetamide hydrolase from *P. savastanoi* (IndP) were aligned by introducing gaps (hyphens) to maximize identities. The dots indicate the presence of the same residue at each position.

To express the amidase gene at high level, we modified the sequence upstream of the ATG codon by means of PCR, using the recombinant plasmid as a template and the following two oligonucleotides as primers (Fig. 5). The sense primer contained a *Sac*I recognition site, a ribosome binding site, a TAG stop codon in frame with the *lac* gene in pUC18 and 18 nucleotides of the amidase structural gene starting with the ATG start codon 9 nucleotides downstream of the ribosome binding site. The antisense primer contained 21 nucleotides of the

gene (complementary to nucleotides 1824-1844 in Fig. 3) 61 nucleotides downstream from the end of the reading frame and a *Hin*dIII recognition site.

Sense primer

SD

5' GGGAGCTCTAAGGAGGAATAGCTCATGTCTTCGTTGACTCCC 3'

Sac I Stop Start

Antisense primer

5' AGGTAAGCTTCCGACAGTCAC 3'

*Hin*dIII

Fig. 5. Sequences of oligonucleotide primers for the expression of the amidase gene.
Each sequence of the oligonucleotide primers is shown in the 5' to 3' end direction. The expression plasmid was constructed as described under Results. SD, ribosome-binding site.

Table 1. Amidase activities of *E. coli* transformants harboring pALJ30 under various conditions.
E. coli JM109 carrying pALJ30 was cultivated in 2 x YT medium under various conditions. The inducer, IPTG, was added at a final concentration of 1 mM.

Time for addition of inducer (h)	Time for cultivation (h)	Cultivation temperature (°C)	Specific activity (nmol•min^{-1}•mg protein^{-1})
0	7	28	276
0	12	28	183
4	7	28	168
4	12	28	201
0	7	37	468
0	12	37	335
4	7	37	405
4	12	37	380

The PCR-product was inserted between the *Sac*I and *Hin*dIII sites of pUC18, resulting in plasmid pALJ30, in which the amidase gene was under the control of the *lac* promoter. A protein corresponding to the predicted molecular mass of 54.6 kDa was synthesized only when the *lac* promoter was induced by IPTG. When *E. coli* JM109 harboring pALJ30 was cultivated for 7 h at 37°C, during which IPTG was added 4 h from the start, the level of amidase activity in the supernatant of the sonicated cell-free extracts of the transformant was 468 nmol•min^{-1}•(mg protein)$^{-1}$ (Table 1), which was much higher than that of *E. coli* containing pALJ20. At this time, as judged by quantitation of the SDS-PAGE track (Fig. 6) with a dual-wavelength

TLC scanner (Shimadzu), the highest amount of amidase formed seemed to correspond to about 8% of the total soluble protein. When the transformant was cultivated at 37°C, a protein band corresponding to the amidase subunit was also observed in the precipitates of the sonicated cell-free extracts from the analysis of SDS-PAGE. The precipitates had no amidase activity, and so they may be inclusion bodies.

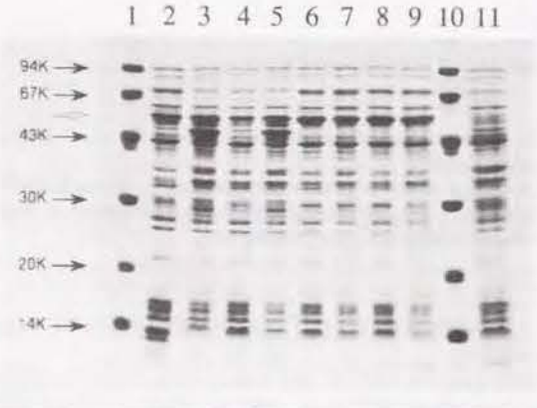

Fig. 6. SDS/PAGE of the supernatant prepared from *E. coli* containing pALJ30.
Lanes 1 and 10 were loaded with the following molecular mass standards: phosphorylase (94 kDa), bovine serum albumin (67 kDa), ovalbumin (43 kDa), carbonic anhydrase (30 kDa), soybean trypsin inhibitor (43 kDa), carbonic anhydrase (14 kDa). Lanes 2-9 and 11 show supernatants of sonicates (100 μg protein). Lane 2, *E. coli* JM109 containing pALJ30, sample taken after a 7 h incubation at 28°C with isopropyl thiogalactoside; lane 3, same as lane 2, but after a 12 h incubation; lane 4, same as lane 2, but after a 7 h incubation, during which isopropyl thiogalactoside was added 4 h from the start; lane 5, same as lane 4, but after a 12 h incubation; lane 6, same as lane 2, but after a 7 h incubation at 37°C; lane 7, same as lane 6, but after a 12 h incubation; lane 8, same as lane 6, but after a 7 h incubation, during which isopropyl thiogalactoside was added 4 h from the start; lane 9, same as lane 8, but after a 12 h incubation; lane 11, *E. coli* JM109 containing the vector plasmid pUC18, as a control. The open arrow indicates the band corresponding to the predicted molecular mass of the amidase.

Purification of the amidase from *E. coli* transformant

Through the purification procedures described in Materials and Methods, the enzyme was purified with a yield of 30.4% from the cell-free extract of *E. coli* containing pALJ30, which was cultured under the optimum conditions for amidase activity, with benzamide as the substrate (Table 2). The purified enzyme showed only one band on SDS-PAGE. The purity of the enzyme preparation was also proven by HPLC on a TSK G3000SW column, which

revealed a single symmetrical protein peak. The purified enzyme catalyzed the hydrolysis of benzamide to benzoic acid at 12.2 μmol•min^{-1}•(mg protein)$^{-1}$ under the standard reaction conditions.

Table 2. Purification of the amidase from the recombinant *E. coli* JM109/pALJ30.
The reaction proceeded under the standard conditions using benzamide as a substrate. One unit (U) of enzyme is the amount catalyzing the production of 1 μmol benzoic acid/min.

Step	Total protein	Total activity	Specific activity	Yield
	mg	U	U/mg	%
Cell-free extract	1410	756	0.536	100
DEAE-Sephacel	158	490	3.10	64.8
$(NH_4)_2SO_4$ (45-60%)	75.4	424	5.62	56.1
FPLC MonoQ HR5/5	29.6	307	10.4	40.6
FPLC Superose^{TM}12	18.9	230	12.2	30.4

Molecular mass and subunit structure

The molecular mass of the enzyme was determined to be 110 kDa by analytical HPLC. When the enzyme was treated with 1% (mass/vol.) SDS and 50 mM 2-mercaptoetanol, a single band was visualized by protein staining; the molecular mass corresponding to the band was estimated to be 55 kDa, consistent with that estimated from the nucleotide sequence. Thus, the enzyme probably consists of 2 subunits identical in molecular mass. The purified amidase from the recombinant *E. coli* had an NH_2-terminal sequence of Ser-Ser-Leu-Thr-Pro-Pro-Asn-Ser-Asn-Gln-Met-Ser-Ala-Leu-Asn-Asn-His-Phe-Arg-Phe. This is the same as that deduced from the DNA sequence with the exception that it lacks a N-terminal methionine.

Effect of temperature and pH

The activity was measured at various temperatures from 10 to 60°C and the optimum was found to be 55°C. Above 60°C, the enzyme activity was rapidly lost (Fig. 7-A). The effect of pH on the activity of the enzyme was examined using benzamide as the substrate (Fig. 7-B). The enzyme showed maximal activity at pH 7.9.

Stability

The enzyme was incubated for 30 min in 10 mM potassium phosphate buffer (pH 7.5) containing 0.5 mM dithiothreitol under various temperature conditions. Aliquots were removed and the amidase activity was assayed under the standard conditions. It exhibited the following

activity: 60°C, 0%; 55°C, 1.0%; 50°C, 2.7%; 45°C, 27%; 40°C, 48%; 35°C, 95%; 30°C, 100%; 25°C, 100%; 20°C, 100%. This enzyme was unstable at its optimal temperature (55°C). After the enzyme was incubated at 30°C for 20 min in buffers at various pH, an aliquot was assayed for amidase activity under the standard conditions. The enzyme was most stable in the broad pH range of 6.7-10.

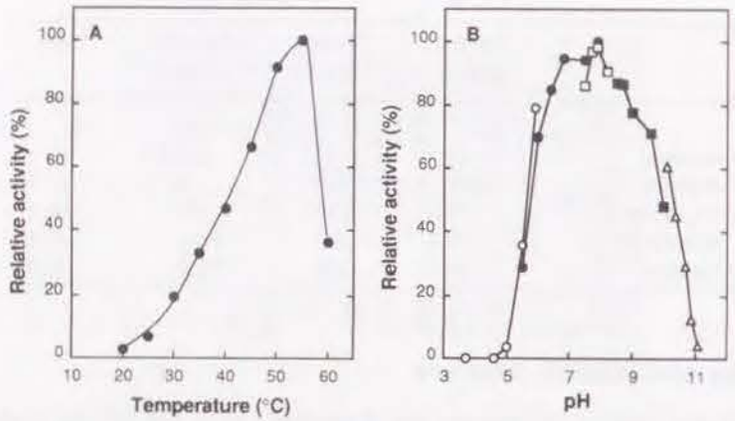

Fig. 7. Effects of temperature and pH on amidase activity.
(A) Reactions proceeded for 20 min at various temperatures. (B) Reactions proceeded for 20 min at 30 °C in the following buffers (final concentration, 0.1 M): acetate (○), potassium phosphate (●), Tris/HCl (□), borate (■) and glycine (△). The relative activity is expressed as a percentage of the maximum activity attained under the experimental conditions.

Inhibitors

The inhibitory effects of various compounds on the enzyme activity were investigated. Incubation proceeded at 30°C for 20 min in standard reaction mixtures containing test compounds at 1 mM. The enzyme was highly sensitive towards $HgCl_2$ and $AgNO_3$ (7 and 22%, respectively, of the original activity). Other metals such as $FeSO_4$, $CuSO_4$ and $CdCl_2$ were also inhibitory to some extent (58, 58 and 87%, respectively). The enzyme was inhibited by 5,5'-dithiobis(2-nitrobenzoic acid) and *p*-chloromercuribenzoic acid to some extent (71 and 64%, respectively), but other thiol reagents such as *N*-ethylmaleimide and iodoacetic acid had no significant effect. Phenylhydrazine caused appreciable inhibition (64%), but other carbonyl reagents such as cysteamine, DL-penicillamine, D-cycloserine and semicarbazide did not influence the activity. Chelating reagents including EDTA, 1,2-dihydroxybenzene-3,5-disulfonic acid disodium salt, *o*-phenanthroline, 8-hydroxyquinoline and α,α'-dipyridyl also had no significant effect on the enzyme.

Substrate specificity

The ability of the enzyme to catalyze the hydrolysis of various amide compounds was examined (Table 3). The synthesis of benzoic acid from benzamide, corresponding to 12.2 $\mu mol.min^{-1}\cdot(mg\ protein)^{-1}$, was taken as 100%. Aliphatic amides such as propionamide, butyramide, isobutyramide, valeramide and capronamide were remarkably active as substrates. Aromatic amides such as benzamide, nicotinamide, 2-thiophenecarboxamide, *m*- or *p*-toluamide and 2-aminobenzamide were also hydrolyzed by the enzyme. When the Michaelis constants for benzamide and propionamide were estimated from Lineweaver-Burk plots, the former (*K*m = 0.15 mM) was found to exhibit somewhat higher affinity for the enzyme than did the latter (*K*m = 0.48 mM). Amino acids containing an amide group such as glutamine and asparagine were inactive as substrates, whereas L-methioninamide was a good substrate.

Table 3. Substrate specificity of the amidase.
The reaction proceeded as described under Materials and methods. The synthesis of benzoic acid from benzamide, corresponding to 12.2 $\mu mol\cdot min^{-1}\cdot mg\ protein^{-1}$, was taken as 100%.

Substrate	Relative activity (%)	Substrate	Relative activity (%)
Benzamide	100	*o*-Hydroxybenzamide	2.6
Formamide	0	*p*-Hydroxybenzamide	14.4
Acetamide	23.8	Nicotinamide	55.9
Propionamide	236	Isonicotinamide	8.0
Butyramide	288	Pyrazinamide	11.8
Isobutyramide	606	2-Thiophenecarboxamide	54.2
Valeramide	519	2-Phenylacetamide	82.8
Pivalamide	90.8	3-Indoleacetamide	23.3
Hexanamide	241	Urea	0
Acrylamide	40.6	Methylurea	25.9
Methacrylamide	112	Ethylurea	81.8
Crotonamide	19.6	Phenylurea	17.2
Cyclohexanecarboxamide	61.3	L-Glutamine	0
Fluoroacetamide	0	D-Glutamine	0
Chloroacetamide	96.2	L-Asparagine	0
Lactamide	83.7	D-Asparagine	0
Malonamide	14.4	Glycinamide	8.5
Succinamide	0	L-Serinamide	5.2
Fumaramide	2.6	DL-Phenylalaninamide	11.8
Adipamide	9.0	L-Threoninamide	28.1
o-Toluamide	3.5	L-Isoleucinamide	0
m-Toluamide	104	L-Methioninamide	189
p-Toluamide	160	L-Tryptophanamide	23.8
o-Aminobenzamide	17.9	L-Lysinamide	0
m-Aminobenzamide	108	L-Argininamide	0
p-Aminobenzamide	15.3		

Stereoselectivity

The ability of the enzyme to hydrolyze racemic amides to optically active acids was investigated. The optical purity of 2-phenylpropionic acid converted from (+/-) 2-phenylpropionamide by the amidase was determined as described in Materials and Methods.

Figure 8 shows the enantioselective hydrolysis of 2-phenylpropionamide to 2-phenylpropionic acid. Until 40 min from the start of the reaction, the *S*-enantiomer was selectively formed (enantiomer excess >95). This amidase appeared to be highly specific for the *S*-enantiomer of 2-phenylpropionamide. Enantioselectivity of the enzyme for 2-chloropropionamide was examined in the same way as used for 2-phenylpropionamide. *R*-(+)- and *S*-(-)-2-Chloropropionamides were converted to (+)- and (-)-2-chloropropionic acids at the same rate in the reaction time, suggesting that the enzyme cannot recognize the configuration of 2-chloropropionamide. Steric hindrance of the enzyme by the chlorine atom of the substrate was less effective upon the stereoselectivity than that by the phenyl group.

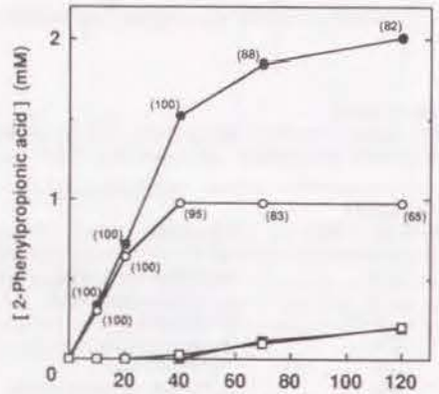

Fig. 8. Enantioselective hydrolysis of 2-phenylpropionamide to 2-phenylpropionic acid. The assay is described in detail under Materials and Methods. (●) The *S*-enantiomer produced from the substrate at the substrate concentration of 4 mM; (■) the *R*-enantiomer produced from the substrate at the substrate concentration of 4 mM; (○) the *S*-enantiomer produced from the substrate at the substrate concentration of 2 mM; (□) the *R*-enantiomer produced from the substrate at the substrate concentration of 2 mM. Numbers in parentheses indicate the optical purity [(*S*-*R*)/(*S*+*R*)x100] of the acid produced.

Acyl transferase activity

The relative activities of the transferase reactions (amide transferase, acid transferase and ester transferase) catalyzed by the amidase were determined. Only amide transferase activity was observed, whereas acid transferase and ester transferase activities were below the detection limits. Compared with that towards benzamide (100%), the activity towards propionamide was 145%. Other amides, namely acetamide (64%), butyramide (734%), isobutyramide (544%), valeramide (943%), acrylamide (542%), crotonamide (139%), nicotinamide (20%), isonicotinamide (26%) and pyrazinamide (39%) functioned as acyl-donors. The substrate spectrum of the amides as acyl donors was in close agreement with the finding of substrate

specificity of the amidase, except that transferase activity using unsaturated aliphatic amides such as acrylamide and crotonamide as a substrate was relatively high.

DISCUSSION

In this section, the author describe the purification and characterization of the protein derived from the cloned amidase gene (*amdA*) linked to the L-NHase gene (*nhlBA*) in a "practical microorganism" *R. rhodochrous* J1, which produces two NHases (H-NHase and L-NHase) depending on the inducer. These NHases differ in substrate specificity: H-NHase preferentially acts on aliphatic nitriles, while L-NHase acts on aromatic nitriles as well as aliphatic nitriles as substrates. Under the conditions in which H-NHase is induced by urea, *R. rhodochrous* J1 cells cannot hydrolyze benzamide as a substrate. On the other hand, under the conditions in which L-NHase is induced by cyclohexanecarboxamide, the cells can hydrolyze benzamide as well as propionamide as a substrate (67). Furthermore, this purified amidase can hydrolyze aromatic amides as well as aliphatic amides as shown in Table 3. The L-NHase and this amidase showed similar trend in substrate specificity for aliphatic and aromatic compounds: for example, L-NHase acts on propionitrile (100%), benzonitrile (75%) and 3-cyanopyridine (50%), while this amidase acts on propionamide (100%), benzamide (42.4%) and nicotinamide (23.7%). These findings suggest that amidase activity derived from the present amidase gene was detected along with L-NHase activity; both enzymes seemed to be induced by the same inducer and cooperate in degrading several nitriles efficiently.

The author found *amdA* 1.9 kb downstream of *nhlA*. This is the first demonstration that an amidase gene involved in nitrile metabolism locates downstream from the NHase gene. In *Rhodococcus* sp. N-774 (14) and another (42) and *P. chlororaphis* B23 (15), each amidase gene is found in the same orientation and just upstream from the genes coding for α- and β-subunits of each NHase. There are two patterns in gene order of nitrile hydratase subunits. In *Rhodococcus* sp. N-774 and *P. chlororaphis* B23, the order is amidase-NHase(α-β), whereas the order is amidase-NHase(β-α) in *Rhodococcus* sp. In this way, gene construction of the nitrile metabolism operon is variously organized. In order to examine the possibility that another amidase gene may be located upstream from *nhlBA*, cloning of the upstream region of *nhlBA* by a gene walking method is now in progress. In *P. chlororaphis* B23, two open reading frames (P47K and OrfE) are present just downstream of the NHase β-subunit gene. The additional sequence of a 38 kDa protein, which is expressed in *E. coli* transformant

harboring NHase-amidase expression plasmid (pPCN4), is also found just upstream of the amidase gene (15). Although nitrile metabolism appears to be simple in the two step reaction of NHase and amidase, other open reading frames such as P38K, P47K and OrfE also might have some functions in the nitrile degradation pathway in *P. chlororaphis* B23. The region between *nhlBA* and *amdA* is of about 1.9 kb long enough to contain one or more open reading frames, which may be involved in nitrile metabolism or control of the expression of L-NHase or amidase. Further analysis of this region is needed for the interpretation of the L-NHase-amidase operon.

Pseudomonas aeruginosa amidase can hydrolyze formamide, acetamide propionamide, hydroxyacetamide and acrylamide but cannot hydrolyze butyramide, isobutyramide, valeramide and lactamide (39). The *Arthrobacter* amidase can act on acetamide, acrylamide and propionamide but cannot hydrolyze formamide, butyramide, valeramide, isobutyramide, methacrylamide, malonamide, succinamide, lactamide, benzamide and nicotinamide (68). The *Brevibacterium* sp. R312 wide spectrum amidase can degrade all the amides mentioned above, but the activities for butyramide, isobutyramide, valeramide and benzamide are very low (69). On the other hand, the *R. rhodochrous* J1 amidase had a wider substrate specificity. Thus, the *R. rhodochrous* J1 amidase is distinct from the above-mentioned enzymes. Furthermore, the *R. rhodochrous* J1 amidase showed enantiomer-selectivity toward 2-phenylpropionamide as the substrate. Purification and characterization of enantiomer-selective amidases from *Brevibacterium* sp. R312 (44) and *Rhodococcus* sp. (42) and cloning of their genes has been reported. Each amidase from these strains is also genetically coupled with each nitrile hydratase, indicating that the enantioselectivity is probably a common feature among the amidases linked with the NHases. However, H- and L-NHases cannot act upon various nitriles enantioselectively (unpublished results). Yamamoto *et al.* (70) reported the production of *S*-(+)-2-(4'-isobutylphenyl)propionic acid [*S*-(+)-ibuprofen], which is useful as a non-steroidal anti-inflammatry drug, from racemic 2-(4'-isobutylphenyl)propionitrile by *Acinetobacter* sp. AK226 nitrilase. Similar reactions can proceed by using a NHase followed by an enantio-selective amidase. The recombinant amidase from *R. rhodochrous* J1 might be useful in the production of higher-value acids from the corresponding nitriles or amides in cooperation with a NHase.

Amidases coupled with NHase have been studied at the gene level in *Rhodococcus* species including N-774, *P. chlororaphis* B23, *Brevibacterium* sp. R312 but their activities regarding transfer of the acylgroup from amides to hydroxylamine have not been mentioned.

The present amidase demonstrated acyl transferase activity as efficient as that of amidases, which are considered not to be involved in nitrile metabolism, such as the wide spectrum amidase from *Brevibacterium* sp. R312 (69) and the aliphatic amidase from *P. aeruginosa* (39).

Under the optimum culture conditions for acrylamide production, *R. rhodochrous* J1 produces a large amount of H-NHase (50% of the total soluble protein) in cell-free extracts whereas amidase activity is very low. Judging from the sequential nitrile degradation by NHase and amidase, and the gene construction of both enzymes from *Rhodococcus* species including N-774, *P. chlororaphis* B23 and here, we consider that *R. rhodochrous* J1 has an amidase, which is induced together with H-NHase by cobalt ions and urea. The amidase gene linked to the H-NHase gene is now being studied.

SUMMARY

The cloned 9.4-kb insert of plasmid pNHJ20L containing low-molecular-mass nitrile hydratase (L-NHase) gene from *Rhodococcus rhodochrous* J1 was digested with various restriction enzymes, and the trimmed fragments were inserted into pUC18 or pUC19. A 1.96-kb *Eco*RI-*Sph*I region located 1.9-kb downstream of the L-NHase gene was found to be essential for the expression of amidase activity in *Escherichia coli*; the gene arrangement of the amidase and the NHase in *R. rhodochrous* J1 differed from those in *Rhodococcus* species including N-774, *Pseudomonas chlororaphis* B23. The nucleotide-determined sequence indicated that the amidase consists of 515 amino acids (54,626 Da) and the deduced amino acid sequence of the amidase had high similarity to those of amidases from *Rhodococcus* species including N-774 and *P. chlororaphis* B23 and to indole-3-acetamide hydrolase from *Pseudomonas savastanoi*.

The amidase gene (*amdA*) modified in the nucleotide sequence upstream from its start codon expressed 8% of the total soluble protein in *E. coli* under the control of *lac* promoter. The level of amidase activity in cell-free extracts of *E. coli* was 0.468 units/mg using benzamide as a substrate. This amidase was purified to homogeneity from extracts of the *E. coli* transformant with 30.4% overall recovery. The molecular mass of the enzyme estimated by HPLC was about 110 kDa, and the enzyme consists of two subunits identical in molecular mass (55 kDa). The enzyme acted upon aliphatic amides such as propionamide and also upon aromatic amides such as benzamide. The apparent *K*m values for propionamide and benzamide were 0.48 and 0.15 mM, respectively. This amidase was highly specific for the *S*-enantiomer

of 2-phenylpropionamide, but could not recognize the configuration of 2-chloropropionamide. It also catalyzed the transfer of an acyl group from an amide to hydroxylamine to produce the corresponding hydroxamate.

Section 3 Regulatory genes required for the amide-dependent induction of L-NHase[e]

In microorganisms that catabolyze nitriles by NHase, this enzyme, if inducible, is generally induced by amides (reaction products), not by nitriles (reaction substrates): an interesting unique phenomenon (10). *Rhodococcus rhodochrous* J1 produces two kinds of NHases: high and low molecular-mass NHases (H-NHase and L-NHase), which exhibit different physicochemical properties and substrate specificities; both H- and L-NHases are composed of α- and β-subunits (α differs in size from β in each case, and the α- and β-subunits of H-NHase differ from those of L-NHase). When this strain is cultured in a medium containing urea and cyclohexanecarboxamide in the presence of cobalt ions, H-NHase and L-NHase are selectively induced, respectively (10). Using immobilized cells containing H-NHase, the industrial production of acrylamide from acrylonitrile was started in 1991 (30,000 tons/year); this is the first case in which biotechnology was applied in the petrochemical industry and also the first successful example of the introduction of an industrial bioconversion process for the manufacture of a commodity chemical. Furthermore, the industrial production of a vitamin nicotinamide from 3-cyanopyridine using cells containing L-NHase, which is induced by crotonamide, is due to start in Europe in 1997. Both H- and L-NHases contain cobalt ions as a cofactor in contrast with ferric-NHases from *Rhodococcus* sp. N-774 (10) and *Pseudomonas chlororaphis* B23 (71), which had been used for the acrylamide manufacture as 1st- and 2nd-generation strains, respectively.

Both H- and L-NHase genes (*nhhBA* and *nhlBA*) were cloned from *R. rhodochrous* J1 and sequenced (13). In each of *nhhBA* and *nhlBA*, an open reading frame (ORF) for the β-subunit (*nhhB* and *nhlB*) is located just upstream of that for the α-subunit (*nhhA* and nhlA). These arrangements of the coding sequences are reverse of the order found in the NHase genes of *Rhodococcus* sp. N-774 (13), *P. chlororaphis* B23 (15) and *Rhodococcus erythropolis* JCM6823 (43). In *R. rhodochrous* J1, The author has found an amidase gene (*amdA*) 1.9-kb downstream of *nhlA* (72); however, in *Rhodococcus* sp. N-774 (14), P. *chlororaphis* B23 (15), *Brevibacterium* sp. R312 (44) and *Rhodococcus* sp. (42), each amidase gene is found just upstream from the genes coding for α-subunit of each NHase. In this manner, construction of the genes responsible for nitrile metabolism is variously organized, suggesting that gene rearrangement had occurred in the genomes of these microorganisms.

Research into the regulatory system of *Rhodococcus* species has recently started by use of a transformation system with a *Rhodococcus-E. coli* shuttle vector (31). In the *nhhBA* gene cluster, The author has found two ORFs (*nhhC* and *nhhD*), which play a positive regulatory role in the process of the H-NHase formation (73). NhhC shares a homology with AmiC, a regulator protein for an aliphatic amidase gene (*amiE*) from *Pseudomonas aeruginosa* (33) and NhhD has similarity to possible repressors MarR (34) and HpcR (35) from *E. coli*. However, the H-NHase gene cluster does not contain an amidase gene. There are no reports on the relationship between NHase and amidase from a standpoint of the gene-regulation mechanism.

In this section, genes required for the amide-dependent induction of *nhlBA* have been identified by using the transformation system in *Rhodococcus*. The author has also shown the coregulation of *nhlBA* and *amdA* in the experiment using various deletion-mutants.

MATERIALS AND METHODS

Strains and plasmids

R. rhodochrous J1 was previously isolated from soil (29). *E. coli* JM109 was the host for pUC plasmid transformation and phage M13 mp18/19 propagation (30). *R. rhodochrous* ATCC12674 was the host for a *Rhodococcus-E. coli* shuttle vector plasmid pK4 (31) and its derivatives, and used for *nhlBA* expression. The plasmid pNHJ20L (13) carrying *nhlBA* of *R. rhodochrous* J1 in the 9.4-kb *Sac*I fragment on pUC19 was used for subcloning and sequencing of genes.

Enzymes and chemicals

Restriction endonuclease, T4 DNA ligase and *E. coli* alkaline phosphatase were purchased from Takara Shuzo Co, Ltd. (Kyoto, Japan) or Toyobo Co. Ltd. (Osaka, Japan). [γ-^{32}P]ATP (180 TBq/mmol) and [α-^{32}P]dCTP (110 TBq/mmol) were from Amersham (Tokyo, Japan). All other chemicals used were from commercial sources and were of reagent-grade.

DNA manipulation

Total DNA of *R. rhodochrous* J1 was prepared as described previously (13). Plasmid DNA was routinely prepared by the alkali lysis method (30) and, if necessary, was purified by ethidium bromide-cesium chloride centrifugation. DNA manipulation was performed

essentially as described by Sambrook et al. (30). The DNA sequence was determined by the dideoxynucleotide chain termination method (58). [α-^{32}P]dCTP and Sequenase (United States Biochemicals, Cleveland, USA) or [γ-^{32}P]ATP and a *Tth* Sequence kit (Toyobo) were used for sequencing.

Transformation of *R. rhodochrous* ATCC12674 by electroporation

A mid-exponential culture of *R. rhodochrous* ATCC12674 was centrifuged at 6,500 x *g* for 10 min at 4°C and washed three times with demineralized cold water. Cells were then concentrated 20-fold in the demineralized cold water and kept on ice. Ice-cold cells (100 µl) was mixed with 1 µg DNA in 1 µl of TE buffer (10 mM-Tris/1 mM EDTA, pH 8.0) in a 1-mm-gapped electrocuvette (Bio-Rad, Richmond, USA), and subjected to a 2.0 kV electric pulse from a Gene Pulser (Bio-Rad) connected to a pulse controller (25 µF capacitor; external resistance, 400Ω). Pulsed cells were diluted immediately with 1 ml of MYP medium (31) and incubated for 2 h at 26°C. They were then spread on MYP medium containing 75 µg kanamycin ml^{-1}.

Preparation of cell extracts and enzyme assay

R. rhodochrous ATCC12674 transformants were grown at 28°C for 24 h in MYP medium containing 0.01% (w/v) $CoCl_2 \cdot 6H_2O$ with (2 g/l) or without crotonamide at several concentrations, harvested by centrifugation at 4,000 x *g* at 4°C, and washed twice with 0.15 M NaCl. The washed cells were suspended in 0.1 M HEPES/KOH buffer (pH 7.2) containing 44 mM *n*-butyric acid, disrupted by sonication for 20 min (19 kHz, Insonator model 201M; Kubota, Tokyo, Japan), and centrifuged at 12,000 x *g* for 10 min at 4°C. The resulting supernatants were used for the enzyme assay. NHase activity was assayed in a reaction mixture (2 ml) containing 50 mM potassium phosphate buffer (pH 7.0), 6 mM benzonitrile and an appropriate amount of the enzyme. The reaction was carried out at 20°C for 10 min and stopped by the addition of 0.2 ml 1 M HCl. The amount of benzamide formed in the reaction mixture was determined as described previously (13). Amidase activity was assayed in a reaction mixture (1 ml) consisting of 10 mM potassium phosphate buffer (pH 7.5), 10 mM benzamide and an appropriate amount of the enzyme. The reaction was carried out at 30°C for 30 min and stopped by the addition of 0.1 ml 1 M HCl. The amount of benzoic acid formed in the reaction mixture was determined as described previously (72). One unit of these enzymes was defined as the amount catalyzing the formation of 1 µmol of benzamide and benzoic

acid/min from benzonitrile and benzamide, respectively, under the above conditions. Protein was determined by the Coomassie brilliant blue G-250 dye-binding method of Bradford (59) using a dye reagent supplied by Bio-Rad.

Western blot analysis

The anti-(L-NHase) antiserum and the anti-(amidase) antiserum were raised in young white female rabbits immunized with the L-NHase purified from *R. rhodochrous* J1 (unpublished results) and the amidase purified from *E. coli* JM109/pALJ30 (72), respectively. Cell extracts prepared by sonication were applied onto SDS-polyacrylamide gel, and transferred to a nitrocellulose membrane by a standard procedure (30). Western blots were probed with anti-(L-NHase) antiserum or anti-(amidase) antiserum and then with anti-rabbit IgG conjugated to horseradish peroxidase. Probing with antibodies and color development were carried out as described by the supplier, Bio-rad.

Computer analysis of amino acid sequences

The DNA sequence was analyzed using the GENETYX sequence analysis program (Software Development Co., Tokyo, Japan). A search of the National Biomedical Research Foundation (NBRF) protein sequence data bank for sequence similarities was carried out with the BLAST algorithm.

RESULTS

Cloning of the 5' upstream region of *nhlBA*

The cloning and characterization of the L-NHase gene (*nhlBA*) of Actinomycete *R. rhodochrous* J1 has previously been described (13). The author cloned the upstream region of *nhlBA* by the DNA-probing method with a 1.35-kb fragment, which was isolated from pNHJ20L digested by *Sac*I plus *Eco*RI, as a probe (Fig. 1). Southern hybridization using this probe against total DNA from *R. rhodochrous* J1 digested with *Eco*RI revealed that this probe hybridized with a single 7.5-kb fragment (data not shown). This DNA fragment was separated by agarose gel electrophoresis, ligated with pUC18 digested with *Eco*RI, and introduced into *E. coli* JM109 by transformation. Colony hybridization with the probe for screening ampicillin-resistant transformants containing the restriction fragment yielded pNLU10 (Fig. 1). This plasmid pNLU10 contained the 7.5-kb fragment derived from *R. rhodochrous* J1 DNA.

Analyses by restriction endonuclease and by sequencing of the fragment showed that two inserts from pNLU10 and pNHJ20L shared a common 1.35-kb *Sac*I-*Eco*RI region. Plasmid pNLUD30 was constructed by inserting a 6.15-kb *Eco*RI-*Sac*I fragment from pNLU10 and a 9.4-kb *Sac*I fragment from pNHJ20L into the *Eco*RI-*Sac*I sites of pBluescriptSK$^+$ (Toyobo).

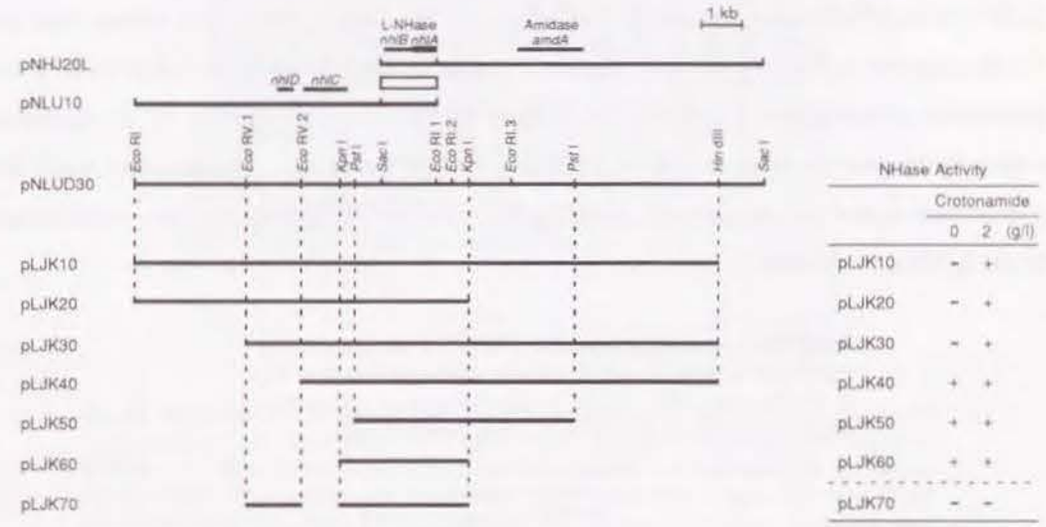

Fig. 1. Genetic organization of the L-NHase gene cluster and construction of a set of plasmids (left panel) and NHase activity of each *R. rhodochrous* ATCC12674 transformant (right panel).
(Left panel) For clarity, only restriction sites discussed in the text are shown. *nhlB* and *nhlA* encode L-NHase β- and α- subunit proteins, respectively (13), and *amdA* encodes an amidase (72). *nhlD* and *nhlC* are the newly identified genes described in this section. The probe used in the experiment are shown by box. Various deletion-plasmids are diagramed below the restriction maps. (Right panel) NHase activity of whole cells, which were cultivated in the medium with (2 g/l) or without crotonamide, was detected as described in Materials and Methods using benzonitrile as a substrate. +, much; -, trace.

Expression of *nhlBA* in *R. rhodochrous* ATCC12674

To identify the sequence elements required for the amide-dependent expression of *nhlBA*, we constructed a set of plasmids (pLJK10~pLJK60) (Fig. 1). Plasmids pLJK10, pLJK30 and pLJK40 contained blunt-ended 15.55-kb, 12.8-kb and 11.3-kb fragments, respectively, from pNLUD30, in the blunt-ended *Eco*RI site of the *Rhodococcus-E. coli* shuttle vector pK4. Plasmids pLJK20 and pLJK60 were constructed by inserting 8.3-kb and 3.1-kb *Kpn*I fragments, respectively, from pNLUD30 into the *Kpn*I site of pK4. Plasmid pLJK50 contained a 5.5-kb *Pst*I fragment from pNLUD30 in the *Pst*I site of pK4. These plasmids were used to transform *R. rhodochrous* ATCC12674 and the resulting transformants were cultured in the $CoCl_2$-containing medium in the presence or absence of crotonamide. In this experiment, *nhlBA* expression was induced by crotonamide, which induces a greater amount of L-NHase

than cyclohexanecarboxamide in *R. rhodochrous* J1 (unpublished data). NHase assays using benzonitrile as a substrate for each cell suspension (Fig. 1) or cell-free extract (Table 1) revealed that, in addition to *nhlBA* themselves, at least a 3.5-kb upstream region (from the 5' end terminus of *nhlB* to *Eco*RV.1 site) is required for the amide-inducible expression of *nhlBA*. On the contrary, transformants harboring plasmids pLJK40, pLJK50 and pLJK60 lacking the *Eco*RV.1-*Eco*RV.2 region, the *Eco*RV.1-*Pst*I region and the *Eco*RV.1-*Kpn*I region from the 3.5-kb upstream region, respectively, showed constitutive *nhlBA* expression irrespective of the addition of crotonamide. These findings suggest the regulatory role of the 3.5-kb upstream region in the process of the amide-dependent L-NHase formation. On the other hand, the downstream region containing *amdA* encoding the amidase (72) appeared to have no influence on the L-NHase induction.

Table 1. NHase activity in cell-free extracts of *R. rhodochrous* ATCC12674 transformants containing various plasmids. *R. rhodochrous* ATCC12674 transformants were cultured in the medium with (+) or without (-) crotonamide (2 g/l).

	NHase activity (U/mg)	
	Crotonamide	
	-	+
pK4	N.D.	N.D.
pLJK10	0.160	8.82
pLJK20	0.320	27.5
pLJK30	0.236	4.12
pLJK40	28.9	17.1
pLJK50	40.3	49.3
pLJK60	28.0	25.1

N.D. : Not detected

The L-NHase formation in *R. rhodochrous* ATCC12674 transformants was examined by SDS-PAGE and Western blot analysis (Fig. 2). Immunostaining of the Western blots in this experiment showed two bands of 29 and 26 kDa corresponding to the accumulated protein detected by Coomassie brilliant blue staining. No immunoreacting bands were detected in the *R. rhodochrous* ATCC12674 transformant carrying pK4 without any inserts, even though the transformant was cultured in the medium supplemented with crotonamide. Expression of NHase activity shown above was dependent on the addition of cobalt ions into the medium, because *R. rhodochrous* ATCC12674 transformants cultured in the medium without cobalt ions had no NHase activity (data not shown). Moreover, none of the *E. coli* JM109 harboring pK4-

derivative plasmids used in this experiment gave NHase activity, even when these transformants were cultured in the medium supplemented with $CoCl_2$ and crotonamide.

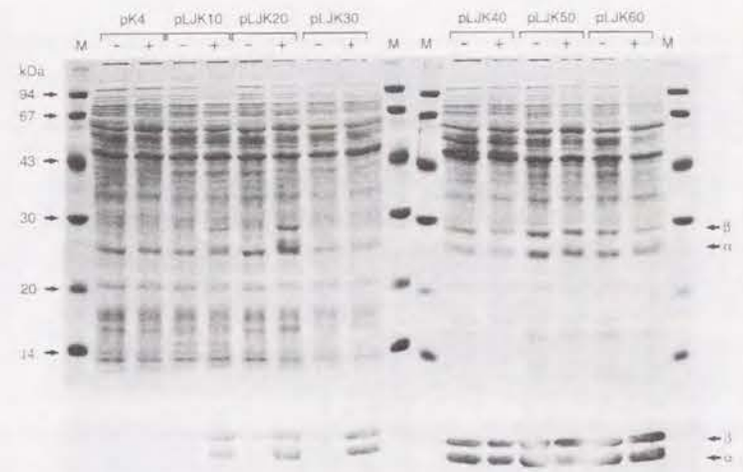

Fig. 2. Expression of L-NHase α- and β-subunit proteins in *R. rhodochrous* ATCC12674. (Upper panel) Coomassie brilliant blue-stained gel showing electrophoretically separated proteins. *R. rhodochrous* ATCC12674 was transformed with pK4 and pK4-derivatives and cultured in the medium with (+) or without (-) crotonamide (2 g/l). The extra bands corresponding to the α- and β-subunit proteins are indicated by arrows. Lanes indicated by 'M' were loaded with the following molecular mass standards: phosphorylase (94 kDa), bovine serum albumin (67 kDa), ovalbumin (43 kDa), carbonic anhydrase (30 kDa), soybean trypsin inhibitor (20 kDa) and a-lactalbumin (14 kDa). (Lower panel) Western blot of a similar gel after immunostaining with antibodies specific for the *R. rhodochrous* J1 L-NHase.

Primary structure of the upstream region of *nhlB*

The *Sac*I-*Eco*RI 1.73-kb fragment containing *nhlBA* was sequenced previously (13). The nucleotide sequence of the *Eco*RV.1-*Sac*I region described above were determined. Fig. 3 depicts the nucleotide and amino acid sequences of two ORFs (*nhlC* and *nhlD*) newly found in the region. The presumptive ATG start codon was found for *nhlC*, but the far less frequent initiation codon TTG was found for *nhlD*. *nhlC* and *nhlD* were preceded by Shine-Dalgarno sequences located within reasonable distances from the presumptive start sites (Fig. 3).

The first ORF named *nhlC* is 1071 nucleotides long, and would encode a protein of 357 amino acids. *nhlC* showed a significant similarity of amino acid sequence with regulatory genes of *nhhC* from *R. rhodochrous* J1 (73) (32.5% identity, 55.4% similarity) and *amiC* from *Pseudomonas aeruginosa* (33) (20.2% identity, 41.0% similarity) (Fig. 4-A, Fig. 6). The AmiC protein (40) is structurally similar to the members of the periplasmic binding protein

family, for example, BraC from *P. aeruginosa* (74). NhlC also showed a relatively weak match with BraC (17.2% identity, 43.3% similarity) (Fig. 4-A).

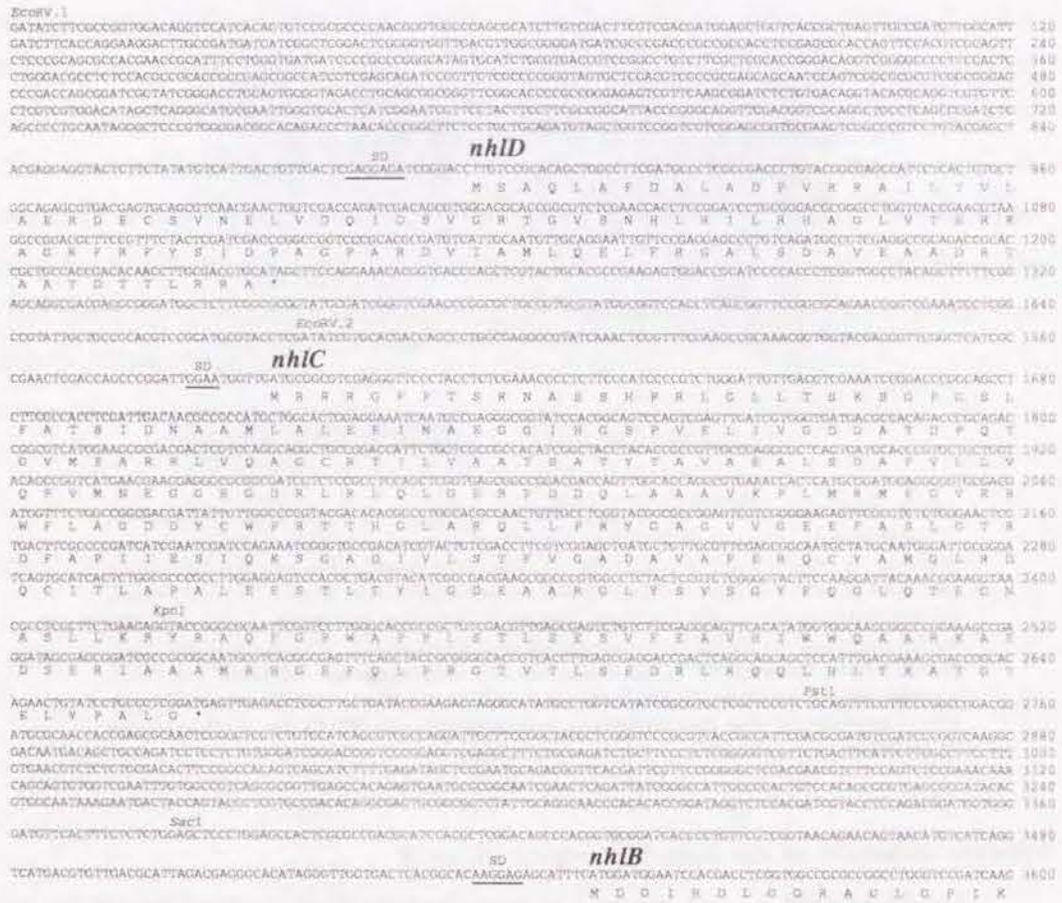

Fig. 3. Nucleotide sequences and the deduced amino acid sequences for *nhlC* and *nhlD*.
The deduced amino acid sequences of the ORFs are shown below the nucleotide sequence in the one-letter code. Potential ribosome-binding sequences are marked as SDs and relevant stop codons are indicated by asterisks. The sequence is numbered from the *Eco*RV.1 site upstream of *nhlD* (Fig. 1).

The second ORF named *nhlD*, is 336 nucleotides long, and would encode a protein of 112 amino acids. A computer-aided FASTA search of the SwissProt protein data base indicated that *nhlD* showed similarity to regulatory genes, *merR* from *Streptomyces lividans* (75) (24.8% identity, 44.8% similarity), *cadC* from *Staphylococcus aureus* (76) (24.7% identity, 43.0% similarity) and *arsR* from *E. coli* (77) (24.3% identity, 45.9% similarity). These genes homologous to *nhlD* are all located upstream of the heavy metal resistance genes (*merAB*, *cadA* and *arsBC*, respectively) and are supposed to have transcriptional regulatory functions for the resistance genes. Although the identity between NhlD (the product of *nhlD*)

and these homologs is relatively low, they are of similar size (112-125 amino acid residues) and 11 consensus amino acid residues are distributed all over the sequence (Fig. 4-B).

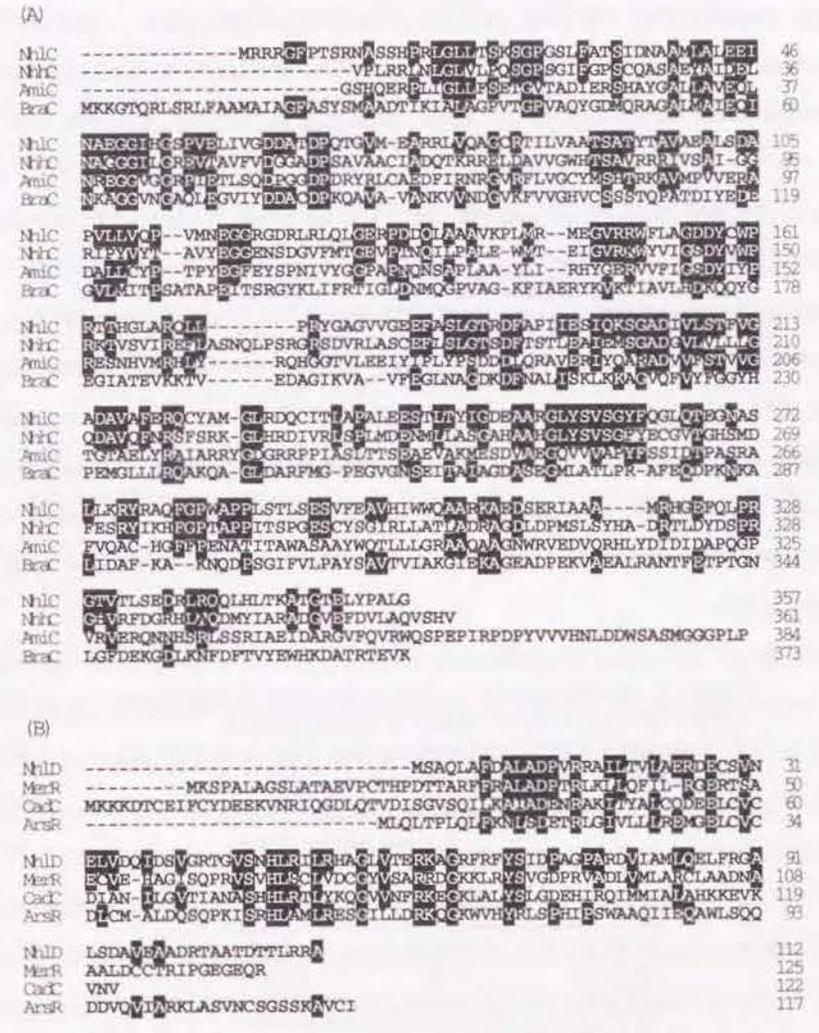

Fig. 4. Alignment of the deduced amino acid sequences of the *R. rhodochrous* J1 *nhlC* (A) and *nhlD* (B) with the respective homologous sequences.
Residues in black boxes indicate identical sequences; dashes denote gaps introduced to maximize alignment. Abbreviations (references); NhhC, a positive regulator of H-NHase from *R. rhodochrous* J1 (73); AmiC, a negative regulator of aliphatic amidase from *P. aeruginosa* (33); BraC, a branched-chain amino acid binding protein from *P. aeruginosa* (74); MerR, a possible regulator for mercury resistance genes from *Streptomyces lividans* (75); CadC, a possible regulator in the cadmium resistance system from *Staphylococcus aureus* (76); ArsR, a transcriptional repressor of ars operon from *E. coli* (77).

There are extensive noncoding sequences between *nhlD* and *nhlC* (357 bp) and *nhlC* and *nhlB* (884 bp), possibly indicating regulatory independence of these three genes thus separated.

The requirement of *nhlC* and *nhlD* for the amide-dependent expression of *nhlBA*

The transformant carrying pLJK30 exhibited the amide-inducible L-NHase expression, whereas the transformant carrying pLJK40, which excludes *nhlD*, expressed L-NHase constitutively (Fig. 1, Table 1). Considering that *nhlC* is present in both pLJK30 and pLJK40, in the presence of amide as an inducer, *nhlD* functions negatively, whereas *nhlC* functions positively for the L-NHase expression. To examine the necessity of *nhlC* for *nhlBA* expression, a plasmid pLJK70 containing the 1477-bp *Eco*RV.1-*Eco*RV.2 fragment in the blunt-ended *Xba*I site of pLJK60 was constructed (Fig. 1). The transformant harboring pLJK70 greatly decreased NHase activity (0.291 and 0.225 U/mg•protein for the uninduced and the induced cells, respectively) compared to the transformant harboring pLJK60, irrespective of the presence of crotonamide in the culture medium. This finding and the above obtained using pLJK30 and pLJK40 suggest that when amide is added to the culture medium, NhlC inhibited the action of repressor NhlD, leading to the L-NHase expression, while NhlC could not function in the absence of amide to the medium, leading to repression of the L-NHase expression by NhlD.

Table 2. Amidase activity in cell-free extracts of *R. rhodochrous* ATCC12674 transformants containing various plasmids.
R. rhodochrous ATCC12674 transformants were cultured in the medium with (+) or without (-) crotonamide (2 g/l).

	Amidase activity (U/mg)	
	Crotonamide	
	-	+
pLJK10	N.D.	0.043
pLJK30	N.D.	0.013
pLJK40	0.111	0.079

N.D. : Not detected

Expression of the L-NHase and amidase genes

Of seven pLJK plasmids constructed above, pLJK10, pLJK30 and pLJK40 contain intact *amdA*. Assay of amidase activity using benzamide as a substrate (Table 2) and Western blot analysis with anti-(amidase) antiserum (Fig. 5) for the transformants harboring each of these three plasmids showed that the transformants carrying pLJK10 or pLJK30 inducibly produced amidase in the presence of crotonamide in the culture medium, but the transformant carrying pLJK40 produced amidase constitutively. This expression pattern of the amidase is

the same as that of L-NHase (Table 1), suggesting that both *nhlBA* and *amdA* are coordinately controlled or cotranscribed in a single mRNA in spite of the relatively long intervening space (1.9 kb). Sequence analysis and characterization of the 1.9-kb region are now in progress.

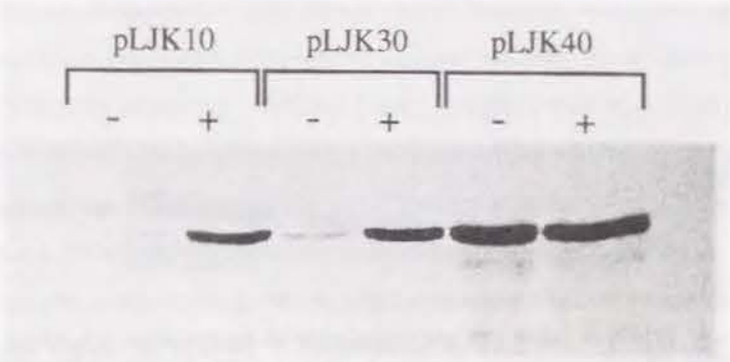

Fig. 5. Expression of amidase in *R. rhodochrous* ATCC12674.
R. rhodochrous ATCC12674 was transformed with pLJK10, pLJK30 or pLJK40, and cultiured in the medium with (+) or without (-) crotonamide (2 g/l). Western blot analysis was carried out as described in Materials and Methods using anti-(amidase) antiserum.

Similarity among NhlD and the bacterial transcriptional regulators, MerR, CadC and ArsR for the metal resistance suggested that the induction of L-NHase and amidase could be affected by the presence of cobalt ions, which is indispensable for the formation of catalytically active L-NHase. To test this possibility, we further investigated the formation of L-NHase and amidase of the transformant carrying pLJK10 cultured in the presence or absence of cobalt ions and in the presence or absence of crotonamide. Western blot analyses with anti-(L-NHase) antiserum (Fig. 6-A) and anti-(amidase) antiserum (Fig. 6-B) for the transformant demonstrated that the formation of each L-NHase and amidase was affected only by the presence of the inducer amide and not by the presence of cobalt ions. Assay for amidase activity of the four kinds of cells cultured as described above agreed with the results of the Western blot analyses; the extracts of cells cultured in the crotonamide-containing medium in the presence and in the absence of cobalt ions showed amidase activities of 0.043 and 0.037 U/mg, respectively, although those in the medium without crotonamide showed no detectable amidase activity irrespective of the presence of cobalt ions. Since cobalt ions are indispensable for the formation of catalytically active L-NHase, we could not investigate the effect of cobalt ions on the expression of *nhlBA* by measuring NHase activity.

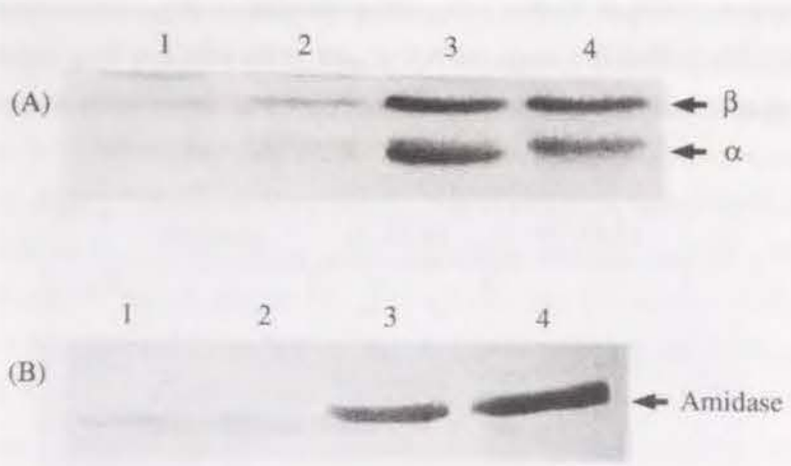

Fig. 6. Effects of cobalt ions and crotonamide on the formation of L-NHase and amidase proteins.
R. rhodochrous ATCC12674 harboring pLJK10 was cultured in the medium with (+) or without (-) $CoCl_2 \cdot 6H_2O$ (0.01 g/l) and with (+) or without (-) crotonamide (2 g/l). Western blot analysis was carried out using anti-(L-NHase) antiserum (A) and anti-(amidase) antiserum (B). Lane 1, cell-free extracts prepared from the transformant cultured in the medium without cobalt ions and crotonamide; lane 2, with cobalt ions and without crotonamide; lane 3, without cobalt ions and with crotonamide; lane 4, with cobalt ions and crotonamide.

DISCUSSION

In this section, the author reports two ORFs (*nhlC* and *nhlD*), which are located upstream *nhlB* in *R. rhodochrous* J1. This gene organization is distinct from that of each NHase gene which has so far been reported. *nhlC* seems to play a positive role for formation of active L-NHase in the presence of amide-inducer. Amino acid sequence deduced from *nhlC* has marked similarity to the negative regulator AmiC of the *P. aeruginosa* aliphatic amidase, which is induced by some low molecular-mass amides such as acetamide and propionamide (39,78). Formation of the *Pseudomonas* amidase derived from the *amiE* gene is positively regulated by AmiR via a transcription anti-termination mechanism (79), and negatively regulated by AmiC which is considered to function by inhibiting the action of AmiR through protein-protein interaction. The AmiC protein has been shown to bind acetamide in equilibrium dialysis studies, and therefore appears to respond to the presence of amides as a sensor protein (40). L-NHase is also induced by amide compounds (not by nitriles), *i.e.*, acetamide, propionamide, acrylamide, methacrylamide, crotonamide and cyclohexane-carboxamide, which

are products of the nitrile hydration reaction catalyzed by NHase. The finding that the *nhlC* (*amiC*-homolog) is responsible for the amide-inducible expression of *nhlBA* is very interesting, while similarity in amino acid sequence is not observed among amide-degrading enzymes; AmiE (the *P. aeruginosa* amidase) (80) does not show any similarity to AmdA from *R. rhodochrous* J1. Assuming that NhlC as well as AmiC functions as a sensor protein sensitive to amide compounds in the culture medium, we suggest that *nhlC* is involved in induction of the L-NHase synthesis in some way. *nhlC* has higher similarity with *nhhC* than with *amiC*.

The author showed the coordinate expression of *nhlBA* and *amdA* in the experiments including enzyme assays and Western blot using various transformants. It has been already reported (72) that L-NHase and the amidase showed similar trends in substrate specificity for aliphatic and aromatic compounds: L-NHase acts on benzonitrile (the synthesis of benzamide from which was taken as 100%), 3-cyanopyridine (66.7%), *n*-capronitrile (200%), methacrylonitrile (97.3%) and crotononitrile (28.0%), while the amidase acts on benzamide (the synthesis of benzoic acid from which was taken as 100%), nicotinamide (55.9%), *n*-capronamide (241%), methacrylamide (112%) and crotonamide (19.6%). These findings suggest that both enzymes are induced by the same inducer (amide) and then cooperate in degrading nitriles efficiently.

nhlD was found to be involved in *nhlBA* expression in *R. rhodochrous* ATCC12674. *nhlD* possibly functions as a repressor in the absence of the inducer amide, and this repression would be relieved by the action of *nhlC* in the presence of amide in the medium. It is interesting to note that *nhlD* is similar to *merR*, *cadC* and *arsR* which regulate the heavy metal resistance systems, *i.e.*, detoxification or transport of heavy metal. L-NHase, the expression of which is regulated by *nhlD* is also associated with heavy metal; L-NHase contains 1.7 atoms cobalt/mol enzyme (unpublished results), and is produced as an active form in *R. rhodochrous* J1 only in the presence of cobalt ions in the culture medium (10). In the experiments using *R. rhodochrous* ATCC12674 transformants, moreover, Co^{2+} is the essential element for the NHase expression in the culture medium. *merR*, *cadC* and *arsR* are considered to repress respective structural genes conferring heavy metal resistance, and the repression may be relieved by the presence of the heavy metal ions, Hg^{2+}, Cd^{2+} and AsO_3^{3-}, respectively (81-83). On the contrary, repression of *nhlBA* expression by *nhlD* appears to be inhibited by *nhlC* in the presence of the inducer amide, instead of cobalt ions. Furthermore, Western blot analysis and assay for amidase activity demonstrated that the presence of cobalt ions had no effect on the formation of L-NHase and amidase; but the former enzyme requires cobalt ions in

active form. These findings raise the possibility that the repressor NhlD might have lost a function as a heavy metal sensor during the course of evolution.

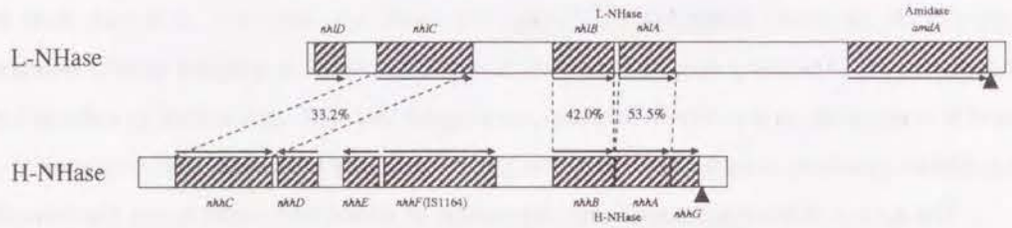

Fig. 7. Organization of the gene clusters *nhlDCBAamdA* and *nhhCDEFBAG* involved in nitrile metabolism in *R. rhodochrous* J1.
Amino acid sequence similarity (percentages of identity) between equivalent genes of both gene clusters are indicated. *nhlBA* and *nhhBA* encode each of β- and α-subunits of L-NHase and H-NHase, respectively. Possible transcriptional terminators are indicated by solid triangles.

Fig. 7 compares the organization of *nhlBA* and *nhhBA* and their flanking genes. In *nhh* genes, both *nhhC* and *nhhD* are required for *nhhBA* expression, whereas *nhhE* and *nhhF* seem to have no effect on *nhhBA* expression. *nhhF* encodes a possible transposase and constitutes a possible insertion sequence (IS*1164*) together with its flanking inverted repeats (84), and *nhhE* is similar to the gene (ORF5) found in a potential transposable element R46 (85). Compared to the arrangement of the *nhl* gene cluster, two extra *nhh* genes (*nhhE* and *nhhF*) exist in the region between the regulatory and structural genes; the insertion event of the *nhhEF* unit into the upstream region of *nhhBA* occurred in the course of evolution. Considering the gene order and relative high homology of both *nhlCBA* and *nhhCBA*, together with the finding that both *nhlC* and *nhhC* may play roles in the L- and H-NHases expression, respectively, although *nhlD* is different from *nhhD* in their structure and regulatory function, it is likely that the gene duplication took place in the *R. rhodochrous* J1 genome, after which extra genes were added.

SUMMARY

The 3.5-kb of 5'-upstream region from *nhlBA* encoding a cobalt-containing low molecular-mass nitrile hydratase (L-NHase) from *Rhodococcus rhodochrous* J1 was found to be required for the amide-dependent expression of *nhlBA* in experiments using a *Rhodococcus* transformation system. Sequence analysis of the 3.5-kb fragment revealed the presence of two open reading frames (*nhlD* and *nhlC*) in this fragment. NhlD has similarity to regulators MerR, CadC and ArsR. NhlC has similarity to the regulators AmiC for the expression of an aliphatic amidase from *Pseudomonas aeruginosa* and NhhC for the expression of a high molecular-mass nitrile hydratase from *R. rhodochrous* J1. Assay for NHase activity of transformants carrying *nhlD* deletion or *nhlC* deletion suggests a negative regulatory role for *nhlD* and a positive regulatory role for *nhlC* in the process of the L-NHase formation. Assay for NHase and amidase activities and Western blot analysis of each *Rhodococcus* transformant carrying various deletion-plasmid, have shown that *nhlBA* and *amdA* encoding an amidase, which is located 1.9-kb downstream of *nhlBA*, were regulated in the same manner. These findings present the genetic evidence for a novel gene cluster of L-NHase induced by the reaction product (amide) in the 'practical microorganism' *R. rhodochrous* J1.

Section 4 Cobalt transporter linked to L-NHase[f]

Cobalt is necessary as a trace element for all cells but is toxic at higher concentrations, a fact of considerable environmental importance. It is the central metal cofactor in the corrine ring of vitamin B_{12} (86) and also plays an important role in biological functions. Methionyl aminopeptidase, which catalyzes the removal of the initiator methionine from nascent polypeptide chains, contain cobalt ions in both prokaryotes and eukaryotes; the N-terminal modification caused by this enzyme appears to be involved in functional regulation, intracellular targeting and protein turnover, although its physiological importance is incompletely understood (87). Methylmalonyl-CoA carboxytransferase from *Propiobacterium shermanii* (88) and glucose isomerase from *Streptomyces albus* (89) are also cobalt-containing enzymes.

Several transition metals, which play an essential role as cofactors in many biochemical processes, must be transported into cells against concentration gradients, *i.e.*, trace concentrations outside and substantial amounts within the cells. Divalent cations of Zn^{2+}, Co^{2+}, Ni^{2+} and Cd^{2+} are transported into the cells by a broad-substrate-range Mg^{2+} transport system in *Alcaligenes eutrophus* (90). The transport of a broad range of metal ions by the relatively unspecific uptake system is an economical solution for most cells and allows the accumulation of trace elements inside the cells for future needs. On the contrary, there seem to be other transport systems for Zn^{2+}, Co^{2+} and Ni^{2+} with higher ion selectivity (91,92). The Ni-specific transporter was identified as a part of the plasmid-encoded hydrogenase (a Ni-containing enzyme) gene cluster in *A. eutrophus* (93). However, there are no reports on the structure and function involved in the uptake of cobalt ions other than by the broad specificity Mg^{2+} transport system in both prokaryotes and eukaryotes.

Nitrile hydratases (NHase; EC 4.2.1.84), which catalyze the hydration of nitriles to the corresponding amides followed by their conversion to the acids plus ammonia by amidase, contain cobalt atoms in an actinomycete *Rhodococcus rhodochrous* J1 (10). Culture of this strain in a medium containing urea and cyclohexanecarboxamide in the presence of cobalt ions, results in the respective production of a high molecular-mass NHase (H-NHase) and a low molecular-mass NHase (L-NHase) with different physicochemical properties and substrate specificities are selectively induced, respectively. Both H- and L-NHases are composed of α- and β-subunits (α differs in size from β in each case, and the α- and β-subunits of H-NHase differ from those of L-NHase).

In the *nhlBA* gene cluster, the author has found two ORFs (*nhlC* as a positive regulator and *nhlD* as a negative regulator required for the amide-dependent induction of *nhlBA*)(94). An amidase gene (*amdA*) is located 1.9-kb downstream of *nhlA* (72), and the expression of *nhlBA* and *amdA* is coordinately regulated (94).

In this section, the author describes the identification of a gene, *nhlF*, which is situated between *nhlBA* and *amdA* and is similar to the bacterial genes encoding nickel transporters previously reported. Furthermore, the author presented evidence that the product of *nhlF*, NhlF transports cobalt ions into the *Rhodococcus* and *Escherichia coli* host cells. By use of the transformation system in *Rhodococcus*, the transporter specific for cobalt ions.has been also characterized.

MATERIALS AND METHODS

Strains, plasmids and media

E. coli JM109 (30) was used as the host strain for recombinant plasmids. *R. rhodochrous* ATCC12674 was the host for a *Rhodococcus-E. coli* shuttle vector pK4 (31) and its derivatives, and was used for the expression of the L-NHase gene (*nhlBA*) and the presumed cobalt transporter gene (*nhlF*). *E. coli* transformants were grown in LB medium (30). *R. rhodochrous* ATCC12674 transformants were grown in MYP medium (31).

Enzymes and chemicals

Restriction endonucleases, calf intestine alkaline phosphatase and T4 DNA ligase were purchased from Takara Shuzo Co. Ltd. Isopropyl β-D-thiogalactopyranoside (IPTG) was obtained from Wako Pure Chemicals (Tokyo, Japan). [α-^{32}P]dCTP (110 TBq/mmol), [γ-^{32}P]ATP (180 TBq/mmol) and $^{57}CoCl_2$ (17.3 TBq/mmol) were from Amersham Japan. Carbonyl cyanide-*m*-chlorophenyl hydrazone (CCCP) was from Nakalai (Kyoto, Japan). 3,5-Di-*tert*-butyl-4-hydroxybenzilidenemalononitrile (SF6847) was kindly provided from Dr. H. Miyoshi. All other chemicals were of the highest purity commercially available.

DNA manipulation

DNA manipulation was performed essentially as described by Sambrook *et al.* (30). The DNA sequence was determined by the dideoxynucleotide chain termination method (58).

[α-^{32}P]dCTP and Sequenase (United States Biochemicals, Cleveland, USA) or [γ-^{32}P]ATP and a *Tth* Sequence kit (Toyobo, Osaka, Japan) were used for sequencing.

Transformation of *R. rhodochrous* ATCC12674 by electroporation

A mid-exponential culture of *R. rhodochrous* ATCC12674 was centrifuged at 6,500 x *g* for 10 min at 4°C and washed three times with demineralized cold water. Cells were then concentrated 20-fold in demineralized cold water and kept on ice. Ice-cold cells (100 µl) were mixed with 1 µg DNA in 1 µl of TE buffer (10 mM-Tris/1 mM EDTA, pH 8.0) in a 1-mm-gapped electrocuvette (Bio-Rad, Richmond), and subjected to a 2.0 kV electric pulse from a Gene Pulser (Bio-Rad) connected to a pulse controller (25 µF capacitor; external resistance, 400Ω). Pulsed cells were diluted immediately with 1 ml of MYP medium (31) and incubated for 2 h at 26°C. They were then spread on MYP medium containing 75 µg kanamycin/ml.

Preparation of cell suspension and enzyme assay

R. rhodochrous ATCC12674 transformants were grown at 28°C for 24 h in MYP medium containing $CoCl_2 \cdot 6H_2O$ at several concentrations, harvested by centrifugation at 6,500 x *g* at 4°C, and washed twice with 0.15 M NaCl. The washed cells were suspended in 0.1 M HEPES/KOH buffer (pH 7.2) containing 44 mM *n*-butyric acid. NHase activity was assayed in a reaction mixture (2 ml) containing 50 mM potassium phosphate buffer (pH 7.0), 6 mM benzonitrile and an appropriate amount of the cell. The reaction was carried out at 20°C for 10 min and stopped by the addition of 0.2 ml 1 M HCl. The amount of benzamide formed in the reaction mixture was determined as described previously (13).

Cobalt uptake experiment

Assay for cobalt uptake was performed using cells grown in MYP medium without cobalt ions for 24 h at 28°C as described above. Cells were centrifuged at 6,500 x *g* for 10 min at 4°C and washed twice with 150 mM NaCl. The washed cells were suspended in buffer A [50 mM Tris-HCl (pH 7.5) containing 10 mM $MgCl_2$] to a concentration of about 10 mg dry cell mass/ml. Cobalt uptake assays were performed in 30 ml Erlenmeyer flasks containing 0.5 mg of dry cell mass in 10 ml of buffer A. Cells were preincubated for 5 min at 30°C before addition of $^{57}CoCl_2$. Assays were shaken at 30°C. To determine the cobalt content of the cells, 0.1 ml of the assay volume was taken at appropriate times and immediately passed through a membrane filter (pore size 0.45 µm; diameter 2.5 cm; Millipore, USA). Cells were

immediately washed on the filter thrice with 3 ml of buffer A. The filters were dried and counted in a γ counter (Packard, USA).

Construction of *nhlF* expression plasmid

To express *nhlF* in *E. coli*, the author improved the sequence upstream from the putative start codon (TTG, nucleotides 5644-5646) by PCR with pLJK50 as a template and two oligonucleotides (Primers 1 and 2) as primers. Primer 1 (5'CTGCAAGCTTTAAGGAGGAA-TAGCGTATGACCAGCACCACCATTACAC3') contained a *Hin*dIII recognition site, a ribosome-binding site, a TAG stop codon in frame with the *lacZ* gene in pUC19 and 22 nucleotides (nucleotides 5644-5665 in Fig. 2) of *nhlF* with the ATG start codon instead of the TTG codon. Primer 2 (5'GTATCTCGGTGGCTGCAGTGATCGTG3') contained 26 nucleotides of the gene (complementary to nucleotides 6710-6735 in Fig. 2) 8 nucleotides downstream from the end of the reading frame and a *Pst*I recognition site. DNA was amplified by the polymerase chain reaction (PCR) using a thermal cycler (Perkin-Elmer, USA). Reaction mixtures contained 1 µg of template DNA, 100 pmol of each oligonucleotide pool, and *Thermus thermophilus* DNA polymerase (Toyobo) in a volume of 100 µl. Thirty thermal cycles consisted of 94°C for 1 min, 55°C for 1 min and 75°C for 3 min each. The plasmids designated as pLCO10 and pLCO20 were constructed by ligation of the gel-purified and *Hin*dIII-*Pst*I digested PCR product with pUC19/*Hin*dIII-*Pst*I and pSTV29/*Hin*dIII-*Pst*I, respectively, and were transformed into *E. coli* JM109.

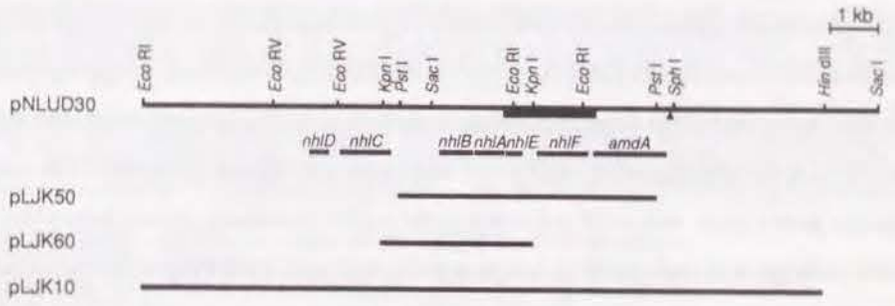

Fig. 1. Genetic organization of the L-NHase gene cluster and the constructed fragments. *nhlB* and *nhlA* are genes encoding L-NHase β- and α- subunit proteins, respectively (13). *nhlC* and *nhlD* have recently been found to be responsible for the amide-dependent L-NHase induction (94). *amdA* encodes the amidase (72). *nhlE* and *nhlF* are the newly identified genes described in this section. Solid triangle represents putative transcription terminator (72). The bold line demonstrates the region corresponding to the sequence shown in Fig. 2

RESULTS

Primary structure of the intervening region among *nhlBA* and *amdA*

A 1.73-kb *Sac*I-*Eco*RI region containing *nhlBA* (13) and a 1.96-kb *Eco*RI-*Sph*I region containing *amdA* (72) from *R. rhodochrous* J1 was previously cloned and sequenced; *nhlA* and *amdA* are separated by the 1.9-kb intervening region (Fig. 1). Furthermore, the author showed that both enzyme genes are coordinately regulated by a positive regulator (*nhlC*) and a negative regulator (*nhlD*), which are located upstream of *nhlB* (94). Here, the author determined the nucleotide sequence of the 1.5-kb *Eco*RI region. Fig. 2 shows the nucleotide sequence of the 1.5-kb *Eco*RI region and its flanking sequence previously determined, as well as amino acid sequences of two ORFs (*nhlE* and *nhlF*) newly found in the region. The presumptive ATG start codon was found for *nhlE*, but the initiation codon TTG was less frequent for *nhlF*. *nhlE* and *nhlF* were preceded by Shine-Dalgarno sequences located within reasonable distances from the respective presumptive start sites. The first ORF (*nhlE*) located just downstream from *nhlA* is 447 nucleotides long, and may encode a protein of 148 amino acids (16,887 Da). *nhlE* showed a low similarity of amino acid sequence with *nhhG* from *R. rhodochrous* J1 (73) (35.6% identity) (data not shown). *nhhG* is also located just downstream from *nhhA* encoding the H-NHase α-subunit protein, and its function has not yet been determined. The second ORF named *nhlF*, is 1059 nucleotides long, and may encode a highly hydrophobic polypeptide of 352 amino acids (37,187 Da); the deduced amino acid sequence of NhlF includes a substantial number of hydrophobic residues (63%). A computer-aided FASTA search of the SwissProt protein data base indicated that NhlF showed similarity to nickel transporters such as HoxN (93) from *A. eutrophus* (36.1% identity), HupN (95) from *Bradyrhizobium japonicum* (37.8% identity), NixA (96) from *Helicobacter pylori* (37.8% identity) and UreH (97) from *Bacillus* sp. (16.9% identity) (Fig. 3). *hoxN* and *hupN* are located in each nickel-containing hydrogenase gene cluster and *ureH* is located in the nickel-containing urease gene cluster. *nixA* is isolated as the gene complementing urease activity in *E. coli* harboring urease structural genes under nickel limitation; this gene is not closely linked to the urease gene cluster. A hydropathy plot by the method of Kyte and Doolittle (98) revealed that NhlF was a markedly hydrophobic protein and contained eight possible transmembrane helices, numbered as 1~8 (Fig. 4).

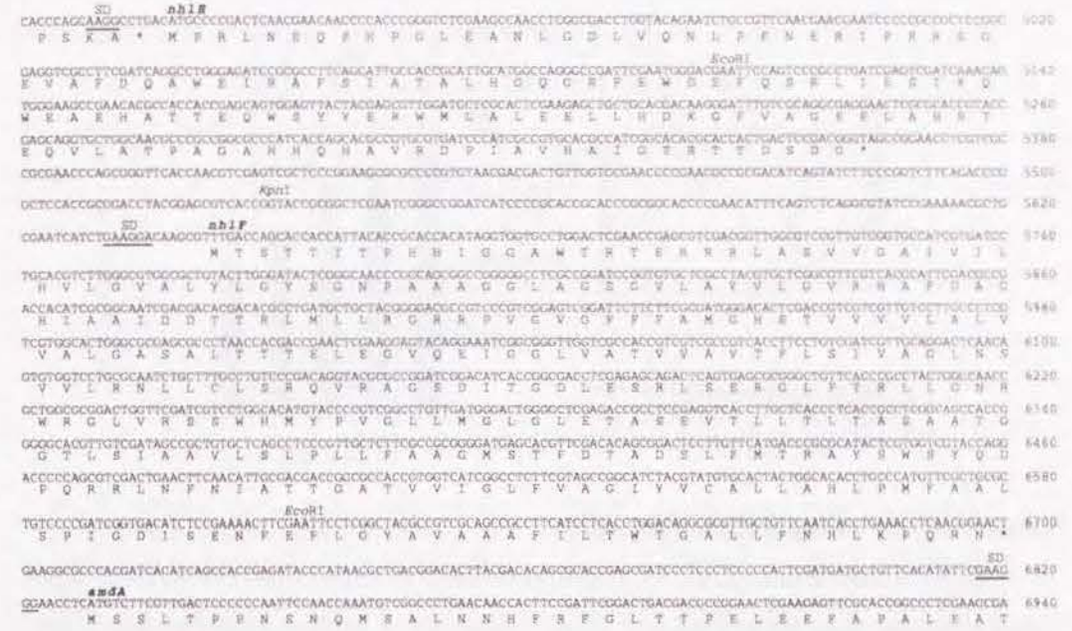

Fig. 2. Nucleotide sequence of the 2040-bp region including the 1506-bp *Eco*RI fragment.
Presumed amino acid sequences of *nhlE* and *nhlF* are indicated. The sequence also includes the 3' end of *nhlA* and 5' end of *amdA*. Probable Shine-Dalgarno (SD) sequences are underlined. The sequence is numbered from the *Eco*RV site upstream of *nhlD* (Fig. 1).

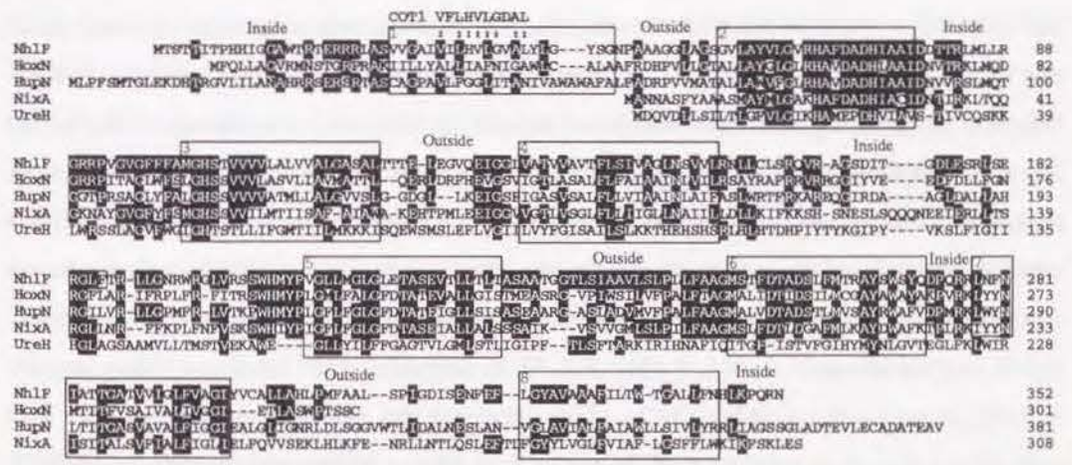

Fig. 3. Alignment of amino acid sequences among NhlF from *R. rhodochrous* J1 and homologous proteins.
Amino acid sequences of NhlF from *R. rhodochrous* J1, HoxN from *A. eutrophus* (93), HupN from *B. japonicum* (95), NixA from *H. pylori* (96) and UreH from *Bacillus* sp (97) were aligned by introducing gaps (hyphens) to achieve maximum homology. Residues in black boxes indicate identical sequences. Putative transmembrane or membrane-associated domains (1~8) is enclosed by boxes. The orientation (Inside, internal; Outside, external) of the nonmembrane loop regions, predicted by the 'positive inside rule' (105) is shown above the sequence. Highly conserved residues between NhlF and COT1 from *Saccharomyces cerevisiae* (107) are marked with colons.

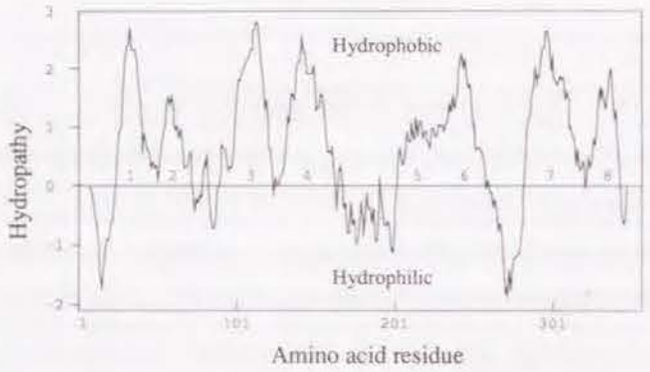

Fig. 4. Hydropathy plot of NhlF.
Hydropathy was calculated for NhlF by using the algorithm of Kyte and Doolittle (98) with a window of 15 amino acid residues.

NHase activity under cobalt limitation

L-NHase enzyme encoded by *nhlBA*, contains 1.7 atoms cobalt/mol enzyme, and L-NHase is formed as an active form in *R. rhodochrous* J1 only in the presence of cobalt ions in the culture medium (10). The position of *nhlF* close to *nhlBA* and the similarity in the amino acid sequence between NhlF and the bacterial nickel transporters suggested that NhlF is a protein that transports cobalt ions into the cell. First, we examined the effect of *nhlF* on the activity of cobalt-dependent L-NHase using a *Rhodococcus-E. coli* host-vector system. As shown in Fig. 1, plasmid pLJK50 contained the *Pst*I fragment covering intact *nhlBAEF* and a part of *amdA* on a *Rhodococcus-E. coli* shuttle vector pK4, and pLJK60 contained the *Kpn*I fragment covering a part of *nhlC* and intact *nhlBAE* on pK4. We transformed each plasmid into *R. rhodochrous* ATCC12674 as a host strain and cultured the resulting transformants in the medium changing final concentrations of $CoCl_2$. NHase assays using benzonitrile as a substrate for each cell suspension prepared as described in Materials and Methods demonstrated that the presence of *nhlF* allows the formation of catalytically active NHase even at very low cobalt concentrations (1, 2, 3, 4, 5 μM) (Fig. 5); in particular, *nhlF* increased NHase activity 3.7 fold, in the case of 1 μM of $CoCl_2$. This suggested that *nhlF* encodes a transporter with high affinity for cobalt ions. With 5 μM of $CoCl_2$, however, NHase activity with the pLJK50-containing transformant was to 2-fold. Furthermore, both transformants showed almost the same NHase activities when they were cultured in the medium supplemented with 0.001% $CoCl_2$ (w/v) (data not shown), corresponding to 42 μM of $CoCl_2$, which is the optimum concentration for the NHase formation in *R. rhodochrous* J1 (99). This indicates the presence

of nonspecific transport system with low affinity for cobalt ions in the *R. rhodochrous* ATCC12674 host strain.

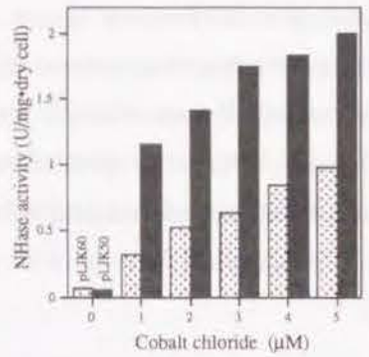

Fig. 5. Effect of *nhlF* on NHase activity of the recombinant *R. rhodochrous* ATCC12674.
Solid boxes, *R. rhodochrous* ATCC12674/pLJK50; shaded boxes, *R. rhodochrous* ATCC12674/pLJK60. Strains were grown for 24 h at 28°C in MYP medium containing $CoCl_2$ as indicated. The NHase activity was measured as described in Materials and Methods.

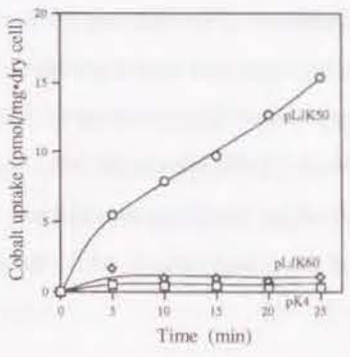

Fig. 6. Cobalt uptake of the recombinant *R. rhodochrous* ATCC12674.
Circle, *R. rhodochrous* ATCC12674/pLJK50; diamond, *R. rhodochrous* ATCC12674/pLJK60; square, *R. rhodochrous* ATCC12674/pK4. The reaction mixture consisted of 10 nM $^{57}CoCl_2$, 10 mM $MgCl_2$ and the cells in a 50 mM Tris-hydrochloride buffer (pH 7.5).

Cobalt uptake of *R. rhodochrous* ATCC12674 transformants

The synthesis of catalytically active NHase by the transformant harboring pLJK50 led the author to examine whether NhlF could function as a cobalt transporter. We measured $^{57}Co^{2+}$ uptake of the *Rhodococcus* transformants. Cell suspensions of *R. rhodochrous* ATCC-12674 con-taining either pLJK50, pLJK60 or pK4 were prepared. Uptake of Co^{2+} was determined by the addition of $^{57}CoCl_2$ (final concentration, 10 nM) to the cell suspension (0.5 mg dry cell mass in buffer A) followed by vacuum filtration after 5, 10, 15, 20 and 25 min. Identical assay without the cells showed that non-specific binding of $^{57}Co^{2+}$ to the membrane filter was negligible. As illustrated in Fig. 6, the presence of *nhlF* significantly increased cobalt uptake.

Effects of uncouplers and divalent cations on cobalt uptake

The effects of uncouplers on the *nhlF*-conferred cobalt uptake were examined. CCCP was added to the cell suspension of the *Rhodococcus* transformant harboring pLJK50 in buffer A, 10 min prior to the addition of $^{57}CoCl_2$. CCCP at the final concentration of 1 μM and 10 μM in the reaction mixture inhibited the uptake by 25% and 85%, respectively, after 25 min of the reaction time. However, CCCP has also been shown to exhibit side effects besides the fun-

ction of a protonophore; it blocks sulfhydryl groups in membrane proteins of *E. coli* and *Staphylococcus aureus* (100,101). Therefore the effect of an uncoupler SF6847 on the cobalt uptake was investigated. SF6847 at the final concentration of 0.1 μM, 1 μM and 10 μM inhibited the uptake by 55%, 85% and 85%, respectively, after the reaction time of 25 min. These findings demonstrated that proton gradients are involved in the cobalt uptake conferred by *nhlF*.

Other divalent cations such as Mn^{2+}, Fe^{2+}, Ni^{2+} and Cu^{2+} were added at the final concentration of 5 μM, 10 min before the addition of $^{57}CoCl_2$ into the cell suspension. The measurement of the cobalt uptake in each condition showed that none of each Mn^{2+}, Fe^{2+} or Cu^{2+} affected the cobalt uptake, while the addition of Ni^{2+} led a marked decrease of the cobalt uptake (Fig. 7).

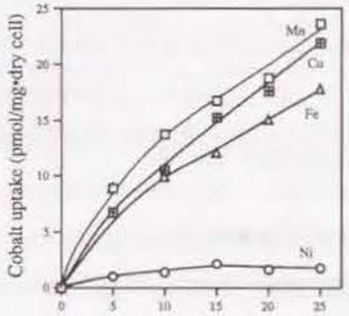

Fig. 7. Effect of other transient metals on the cobalt uptake of the *R. rhodochrous* ATCC12674/pLJK50.
Square, $MnCl_2$; triangle, $FeSO_4$; circle, $NiCl_2$; cross in square, $CuSO_4$. The metals were added to the cell suspension 10 min prior to the addition of $^{57}CoCl_2$.

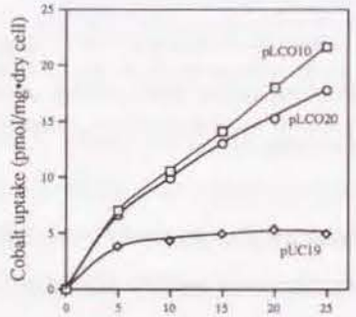

Fig. 8. Cobalt uptake by the recombinant *E. coli* JM109.
Square, *E. coli* JM109/pLCO10; circle, *E. coli* JM109/pLCO20; diamond, *E. coli* JM109/pUC19. The reaction mixture consisted of 10 nM $^{57}CoCl_2$, 10 mM $MgCl_2$ and the cells in a 50 mM Tris-hydrochloride buffer (pH 7.5).

Expression of the cobalt transporter in *E. coli*

Plasmid pLJK50 containing *nhlBAEF* and a part of *amdA* conferred the energy-dependent cobalt uptake upon the *Rhodococcus* host, whereas pLJK60 containing a part of *nhlC* and *nhlBAE* did not. These observations suggest that NhlF is a single component responsible for the cobalt uptake. To test this possibility, *nhlF* was introduced into an *E. coli* strain, and its cobalt uptake activity was investigated. To enhance *nhlF* expression in *E. coli*, the author altered the sequence upstream from TTG start codon by PCR as described in Materials and Methods. The resulting *nhlF* was introduced on a high-copy-number-plasmid pLCO10 derived from pUC19 or a low-copy-number-plasmid pLCO20 de-rived from pSTV29 into an *E. coli* JM109. The *E. coli* transformants harboring each pLCO10, pLCO20 and pUC19 were cultured in LB medium supplemented with 1 mM of IPTG for 12 h at 28°C. Cells were harvested and the cell suspensions were prepared by the method as in the case of the *Rhodococcus* transformants. The cobalt uptake experiments indicated that pLCO10 and pLCO20 confers significantly cobalt uptake activity upon the *E. coli* strain (Fig. 8), suggesting that only *nhlF* is required for the functional cobalt uptake and that the NhlF poly-peptide folded in a functionally active form probably in the *E. coli* inner membrane. The uptake activity seemed to be independent of the copy number of the plasmids within the *E. coli* cells.

DISCUSSION

H- and L-NHases are selectively produced in *R. rhodochrous* J1 cultured only in the presence of cobalt ions with each inducer (10). Both purified enzymes contain cobalt atoms as a prosthetic metal and require this divalent cation for the catalytically active enzyme; these cobalt atoms bind tightly to the enzyme and are not released from the protein even after dialysis for five days (12). No other metals such as Ni, and Fe which is a cofactor of NHases from *Pseudomonas chlororaphis* B23 (71) and *Brevibacterium* sp. R312 (102), can replace cobalt ions in both NHases. To provide the NHase enzyme with sufficient cobalt, the metal ions should be actively transported into the *R. rhodochrous* J1 cell.

The present study in this section on the nucleotide sequence of the intervening region between *nhlBA* and *amdA* suggests that *nhlF* located in this region possesses significant similarities to the previously known genes encoding potential nickel transporters from Gram-negative and Gram-positive bacteria. The author also found that *nhlF* significantly enhanced *nhlBA*-derived L-NHase activity in *Rhodococcus* transformants in the cobalt-limiting conditions and that *nhlF* on the vector plasmid conferred the cobalt uptake activity upon *Rhodococcus* and *E. coli* hosts. The studies using uncouplers suggested that proton gradients are involved in the cobalt transport. These findings suggest that NhlF located in cell membrane energy-dependently mediates the transport of cobalt ions into the cell and therefore facilitates its incorporation into the L-NHase enzyme.

It is interesting to note that *nhlF* is part of a L-NHase gene cluster spanning a DNA region of 8.6-kb. This region contains the structural genes involved in nitrile metabolism by the combination of L-NHase and the amidase, together with the regulatory genes responsible for the amide-dependent induction of both enzymes (94). The cobalt uptake experiments using

the *Rhodococcus* transformant harboring pLJK10 (see Fig. 1) cultured in the medium supplemented with or without an inducer crotonamide for the formation of L-NHase and the amidase showed that NhlF activity appeared only in the presence of crotonamide (data not shown). These findings suggested the coordinate regulation of *nhlBA*, *nhlF* and *amdA*, which is probably due to a cotranscription of these genes in a single mRNA, consistent with the presence of ρ-independent potent transcriptional terminator found in the downstream region of *amdA* (72) and with the absence of such a sequence between *nhlA* and *nhlF* or *nhlF* and *amdA*.

NhlF-related proteins previously reported have been directly or indirectly shown to be involved in the uptake of nickel ions. Among these nickel transporters, HoxN from *A. eutrophus* has been most intensively studied. In *A. eutrophus*, two transport systems for nickel ions exist: a nonspecific high-capacity magnesium transport system and a high-affinity low-capacity nickel transporter, HoxN. Nickel uptake by the magnesium transport system was competitively inhibited by Mg^{2+}, Mn^{2+}, Zn^{2+} and Co^{2+}, whereas the activity of the HoxN-mediated transport system was inhibited by only Co^{2+} (103). In this study, the author demonstrated that the cobalt uptake activity derived from *nhlF* was markedly inhibited by adding excess Ni^{2+} to the cell suspension; the other metals tested, *i.e.*, Mn^{2+}, Fe^{2+} and Cu^{2+} had no effect on the cobalt uptake. These observations suggested that NhlF is responsible for nickel uptake as well as cobalt uptake and also that HoxN is involved in cobalt uptake as well as nickel uptake; unfortunately, HoxN has not been reported to be involved in the cobalt uptake from *A. eutrophus*. However, the author could not detect nickel uptake by pLJK50-containing *Rhodococcus* using radioactive $^{63}NiCl_2$ (data not shown), which indicates that nickel ion is not a substrate for NhlF. Consequently, NhlF is a cobalt-specific transporter.

Hydropathy plots of amino acid sequence of NhlF, the topological model for HoxN proposed by Eitinger *et al.* (104) and the positive inside rule developed by von Heijne (105) suggested that NhlF is a membrane protein including eight transmembrane helices with the orientation of locating N-terminus in the cytoplasm (Fig. 3). Alignment of amino acid sequences of NhlF and its related nickel transporter proteins (Fig. 3) provides some information about the structure of NhlF. Wolfram *et al.* (106) presented two segments conserved among the nickel transporters as potent domains involved in the high-affinity nickel binding or in the translocation process; their positions are from aa. 44 to 72 and from aa. 89 to 99 of HoxN. Both segments include histidine residues (aa. 62, 68 and 97 of HoxN), which are generally considered to be potential metal ligands. The regions corresponding to both segments are highly conserved in NhlF, and the above-mentioned histidine residues also exist

in NhlF (aa. 68, 74 and 103 of NhlF). On the other hand, compared with the nickel transporters, quite different amino acid residues appeared in the corresponding sequence of NhlF; histidine (aa. 10), tryptophan (aa. 15), tyrosine (aa. 44), alanine (aa. 50), leucine (aa. 87), threonine (aa. 143, 254 and 284), arginine (aa. 179), serine (aa. 200), where different amino acids are conserved among the nickel transporters. Therefore, these amino acid residues may be involved in the cobalt-specificity.

Conklin *et al.* reported that *COT1*, isolated as a suppressor of cobalt toxicity, is responsible for the reduction of the cytoplasmic Co^{2+} ion concentration within cells of *Saccharomyces cerevisiae* (107,108). The increased tolerance to cobalt ions in the *COT1*-overexpressing yeast is due to the *COT1*-dependent increased sequestration or compartmentalization within the mitochondria of cobalt ions that cross the plasma membrane. COT1 was presumed to be a 48-kDa membrane protein with six membrane-spanning domains and found in the mitochondrial membrane fraction of cells. The similar function of cobalt uptake suggests some similarity in the primary or secondary structures of NhlF and COT1. Computer analysis of the amino acids sequences of NhlF and COT1 did not show overall similarity between them. However, as shown in Fig. 3, helix 1 of NhlF contains a segment highly similar to a segment in helix 5 of COT1 (8 of 10 residues). In this region, both NhlF and COT1 contain a histidine residue which is a potential metal-binding amino acid, but neither HoxN nor HupN contains histidine at the corresponding site, suggesting the functional role for the cobalt-specific recognition.

On the other hand, the *COT2* gene (presently *GRR1*) was also isolated from *Saccharomyces cerevisiae* (108,109); *COT2* mutant tolerates increased level of Co^{2+} through the reduction in the rate of glucose-dependent transport of cobalt into cells. However, COT2 does not appear to be responsible for the cobalt transport; this protein may play a more general role in yeast physiology that indirectly controls the permeability of the membrane to cobalt ions or the driving force for the uptake, and COT2 might be involved in the glucose activation of the plasma membrane ATPase. As expected, there is no sequence similarity between NhlF and COT2.

NhlF also exhibited no sequence similarity to the genes involved in the active efflux system of broad specificity for metals of Ca^{2+}, Zn^{2+} and Co^{2+}, which have been characterized in detail by genetic analyses on resistance of these metals in *A. eutrophus* (95,110,111).

SUMMARY

Cobalt is an essential component of a low molecular-mass nitrile hydratase (L-NHase) from *Rhodococcus rhodochrous* J1. A new gene, *nhlF*, was found in the DNA region between *nhlBA* and *amdA*, which are involved in the degradation of nitriles. The product of *nhlF* shows a significant sequence similarity with those of *hoxN* from *Alcaligenes eutrophus*, *hupN* from *Bradyrhizobium japonicum*, *nixA* from *Helicobacter pylori* and *ureH* from *Bacillus* sp., which are considered to be involved in nickel uptake into these cells. Sequence and hydropathy plot analyses have shown that NhlF would be a 352-amino acid protein with eight hydrophobic putative membrane-spanning domains. The *nhlF* expression in *R. rhodochrous* ATCC12674 and *E. coli* JM109 confers uptake of ^{57}Co in their cells, but not of ^{63}Ni. These findings together with the finding that the cobalt uptake was inhibited by the addition of uncouplers such as CCCP and SF6847 have suggested that NhlF specially mediates the cobalt transport into the cell energy-dependently.

CHAPTER III Genetic Analysis of Nitrilase

Section 1 Sequencing and overexpression of the nitrilase gene (*nitA*) and identification of an essential cysteine residue[g]

Nitrilase catalyzes the direct cleavage of nitriles to yield the corresponding acids and ammonia. When *Rhodococcus rhodochrous* J1 is cultivated in medium containing isovaleronitrile as an inducer, only nitrilase is inducibly formed (11). Nitrilases have also attracted increasing attention as catalysts for organic chemical processing, because of the mild conditions, quantitative yields, absence of by-products and in some cases, enantio- or regioselectivity that result from their reactions (112,113).

Nitrilases that utilize benzonitrile and related aromatic nitriles as substrates have been purified from *Pseudomonas* (17,18), *Nocardia* sp. NCIB 11215 (19) and NCIB 11216 (20), *Fusarium solani* (21), *Arthrobacter* sp. (22), *Rhodococcus rhodochrous* J1 (23) and *Escherichia coli* transformed with a *Klebsiella ozaenae* plasmid DNA (24). In the author's laboratory, nitrilases that act on aliphatic nitriles and arylacetonitriles were also purified from *Rhodococcus rhodochrous* K22 (25) and *Alcaligenes faecalis* JM3 (26), respectively and characterized. However, there is only one report of cloning the nitrilase gene for *K. ozaenae* bromoxynil nitrilase (24).

All nitrilases so far reported are classified as sulfhydryl enzymes since they are inactivated by thiol reagents. The *R. rhodochrous* J1 nitrilase is also inactivated by thiol reagents (23). An active cysteine residue has not yet been identified in any nitrilase.

In this section, the author describes the cloning and sequencing of the nitrilase gene (*nitA*) from *R. rhodochrous* J1, and presents evidence that a cysteine residue (Cys-165) plays an important role in the function of the active site.

MATERIALS AND METHODS

Bacterial strains and plasmids

Rhodococcus rhodochrous J1 was previously isolated from soil samples (29). *Escherichia coli* JM105 (30) was used for pUC plasmid 18/19 transformation.

Media

R. rhodochrous J1 was cultivated as described previously (23). M13 phage was propagated and the nitrilase gene was expressed in 2 x YT medium (30).

Enzymes and chemicals

Lysyl-endopeptidase and 5,5'-dithiobis(2-nitrobenzoic acid)(DTNB) were obtained from Wako Pure Chemicals (Tokyo, Japan). Restriction endonucleases and T4 DNA ligase were purchased from Takara Shuzo Co. Ltd. [γ-^{32}P]ATP (180 TBq/mmol), [α-^{32}P]dATP (15 TBq/mmol) and [α-^{32}P]dCTP (110 TBq/mmol) were from Amersham Japan. A low molecular mass standard kit was obtained from Pharmacia LKB Biotechnology Inc. Cellulofine GCL-2000 superfine was purchased from Seikagaku Kogyo Co. (Tokyo). All other chemicals used were from commercial sources and of reagent grade.

NH_2-Terminal sequence analysis

Nitrilase was purified from *R. rhodochrous* J1 as described previously (23), and the enzyme (1 mg in 1 mM potassium phosphate buffer, pH 7.5) was used directly for the NH_2-terminal sequence analysis by automated Edman degradation with an Applied Biosystems 470A gas-phase amino acid sequencer. The phenylthiohydantoin-derivatives were separated and identified by an on-line phenylthiohydantoin analyzer (Model 120A, Applied Biosystems Japan, Tokyo) with a phenylthiohydantoin C_{18} column.

Isolation of peptide fragments and peptide sequencing

Nitrilase (1.56 mg) was incubated in 20% (v/v) trichloroacetic acid at 37°C for 6 h and digested with 0.41 µg lysylendopeptidase in 0.6 ml 0.01 M Tris/HCl (pH 7.6) at 37°C for 24 h. The mixture (70 µl) was applied to high-pressure liquid chromatography equipped with a Ultron N C_{18} (4.6 x 150 mm Shinwa Kako, Kyoto, Japan) and eluted with a linear gradient of acetonitrile (0-60%, v/v) in the presence of 0.1% (v/v) trifluoroacetic acid at a flow rate 1.0 ml/min. The peptide fragments isolated were sequenced by automated Edman degradation.

Cloning of a nitrilase gene from *R. rhodochrous* J1

Oligonucleotide primers were synthesized based upon the amino acid sequences of the NH_2 termini and the internal fragment generated with lysyl-endopeptidase. The amino acid sequence Val-Ala-Ala-Val-Gln-Ala-Gln-Pro-Val-Trp-Phe-Asp-Ala was used to model the

oligodeoxynucleotide pool 5'-GTCGCTGCAGT(C,G,T)CAGGC(A,C)CA(A,G)CC(G,T)GT-(A,C,G)TGGTT(C,G)GA(C,T)GC-3' (sense strand), and Phe-Ala-Arg-Ile-Ile-Gly-Pro-Asp-Gly to model 5'-CC(A,G)TC(A,C,G)GG(A,C,G)CC(A,G,T)ATGAT(C,G)CG(C,G)GC-(A,G)AA-3' (antisense strand). These oligonucleotides were synthesized by the phspho-ramidite method (114) using an Applied Biosystems Model 381A automatic synthesizer. Total DNA of *R. rhodochrous* J1 was prepared after cell lysis (wet mass, 15 g) with lysozyme and *Achromobacter* peptidase (Wako Pure Chemicals, Tokyo, Japan) following the method of Saito and Miura (49). DNA was amplified by the polymerase chain reaction (PCR) using a thermal cycler (Perkin-Elmer/Cetus, U.S.A.). Reaction mixtures contained 10 µg of DNA, 100 pmol of each oligonucleotide pool, and *Thermus thermophilus* DNA polymerase (Toyobo) in a volume of 100 µl. Thirty thermal cycle consisted of 93°C for 1 min, 55°C for 2 min, and 73°C for 3 min each. The gel-purified PCR-synthesized product [750 base pairs (bp)] was cloned into the *Pst*I-*Sma*I sites of M13mp18 replicative-form DNA and designated as pNJ1. The gel-purified PCR-product was further used as a radiolabeled probe by random priming (115), to clone the full-length nitrilase gene. Nucleotides were sequenced by chain-termination (58) using Sequenase version 2 (United States Biochemical Corp., Cleveland, U.S.A.). Deoxy-ITP or 2'-deoxy-7-deaza GTP was used as a substitute for dGTP during M13 sequencing, to minimize compression.

Preparation of crude extracts from *Escherichia coli* transformants

Recombinant *E. coli* JM105 was cultured to full growth in 10 ml of 2 x YT medium containing 50 µg/ml ampicillin in a 50-ml test tube at 37°C, then transferred to 100 ml of the same medium in a 500-ml shaking flask with IPTG added to a final concentration of 1 mM, to induce the *lac* promoter. After various culture periods, the cells were harvested by centrifugation, suspended in 3 ml of 0.1 M potassium phosphate buffer (pH 7.5) containing 1 mM dithiothreitol, disrupted by sonication for 5 min (19 kHz, Insonator model 201M; Kubota, Tokyo, Japan) and centrifuged at 12,000 x *g* for 30 min. The resulting supernatants were used in the enzyme assay. Sodium dodecyl sulfate-polyacrylamide gel electrophoresis (SDS-PAGE) was performed by the method of Laemmli (60).

Site-directed mutagenesis

Site-directed mutagenesis was carried out using the oligonucleotide directed *in vitro* mutagenesis system of Amersham Japan according to the procedure recommended by the

supplier, and which was basically developed by Eckstein and co-workers (116). To prepare both sense and antisense single-stranded DNAs, *Eco*RI and *Bam*HI sites of replicative-form M13mp18 and M13mp19 were ligated with the 593-bp *Eco*RI-*Bam*HI fragment (nucleotide positions 318-910) isolated from plasmid pNJ10. After transformation into the competent strain JM105, the recombinant phages were screened initially for white plaques on plates containing IPTG and 5-bromo-4-chloro-3-indolyl β-D-galactopyranoside. Two oligonucleotides were synthesized for mutagenesis: 5'-CGCTCAACA*GCTGGGAGC-3' for replacement of Cys-165 by Ser and 5'-GGCGCGCTCAACG*C*G*TGGGAGCATTTC-CAG-3' for replacement of Cys-165 by Ala (the positions of the introduced *Pvu*II and *Mlu*I restriction sites are underlined, respectively), where asterisks indicate mismatched bases. The mutants were initially screened by restriction enzyme mapping on replicative-form DNA prepared from several plaques and then by DNA sequencing. Typically, 65-100% of the transformants contained the desired mutation. A 198-bp *Eco*RV-*Xho*I fragment (nucleotide positions 537-734) was excised from each of the mutated phage DNAs and inserted between the *Eco*RV and *Xho*I sites of plasmid pNJ20 instead of the parental fragment. The two mutant plasmids thus obtained were designated pNJ20-165S and pNJ20-165A, using the one-letter code for each substituted amino acid residue. The constructs were confirmed by restriction mapping.

Reaction with DTNB

Various amounts of DTNB (1-5.6 μmol) were incubated with the enzyme (2.8 μmol of subunit) in 10 mM potassium phosphate buffer (pH 7.2) at 0°C for 2 h (final volume, 1 ml). DTNB was replaced by water in a blank. After the reaction, the 412 nm was monitored, and an aliquot of the reaction mixture was removed to determine the remaining activity. The amount of 5-thio-2-nitrobenzoate (TNB) released was estimated with the published molar absorption coefficient in 8 M urea, 14,290 M^{-1} cm^{-1} (117).

Enzyme assays

Nitrilase activity for *R. rhodochrous* J1 was assayed by the same method as previously described (23). The protein concentration was determined according to Bradford (59). One unit of nitrilase activity was defined as the amount of enzyme that catalyzed the formation of 1 μmol benzoic acid/min under the above conditions. The specific activity was expressed as units/milligram of protein.

RESULTS AND DISCUSSION

Cloning and nucleotide sequence of the nitrilase gene from *R. rhodochrous* J1

The nitrilase from *R. rhodochrous* J1 was purified and the amino acid sequences of the peptides were determined by digesting the nitrilase with lysyl-endopeptidase. The purified enzyme had an NH_2-terminal sequence of Val-Glu-Tyr-Thr-Asn-Thr-Phe-Lys-Val-Ala-Ala-Val-Gln-Ala-Gln-Pro-Val-Trp-Phe-Asp-Ala-Ala-Lys-Thr-Val-Asp-Lys-Thr-Val-Ser-Ile-Ile-Ala-Glu-Ala. Sequences of two peptides were Phe-Ala-Val-Arg-Tyr-His-Glu-Asn and Leu-Ile-Gly-Arg-Gly-Gly-Gly-Phe-Ala-Arg-Ile-Ile-Gly-Pro-Asp-Gly-Arg-Asp-Leu-Ala-Thr-Pro-Leu-Ala-Glu-Asp, respectively (see Fig. 2). The oligonucleotide sense primer containing the *Pst*I site synthesized was a 38 mer with 288 variants (corresponding amino acid positions 10-22 in Fig. 2), and the antisense primer was a 26 mer with 432 variants (corresponding amino acid positions 253-261 in Fig. 2). The nucleotide sequence corresponding to both primers was detected in the cloned pNJ1 containing a 750-bp-length fragment generated by PCR amplification.

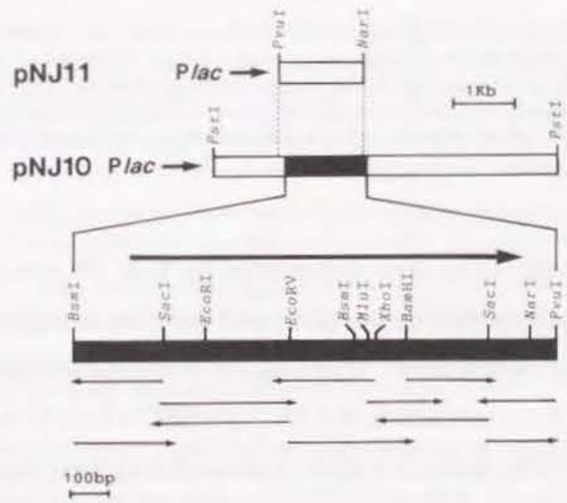

Fig. 1. Restriction map, sequencing strategy of plasmid pNL10, and construction of plasmid pNL11 for expression of nitrilase gene.
Plasmid pNJ10 contains a 5.4-kb fragment at the *Pst*I site of pUC19. A sequencing strategy for the nitrilase gene is shown under the restriction map of pNJ10. Arows indicate the direction and extent of the sequence determination. Plasmid pNJ11 contains a 1.3-kb fragment at the *Sma*I and *Acc*I sites of pUC18. The location and direction of the *lac* promoter are also indicated.

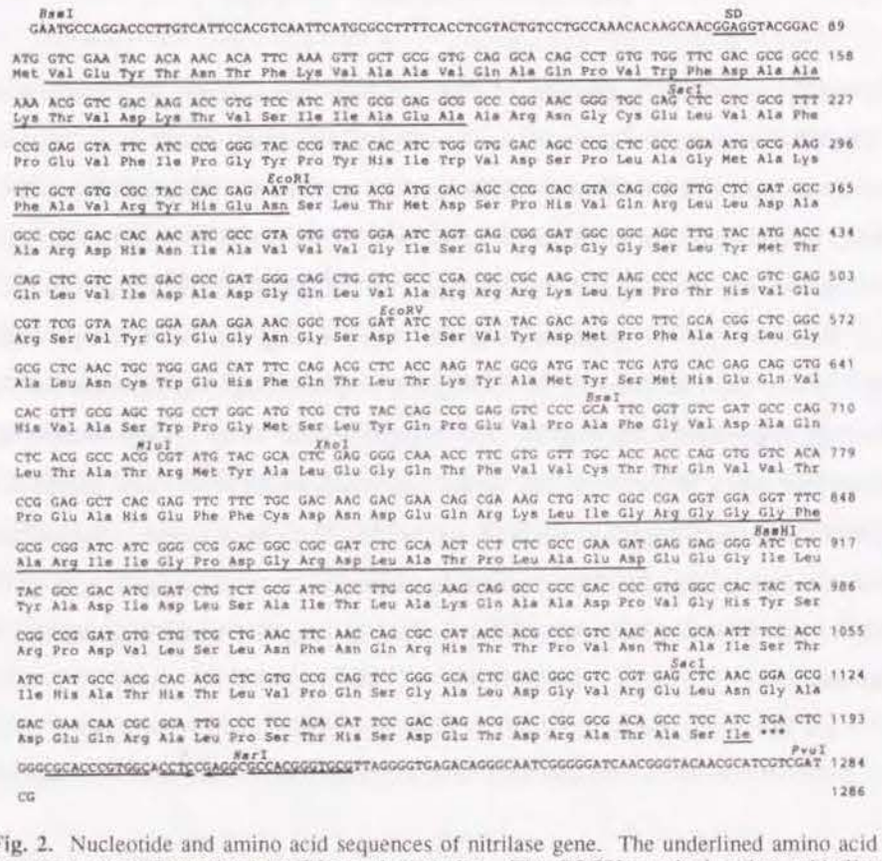

Fig. 2. Nucleotide and amino acid sequences of nitrilase gene. The underlined amino acid sequences were determined by Edman degradation. The COOH-terminal amino acid (Ile) agreed with that determined by carboxypeptidases. Potential ribosome-binding sequences are marked SD (Shine-Dalgarno), and a relevant stop codon is indicated by asterisks. An inverted repeat sequence downstream from the nitrilase gene is indicated by opposing arrows.

To obtain the entire gene, after digestion of the total DNA with several restriction endonucleases, Southern hybridization was performed using the radiolabeled PCR-synthesized probe with the following modifications. Hybridization proceeded at higher stringency, using a buffer containing 35% (v/v) formamide, 5 x SSC (1 x SSC = 0.15 M NaCl, 15 mM sodium citrate) and 0.1% (m/v) SDS at 42°C for 12 h. A single 5.4-kb band was detected from a *Pst*I digest of the total DNA. This fragment was recovered and ligated with T4 DNA ligase to linear pUC19 DNA successively treated with *Pst*I and bacterial alkaline phosphatase. The ligated mixture was introduced by transformation into *E. coli* JM105 and ampicillin-resistant transformants were selected on 2 x YT agar medium containing 50 µg/ml ampicillin. Colony hybridization with the PCR-generated probe for screening the clones containing the restriction fragment result in pNJ10 containing a 5.4-kb *Pst*I fragment (Fig. 1). Restriction endonuclease

digestion together with Southern hybridization with the above probe indicated the location of the nitrilase gene (*nitA*). The nucleotide sequence was determined in both orientations and all the restriction sites used for cloning were verified by determination as part of an overlapping sequence. An open reading frame encoding 366 amino acids (Fig. 2), which started with methionine and terminated with a TGA codon, also encoded sequences corresponding precisely to those determined using purified nitrilase. The amino acid composition of the enzyme calculated from the nucleotide sequence is similar to that obtained by chemical analysis of the purified enzyme (23). This sequence encodes a putative polypeptide of a molecular mass of 40,189 Da, which is in close agreement with that of 41.5 kDa separated by SDS-PAGE (23).

A typical Shine-Dalgarno sequence (64) was present 8 bp upstream from the initiation codon, but none of the consensus promoter sequences found in other prokaryotes (65) were observed in the upstream region. A strong hairpin structure (ΔG = -44.6 kcal/mol) located just downstream of the termination codon of the *nitA*. The overall G + C composition of positions 1, 2 and 3 of the codons for the nitrilase is 64.3, 43.6 and 80.1%, respectively. This gene was characterized by the high frequency of G/C at the third letter of the codon within the coding region, as observed in some organisms such as *Streptomyces* (118) and *Thermus* (119) having DNA with a high G + C content.

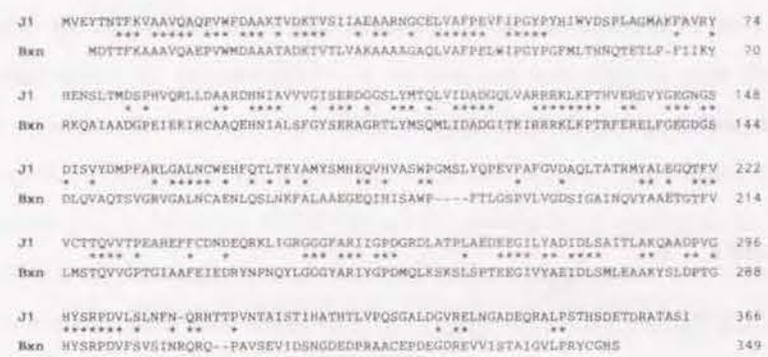

Fig. 3. Comparison of deduced amino acid sequences of nitrilases from *R. rhodochrous* J1 and *K. ozaenae*. Two sequences were aligned by introducing gaps (hyphens) to maximize identities. Identical residues are denoted by asterisks between the sequences. Bxn, bromoxynil.

The amino acid sequence of *R. rhodochrous* J1 nitrilase was compared with that of the *K. ozaenae* bromoxynil nitrilase (Fig. 3). There was a 42.7% match of amino acids in 347 overlapping residues between *R. rhodochrous* J1 and *K. ozaenae*. The bromoxynil nitrilase from *K. ozaenae* (24) is highly specific for benzonitrile-derivatives with two meta-positioned

halogen atoms, but it does not act upon benzonitrile, which is a good substrate for the *R. rhodochrous* J1 nitrilase (23). A small difference in amino acid sequence between both nitrilases seems to bring about a large difference in substrate specificity. The protein sequence data base of the NBRF (National Biochemical Research Foundation)(120) was searched for sequences similar to the nitrilases from *R. rhodochrous* J1 and *K. ozaenae*. However, no homology was found. Comparison with the amino acid sequences of the *R. rhodochrous* J1 nitrilase revealed no similaritiy to those of two nitrile hydratases from *R. rhodochrous* J1 (13), although both nitrilase and nitrile hydratases acts upon a nitrile compound, suggesting that they have different enzymatic reaction mechanisms.

Production and purification of the nitrilase protein in *E. coli*

To overproduce the nitrilase in *E. coli*, a 1.3-kb *Pvu*I-*Nar*I fragment was inserted between the *Sma*I and *Acc*I sites of pUC18, resulting in pNJ11 (Fig. 1), in which the nitrilase gene was under the control of the *lac* promoter. When *E. coli* harboring pNJ11 was cultivated in the presence of IPTG at 37°C, nitrilase activity was detected in the supernatant of the sonicated cell-free extracts obtained at 12,000 x *g*. The author analyzed the production of the nitrilase in the supernatant of the sonicated extracts by SDS-PAGE and detected a 41.5-kDa synthesized protein corresponding to the subunit of the purified *R. rhodochrous* J1 nitrilase. However, the level of nitrilase activity in the supernatant was 0.080 unit/mg, which was low compared with that in cell-free extracts of *R. rhodochrous* J1 cells cultivated with isovaleronitrile (with benzonitrile as a substrate) (23).

primer 1

```
                SD
5' CCCAAGCTTTAAGGAGGAATAGGACATGGTCGAATACACAAAC 3'
     HindIII          Stop   Start
```

primer 2

```
5' ATCTCTAGATTGCCCTGTCTCA 3'
     XbaI
```

Fig. 4. Sequences of the oligonucleotide primers for expression of nitrilase gene. Primers 1 and 2 are the sense and antisense primers, respectively. The sequences are shown in the 5' to 3' direction.

To enhance the nitrilase activity, the author improved the sequence upstream of the ATG codon using PCR with pNJ10 as a template and two oligonucleotides as primers (Fig. 4). Primer 1 contained a *Hin*dIII recognition site, a ribosome binding site, and a TAG stop codon in-frame with the *lacZ* gene in pUC19 and 18 nucleotides (nucleotides 90-107 in Fig. 2) of *nitA* starting with the ATG start codon 9 nucleotides downstream of the ribosome-binding site. Primer 2 contained 22 nucleotides of the gene (complementary to nucleotides 1239-1260 in Fig. 2) 46 nucleotides downstream from the end of the reading frame, and a *Xba*I recognition site. The plasmid designated as pNJ20 was constructed by ligation of the PCR-product with pUC19/*Hin*dIII-*Xba*I, and transformed into *E. coli* JM105.

Table 1. Nitrilase activities of *E. coli* transformants under various culture conditions
The concentration of IPTG was 1 mM in 2 x YT medium.

IPTG feeding time	Cultivation time	Cultivation temperature	Specific activity
h	h	℃	units/mg
0[a]	6	28	0.150
0[a]	12	28	0.166
4[b]	7	28	0.140
4[b]	12	28	0.190
0[a]	6	37	3.68
0[a]	12	37	7.87
4[b]	7	37	3.72
4[b]	12	37	8.04

[a]IPTG was added to 2 x YT medium at the same time the culture was started.
[b]IPTG was added to 2 x YT medium 4 h after the start of culture.

In this construction, the *nitA* was under the control of the *lac* promoter. A protein corresponding to the purified *R. rhodochrous* J1 nitrilase subunit was synthesized only when the *lac* promoter was induced by IPTG. When *E. coli* carrying pNJ20 was cultured in the presence of IPTG, nitrilase activity was observed in the supernatant of the sonicated cell-free extracts, but not in the pellet obtained at 12,000 x *g*. The maximum level of nitrilase activity in the supernatant was 8.04 units/mg (Table 1). This value corresponded to 50.6% compared with the specific activity in the purified nitrilase from *R. rhodochrous* J1. The expression of the *nitA* was examined in the supernatant of the sonicated cell-free extracts by SDS-PAGE (Fig. 5). As judged by quantitative evaluation of the gel track with a dual-wavelength TLC Scanner CS-930 system (Shimadzu, Kyoto, Japan), the highest amount of the nitrilase formed corresponded to about 50% of the total soluble protein. Therefore, hyperproduction of the nitrilase was attained in the active form, whereas nitrile hydratases from *R. rhodochrous* J1 were produced as the insoluble form in *E. coli* (13).

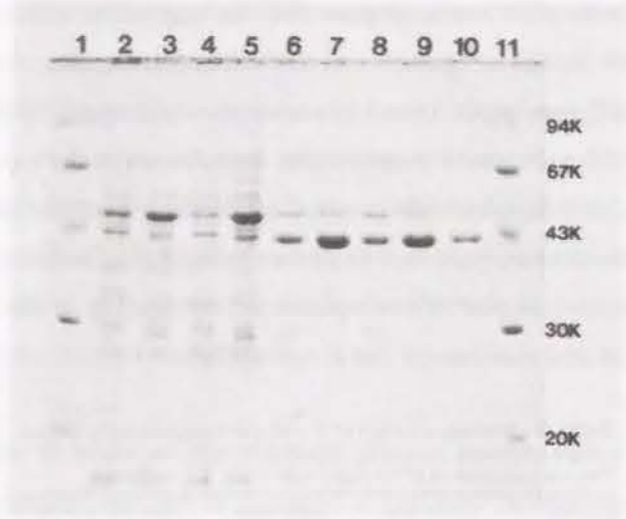

Fig. 5. SDS/PAGE of supernatant prepared from *E. coli* containing pNJ20.
Lanes 1 and 11 were loaded with the following molecular mass standards: phosphorylase (94 kDa), bovine serum albumin (67 kDa), ovalbumin (43 kDa), carbonic anhydrase (30 kDa), soybean trypsin inhibitor (43 kDa), carbonic anhydrase (14 kDa). Lanes 2-9 show supernatants of sonicates (60 µg protein). Lane 2, *E. coli* containing pNJ20, sample taken after a 6-h incubation at 28°C with IPTG; lane 3, same as lane 2, but after a 12-h incubation; lane 4, same as lane 2, but after a 7-h incubation, during which IPTG was added 4 h from the start; lane 5, same as lane 4, but after a 12-h incubation; lane 6, same as lane 2, but after a 6-h incubation at 37°C; lane 7, same as lane 6, but after a 12-h incubation; lane 8, same as lane 6, but after a 7-h incubation, during which IPTG was added 4 h from the start; lane 9, same as lane 8, but after a 12-h incubation; lane 10, purified nitrilase (15 µg of protein) from the sample derived from lane 9 as described in the text, as a control.

The nitrilase produced in the recombinant cells was purified through the following one-step column procedure at 0-4°C. Cell-free extract was fractionated with ammonium sulfate (33-50%, m/v), followed by dialysis against 0.01 M potassium phosphate buffer pH 7.5, containing 1 mM dithiothreitol. The dialyzed enzyme solution was applied to a Cellulofine GCL-2000 superfine column and eluted with 0.01 M potassium phosphate buffer (pH 7.5) containing 1 mM dithiothreitol. Active fractions were precipitated with 60% saturated ammonium sulfate and dialyzed against the above buffer. The purified enzyme, which showed only one band on SDS-PAGE (Fig. 5), gave almost the same physicochemical properties such as, specific activity and molecular mass, as the purified parental nitrilase from *R. rhodochrous* J1.

Reactivity with DTNB

Previous studies on *R. rhodochrous* J1 nitrilase (23) indicated that the enzyme is susceptible to thiol reagents and is therefore classfied as a sulfhydryl enzyme. In previous studies (23), incubation of the enzyme with DTNB for 10 min at 0°C resulted in loss of 92.2% of the activity. After incubation of the enzyme with DTNB for 2 h at 0°C in the presence of 8 M urea, 3.82 mol of TNB was detected per mol of enzyme subunit. By analyzing the amino acid composition (23) and the nucleotide sequence, the enzyme subunit was found to contain 4 mol of half-cystine. These findings indicate that each subunit has 4 free cysteine residues, but no disulfide bonds. Thereafter, DTNB was incubated with the enzyme in the absence of urea. The enzyme was fully inactivated when ~1 mol of DTNB reacted with 1 mol of enzyme subunit (Fig. 6). The relationship between the inactivation and modification (*i.e.*, TNB release) was proportional, that is, among four free sulfhydryl groups present in a subunit, only one reacted with DTNB. This relationship between the quantity of DTNB that reacted and the degree of inhibition, showed that modification of one sulfhydryl group per subunit by DTNB resulted in the complete loss of the catalytic activity of the parental nitrilase.

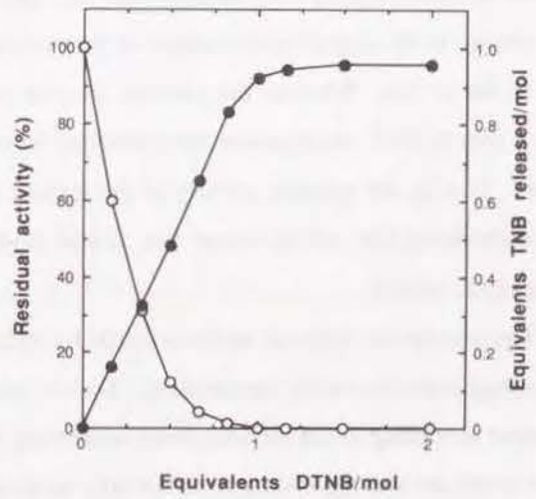

Fig. 6. Titration of sulfhydryl group of nitrilase with DTNB.
TNB released was determined by measuring the absorbance at 412 nm. Residual activity (○) and TNB released (●) were determined as described under "Materials and Methods".

The *R. rhodochrous* J1 nitrilase contains 4 cysteinyl residues (at positions 41, 165, 224, 238) (Fig. 3). Of these cysteine residues, only Cys-165 is conserved at the corresponding

position in the *K. ozaenae* nitrilase, and there is high sequence similarity around this cysteine. Judging from the comparison of overall amino acid sequences between these nitrilases, it seems that there is a considerable structural similarity. To determine whether Cys-165 is essential for nitrilase activity, this residue was replaced by site-directed mutagenesis.

Expression of mutant nitrilase genes

The author constructed two mutant enzymes in which Cys-165 was replaced with Ala or Ser. SDS-PAGE of cell-free extracts from the transformant cells harboring plasmids pNJ20-165S or pNJ20-165A, which were cultured under the same conditions used to overproduce the active nitrilase in the transformant carrying pNJ20, revealed a predominant protein band with a mobility identical to that of the non-mutationed nitrilase. Both mutant proteins were purified to homogeneity by SDS-PAGE according to the procedure used to purify nitrilase from extracts of the transformant cells harboring pNJ20. The purified C165S and C165A enzymes were immunochemically indistinguishable from the parental enzyme when examined by Ouchterlony double-diffusion analysis (121) using the anti-(nitrilase) anti-serum prepared as previously described (23). Their circular dichroism spectra in the far-UV region and molecular mass were also identical with those of the parental enzyme (data not shown). These results demonstrate that essentially no major change in the overall conformation of the enzyme protein was elicited by mutation of Cys-165 to Ser or Ala. Whereas the parental enzyme produced benzoic acid from benzonitrile within 5 min at 25°C, no products were detected from the mutant enzymes even after a 24 h reaction. That is, the specific activity of the mutant enzymes is below the detection threshold due to changing Cys-165 to Ala or Ser. These findings demonstrate that Cys-165 is essential for catalytic activity.

R. rhodochrous J1 produces one nitrilase and two nitrile hydratases depending on the inducer. This strain exhibited versatile nitrile metabolism. That in one strain the metabolic pathway completely changes according to the inducer, is an interesting phenomenon. Studies on nitrile-metabolizing enzymes are also significant from not only an academic standpoint such as the analysis of their gene-regulation but also from a biotechnological perspective including the production of useful acids or amides.

SUMMARY

The amino acid sequences of the NH_2 terminus and internal peptide fragments of a *Rhodococcus rhodochrous* J1 nitrilase were determined in order to prepare synthetic oligonucleotides as primers or the polymerase chain reaction. A 750 base DNA fragment thus amplified was used as the probe to clone a 5.4-kb *Pst*I fragment coding for the whole nitrilase. The nitrilase gene (*nitA*) modified in the sequence upstream of the presumed ATG start codon was expressed to about 50% of the total soluble protein in *Escherichia coli*. The predicted amino acid sequence from the *nitA* showed similarity with that of the bromoxynil nitrilase from *Klebsiella ozaenae*. The 5,5'-dithiobis(2-nitrobenzoic acid) modification of the nitrilase from *R. rhodochrous* J1 resulted in inactivation with the loss of one sulfhydryl group per enzyme subunit. Of four cysteine residues in the *Rhodococcus* nitrilase, only Cys-165 is conserved in the *Klebsiella* nitrilase. Mutant enzymes containing Ala or Ser instead of Cys-165 did not exhibit nitrilase activity. These findings suggest that Cys-165 plays an essential role in the function of the active site.

Section 2 Transcriptional regulation of *nitA*^{h}

Four cDNAs encoding nitrilases that convert indole-3-acetonitrile to IAA have been cloned and characterized from *Arabidopsis thaliana* (6-8). Pathogenic fungal species such as *Taphrina wiesneri*, *Taphrina deformans* and *Taphrina pruni*, which cause hyperplastic diseases in plants such as cherry, peach and plum, respectively, also form nitrilase involved in IAA biosynthesis, resulting in growth and division of infected plant cells (122).

In the author's laboratory, nitrilases from *Rhodococcus rhodochrous* J1 (23,123), *Rhodococcus rhodochrous* K22 (25,124) and *Alcaligenes faecalis* JM3 (5,26), which act on aromatic nitriles, aliphatic nitriles and arylacetonitriles, respectively were characterized in the protein and genetic studies. Stalker *et al.* have also cloned the bacterial *Klebsiella ozaenae* gene encoding nitrilase that degrades bromoxynil (24). However, the mechanisms that regulate nitrilase expression have not been reported. The nitrilases from *R. rhodochrous* J1, *R. rhodochrous* K22 and *A. faecalis* JM3 are all strongly induced by the addition of isovaleronitrile to the medium (23,25,26), making large amounts of enzyme available for application in industrial production of a wide range of useful acids from nitriles. In this section, the author describes characterization of the promoter and regulation of the nitrilase gene (*nitA*) in *R. rhodochrous* J1.

MATERIALS AND METHODS

Strains and plasmids

R. rhodochrous J1 was previously isolated from soil (29). *E. coli* JM109 (30) was the host for pUC plasmids. *R. rhodochrous* ATCC12674 was the host for a *Rhodococcus-E. coli* shuttle vector plasmid pK4 (31) and its derivatives, and was used for the expression of the nitrilase gene (*nitA*). The plasmid pNJ10 (123) carrying *nitA* in a 5.4-kb *Pst*I fragment on pUC19 was used for subcloning and sequencing of genes.

Transformation of *R. rhodochrous* ATCC12674 by electroporation

DNA manipulation was performed essentially as described by Sambrook *et al.* (30). A mid-exponential culture of *R. rhodochrous* ATCC12674 was centrifuged at 6,500 x *g* for 10 min at 4°C and washed three times with demineralized cold water. Cells were then concentrated 20-fold in demineralized cold water and kept on ice. Ice-cold cells (100 µl) were mixed with 1

µg DNA in 1 µl of TE buffer (10 mM-Tris/1 mM EDTA, pH 8.0) in a 1-mm-gapped electrocuvette (Bio-Rad, Richmond), and subjected to a 2.0 kV electric pulse from a Gene Pulser (Bio-Rad) connected to a pulse controller (25 µF capacitor; external resistance, 400Ω). Pulsed cells were diluted immediately with 1 ml of MYP medium (31) and incubated for 2 h at 26°C. They were then spread on MYP medium containing 75 µg kanamycin/ml.

Preparation of cell extracts and enzyme assay

R. rhodochrous ATCC12674 transformants were cultured at 28°C for 24 h in MYP medium in the presence or absence of isovaleronitrile (0.1% v/v), harvested by centrifugation at 4,000 x g at 4°C, and washed with 10 mM potassium phosphate buffer (pH 7.5). The washed cells were suspended in 0.1 M potassium phosphate buffer (pH 7.5) containing 1 mM dithiothreitol and 20% (v/v) glycerol, disrupted by sonication for 20 min (19 kHz, Insonator model 201M; Kubota, Tokyo, Japan), and centrifuged at 12,000 x *g* for 10 min at 4°C. The resulting supernatant was assayed for nitrilase as previously described (123). One unit of nitrilase catalyzes the formation of 1 µmol of benzoic acid/min under the above conditions. The protein was determined according to Bradford (59). The specific activity is expressed as units/mg of protein.

RNA preparation

R. rhodochrous J1 collected from an agar slant was inoculated into a test tube containing 5 ml of a medium consisting of 5 g Polypepton (Daigo, Osaka, Japan), 5 g meat extract (Mikuni, Tokyo, Japan), 0.5 g yeast extract (Oriental Yeast, Tokyo, Japan) and 2 g NaCl/l tap water (pH 7.0), and incubated at 28°C for 24 h with reciprocal shaking. From this, 1.6 ml was inoculated into a 500-ml shaking flask containing 100 ml of a medium [10 g glycerol, 5 g Polypepton, 3 g malt extract and 3 g yeast extract/l tap water (pH 7.2)] with or without isovaleronitrile (0.1%, w/v), and incubated at 28°C for 48 h with aeration. Cells were collected from 60 ml of such cultures by centrifugation, and total RNA was extracted by the AGPC (acid-guanidium-phenol-chloroform) method (32).

Northern (RNA) blot hybridization

For Northern blot hybridization, each RNA sample (30 µg) was subjected to electrophoresis on a 1% agarose-formaldehyde gel, and transferred to a nitrocellulose membrane filter (Schleicher & Schuell, Germany) in 20 x SSC (1 x SSC = 0.15 M NaCl, 15

mM sodium citrate). Prehybridization and hybridization were carried out at 42°C in a solution consisting of 40% (v/v) formamide, 5 x SSC, 0.1% (w/v) SDS and 100 mg/ml of sonicated salmon sperm DNA. The DNA fragments used as probes were radiolabeled with a multiprime DNA labeling system (Amersham). Filters were washed twice at room temperature in 40% formamide, 5 x SSC, 0.1% SDS, and then washed three times at room temperature in 2 x SSC solution with 0.1% SDS.

Primer extension analysis

The primer 5'-GAATGTGTTTGTGTATTCGACCATG-3', complement-ary to positions 620 to 644 (Fig. 3), was synthesized, and then labeled with [^{32}P] at the 5' end by polynucleotide kinase. Reverse transcriptase-mediated primer extension was performed by the method of Sambrook *et al.* (30).

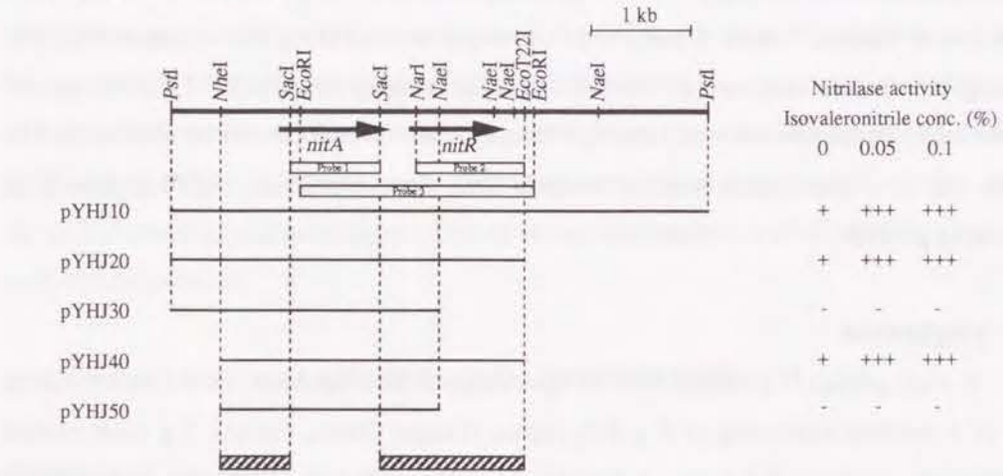

Fig. 1. Construction of a set of plasmids (left column) and nitrilase activity of each *R. rhodochrous* ATCC12674 transformant (right column).
(Left column) For clarity, only restriction sites discussed in the text are shown. Various deletion plasmids are diagrammed below the restriction map. Plasmids (pYHJ10~50) were constructed by inserting each restriction fragment from pNJ10 into the *Pst*I site or *Pst*I site that had been filled in with T4 DNA polymerase, of pK4. In the case of pYHJ40 and pYHJ50, the *Nhe*I sites of their inserted fragments were also filled in with T4 DNA polymerase during the construction. The region sequenced this time is indicated by shaded boxes. The probes used in the Northern blot analysis are shown by boxes. (Right column) Nitrilase activity of whole cells was detected as described in Materials and Methods using benzonitrile as a substrate. +++, much; +, trace; -, not detected.

RESULTS

Expression of *nitA* in *R. rhodochrous* ATCC12674

To identify the sequence element required for the expression of *nitA*, I constructed a set of plasmids containing sub-fragments of a 5.4-kb *Pst*I fragment from pNJ10 (123) inserted at

the *Pst*I site of the *Rhodococcus-E. coli* shuttle vector pK4 (Fig. 1). These plasmids were used to transform *R. rhodochrous* ATCC12674 and the resulting transformants were cultured in MYP medium (31) with or without isovaleronitrile (0.1% v/v). Enzyme assays using benzonitrile as a substrate for each cell suspension (Fig. 1) or cell-free extract (Table 1) revealed that, in addition to *nitA* itself, at least a 0.6-kb upstream region (from the *Nhe*I site to the 5' end terminus of *nitA*) and a 1.4-kb downstream region (from the 3' end terminus of *nitA* to the *Eco*T22I site) are required for the appearance of nitrilase activity, as in pYHJ40. As previously found in *R. rhodochrous* J1 (11, 23), the presence of isovaleronitrile in the culture medium showed salient enhancement of nitrilase activity in the *Rhodococcus-E. coli* host-vector system used in this experiment. The transformant harboring pYHJ20 exhibited the highest activity [0.537 μmol•min^{-1}•(mg protein)$^{-1}$].

Table 1. Nitrilase activity in cell-free extracts of *R. rhodochrous* ATCC12674 transformants containing various plasmids.

Plasmid	Isovaleronitrile	Specific activity (U/mg)
pK4	-	N.D.
	+	N.D.
pYHJ10	-	0.003
	+	0.193
pYHJ20	-	0.019
	+	0.537
pYHJ30	-	N.D.
	+	N.D.
pYHJ40	-	0.002
	+	0.297
pYHJ50	-	N.D.
	+	N.D.

N.D. : not detected.

Nitrilase formation in the transformants was examined by SDS-PAGE (Fig. 2). The transformants carrying pYHJ10, pYHJ20 or pYHJ40 expressed larger amounts of a protein of 41.5 kDa, in the presence of isovaleronitrile, than the transformants carrying pK4, pYHJ30 or pYHJ50. The protein, which corresponded to about 4% of all soluble protein in the supernatant of cell-free extracts of the pYHJ20-carrying transformant cultured in the presence of isovaleronitrile, were found to be the nitrilase encoded by *nitA* by its N-terminal amino acid sequence on a gas-phase amino acid sequencer (Applied Biosystems Japan, 470A, Tokyo) (Fig. 3). When the pK4-derivative plasmids used in this experiment were introduced into *E. coli* JM109, nitrilase activity could not be detected, even after culture in the presence of

isovaleronitrile (data not shown), suggesting that an *E. coli* RNA polymerase could not recognize the promoter of *nitA* from *R. rhodochrous* J1.

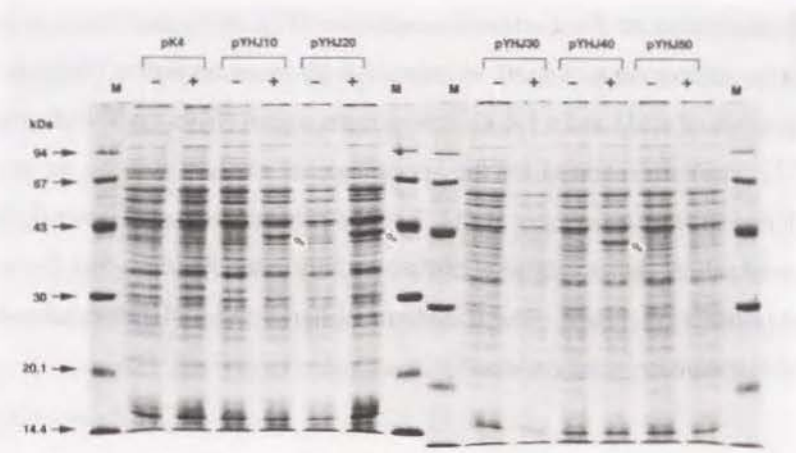

Fig. 2. Coomassie-stained SDS-PAGE showing nitrilase formation in *R. rhodochrous* ATCC12674 transformants.
Lanes indicated by M were loaded with the following molecular mass standards: phosphorylase (94 kDa), bovine serum albumin (67 kDa), ovalbumin (43 kDa), carbonic anhydrase (30 kDa), soybean trypsin inhibitor (20.1 kDa) and a-lactalbumin (14.4 kDa). Lanes indicated by +, 100 μg of cell-free extracts from the *R. rhodochrous* ATCC12674 transformants cultured in the medium supplemented with (0.1%, v/v) isovaleronitrile; Lanes indicated by -, 100 μg of cell-free extracts from the *R. rhodochrous* ATCC12674 transformants cultured in the absence of isovaleronitrile. The open arrows indicate the band corresponding to the nitrilase.

Primary structure of the flanking region of *nitA*

The *Bsm*I-*Pvu*I 1.29-kb fragment containing *nitA* was sequenced previously (123). The author further sequenced the *Nhe*I-*Bsm*I upstream region and the *Pvu*I-*Eco*T22I downstream region required for nitrilase production (Fig. 3).

An ORF (start and stop codons at nucleotides 1970 ATG and 2927 TAG, respectively) downstream of *nitA* was 957 nucleotides long, and encoded a protein of 319 amino acids (35.1 kDa). The ORF was designated *nitR*. The *nitR* gene product (NitR) is significantly similar in amino acid sequence to the positive regulator XylS of a xylene-metabolism in *Pseudomonas putida* (125) and to AraC, the positive regulator of arabinose-metabolism in *E. coli* (126): 20.3% identity of amino acids in 310 overlapping residues between NitR and XylS; 17.1% identity in 282 residues between NitR and AraC (Fig. 4). The similarities were confined to the carboxyl termini of the proteins. The similarity of NitR to XylS and AraC, and the importance of nitR for nitrilase production, provided strong evidence that NitR is a positive regulator of *nitA* expression.

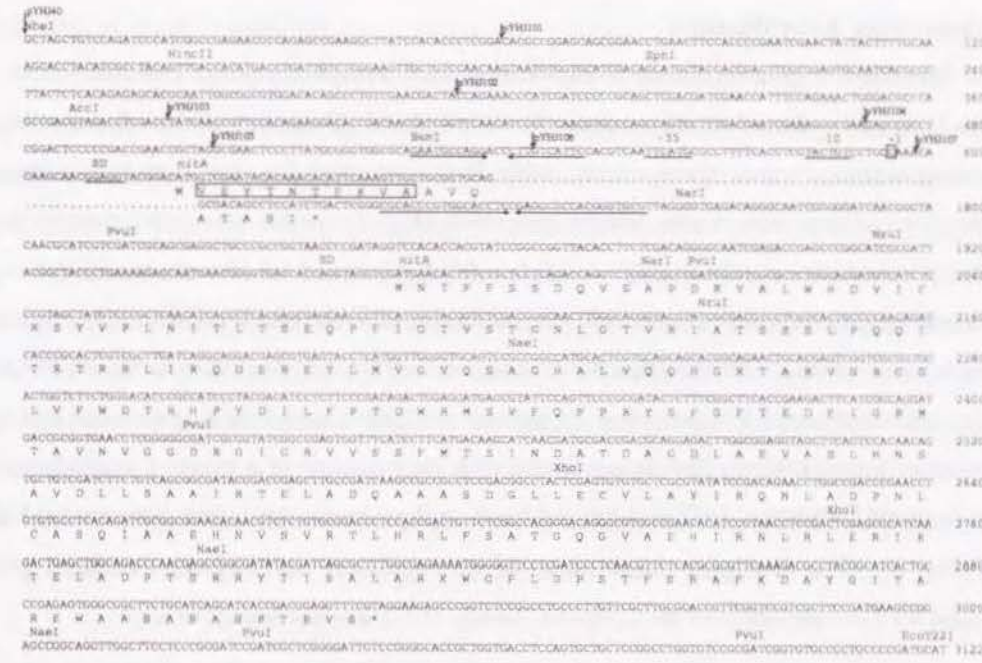

Fig. 3. Nucleotide sequence of flanking region of *nitA* from *R. rhodochrous* J1.
The deduced amino acid sequences using standard one-letter amino acid abbreviations are shown below their respective nucleotide sequences. Boxed amino acid residues indicate the N-terminal sequence of nitrilase determined by Edman degradation. Shine-Dalgarno sequences are underlined. The stop codons are indicated by asterisks. The cytidine residue in a box is the transcriptional start site of *nitA* determined by primer extension analysis. The *nitA* sequence (denoted with gaps) was published earlier (13, GenBank accession no. D11425). Endpoints of deletions introduced from upstream are marked by vertical arrows. Inverted repeats are shown by converging arrows.

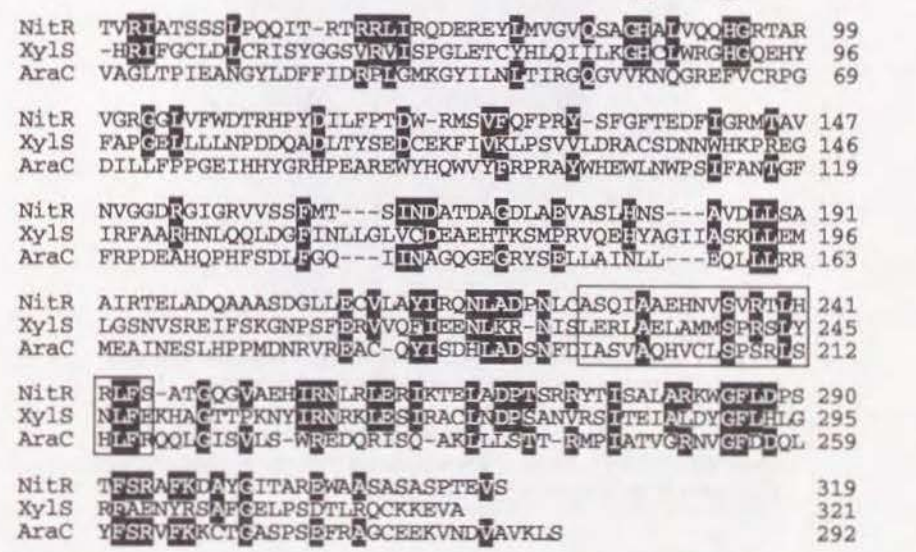

Fig. 4. Comparison of amino acid sequences of NitR from *R. rhodochrous* J1 and homologous proteins.
Amino acid sequences of NitR from *R. rhodochrous* J1, XylS from *P. putida* (125) and AraC from *E. coli* (126) were aligned by introducing gaps (hyphens) to achieve maximum homology. Residues in black boxes indicate identical sequences. The helix-turn-helix motif (amino acids 226-245 of NitR) is enclosed by boxes.

Northern blot hybridization

The DNA fragments shown in Fig. 1 were used as probes against total RNA from *R. rhodochrous* J1 cultured in the medium in the presence or absence of isovaleronitrile, to determine whether transcription of *nitA* and *nitR* was altered by the culture conditions. Northern blots were probed with labeled fragments (Fig. 1) specific for *nitA* (probe 1), *nitR* (probe 2) or *nitA* plus *nitR* (probe 3). A single mRNA species of 1.4 kb corresponding to *nitA* was found only in induced cultures (Fig. 5), indicating that nitrilase formation is regulated at the transcriptional level. On the other hand, almost no mRNA corresponding to the *nitR*-coding region could be detected irrespective of the culture conditions, demonstrating that *nitA* and *nitR* are separately transcribed. This is consistent with the presence of a putative ρ-independent transcriptional terminator (ΔG = -44.6 kcal/mol) in the non-coding region between *nitA* and *nitR* (Fig. 3). The divergent transcription of the regulatory and cognate structural genes observed for most members of the xylS/araC family (127) was not found for *nitR*.

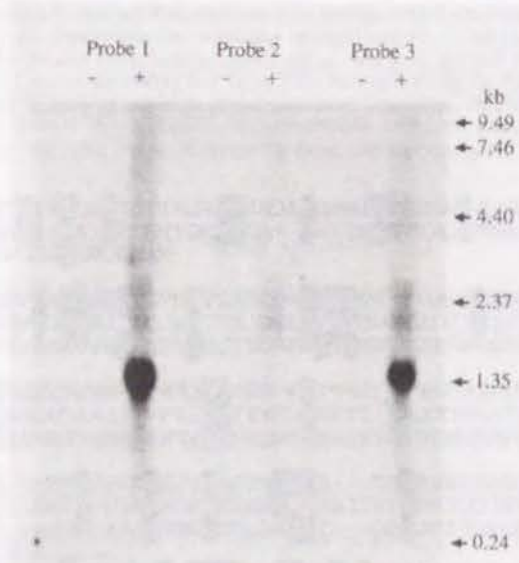

Fig. 5. Northern blot analysis of *R. rhodochrous* J1
An RNA ladder (Bethesda Research Laboratories) was used as a size marker. The probes used in the experiment are shown in Fig. 1. Lanes indicated by +, 30 μg of RNA extracted from the *R. rhodochrous* J1 cultured in the medium supplemented with (0.1%, v/v) isovaleronitrile; Lanes indicated by -, 30 μg of RNA extracted from the *R. rhodochrous* J1 cultured in the absence of isovaleronitrile.

Mapping of *nitA* transcript

Since nitrilase is produced at high levels in *R. rhodochrous* J1 (23) and in the appropriate *R. rhodochrous* ATCC12674 transformants after induction (Fig. 2), a strong promoter containing a binding site specific for NitR was expected to be present close to *nitA*. To map the initiation site of *nitA* transcription, the author used primer extension analysis with total RNA from *R. rhodochrous* J1 grown in the medium in the presence or absence of isovaleronitrile. A single site of initiation of transcription was identified at nucleotide position 595, only in RNA from the induced culture (Fig. 6). This nucleotide is 26 bp upstream from the ATG initiation codon of *nitA* (Fig. 3). Around 35 bp upstream of the transcriptional start site, possible -35 (TTCATG) and -10 (TACTGT) sequences have been found, which were similar to those of *casA*, a cellulase gene from *Streptomyces* sp., [(TTCACC) for -35 and (TACCGT) for -10] (128).

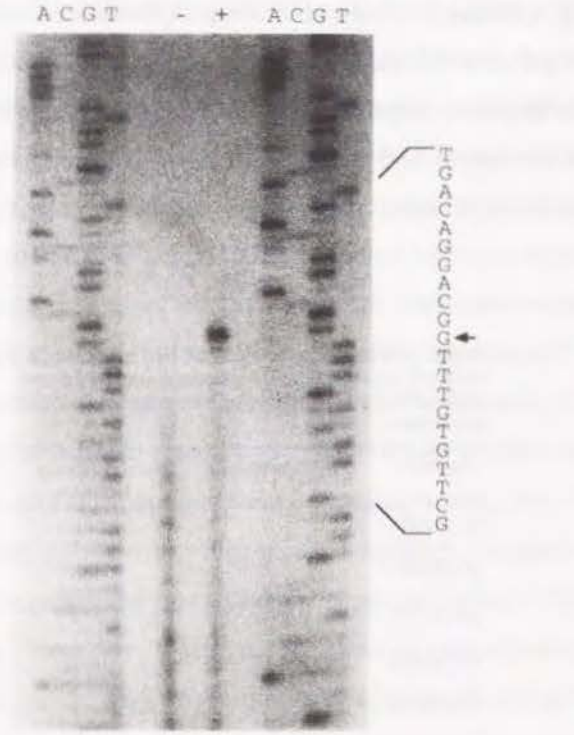

Fig. 6. Mapping of the 5' end of the *nitA* transcript.
Primer extension analysis using total RNA isolated from *R. rhodochrous* J1 cultured in the presence (lane indicated by +) or absence (lane indicated by -) of isovaleronitrile was carried out. Primer extended products were electrophoresed in parallel with sequence ladders generated with the same primer. The position of the transcription start site is marked by an arrow.

Truncation of the upstream sequence of *nitA*

To define more precisely the region of the promoter essential for the isovaleronitrile-inducible expression of *nitA*, deletions were introduced in the upstream region of *nitA*. The *Nhe*I-*Eco*T22I fragment (= the inserted fragment of pYHJ40) from pNJ10 was inserted into the *Eco*RV-*Pst*I sites of pBluescript SK(+) after the *Nhe*I end was filled in with T4 DNA polymerase. The resulting plasmid pNITUP was used to generate deletions from the *Nhe*I/*Eco*RV site. The area deleted from the insert was determined by restriction endonuclease mapping and subsequent DNA sequence analysis of the deletion mutants, as shown in Fig. 3. Each shortened fragment was ligated into pK4, and the resulting plasmids (pYHJ101~pYHJ107) were used to transform *R. rhodochrous* ATCC 12674. The transformants were assayed for the ability to produce nitrilase with or without isovaleronitrile using MYP medium. In *R. rhodochrous* ATCC12674, the smallest insert conferring nitrilase activity was pYHJ105 containing an 89 bp sequence upstream from the transcriptional start site. Transformants harboring pYHJ106 containing a 47 bp upstream sequence of the transcriptional start site or pYHJ107 containing a 22 bp upstream sequence of the translational start codon, showed no nitrilase activity (Table 2). An inverted repeat sequence centered at -52 was entirely contained in pYHJ105, but all of the left hand half of the repeat and 3 bp of the right hand half were missing in pYHJ106, suggesting that the inverted repeat could possibly serve as a binding site for NitR.

Table 2. Nitrilase activity in cell-free extracts of *R. rhodochrous* ATCC12674 transformants containing plasmids in which the upstream sequence of *nitA* was deleted.

Plasmid	Isovaleronitrile	Specific activity (U/mg)
pYHJ40	-	0.002
	+	0.297
pYHJ101	-	0.008
	+	0.425
pYHJ102	-	0.009
	+	0.433
pYHJ103	-	0.004
	+	0.514
pYHJ104	-	0.009
	+	0.530
pYHJ105	-	0.005
	+	0.476
pYHJ106	-	N.D.
	+	N.D.
pYHJ107	-	N.D.
	+	N.D.

N.D. : not detected.

DISCUSSION

In this section, a *Rhodococcus* host-vector system was used to examine the mechanism involved in the control of *nitA* expression, using as host *R. rhodochrous* ATCC12674, which exhibited no detectable nitrilase activity (Fig. 1, Table 1). The author has demonstrated that the transcription of *nitA* is regulated in response to isovaleronitrile added to the culture medium both in the original *nitA*-containing *R. rhodochrous* J1 and in the appropriate transformants of *R. rhodochrous* ATCC 12674. Evidence is also presented for the existence of the regulatory gene, *nitR*, the product of which (NitR) is required for the isovaleronitrile-dependent induction of *nitA*. NitR is related to bacterial transcriptional regulators belonging to the XylS/AraC family. This family, members of which are positive regulators involved in metabolism of carbon sources and in pathogenesis, is characterized by the sequence similarity within the carboxyl terminus, which is the region containing a helix-turn-helix DNA binding motif (127, 129). Among this family, for regulators recognizing chemical signals (inducers), the non-conserved N-terminal region is presumed to be responsible for binding the activator molecule. Deletion of the central and 3'-terminal region of *nitR* resulted in the complete loss of *nitA*-encoded nitrilase activity. In the previous section, the author showed that *nitA* modified in the sequence upstream of the ATG start codon is expressed under the control of the *lac* promoter to ~50% of the total soluble protein in *E. coli* JM105, even when *nitR* is absent in the downstream region of *nitA* (123). This finding as well as the result from the Northern blot analysis indicates that *nitR* functions as a transcriptional activator for the formation of NitA.

The author described the mapping of a transcript in *Rhodococcus* species for the first time. Since the amount of nitrilase produced by *R. rhodochrous* J1 after induction can reach 35% of all soluble protein, *nitA* is expected to have a strong promoter. The -35 and -10 regions for the transcriptional start site of *nitA* were selected by their sequence similarity to the Actinomycete, mainly Streptomycete consensus promoter sequence, TTGAC(A/G) -17bp-TAg(A/G)(A/G)T (130). However, the relatively short (15 bp) distance between these hexamers in *R. rhodochrous* J1 may imply that the putative -35 region does not play an important role, a situation not uncommon among promoter dependent on additional transcriptional activator including those dependent on XylS or AraC. On the other hand, the similarity of the *nitA* promoter sequence to the *E. coli* consensus is relatively low, consistent with the failure of the pK4-derivative plasmids used in this experiment to direct detectable

nitrilase production in *E. coli* JM109. Deletion analysis suggested the possible participation of an inverted repeat sequence, centered on bp -52, in induction of *nitA* transcription.

A new family of carbon-nitrogen hydrolases has recently been proposed (131,132) by several conserved motifs, one of which contains an invariant cysteine as demonstrated in the nitrilases (5,123,124). Nitrilases are significantly similar to aliphatic amidases, cyanide hydratases and β-alanine synthase. The expression of an aliphatic amidase, which is induced by amides such as acetamide and propion-amide, is regulated by both a negative regulator, AmiC and a positive regulator, AmiR in *Pseudomonas aeruginosa* (40). The regulation mechanism of *nitA* in *R. rhodochrous* J1 is different from that of the aliphatic amidase. Further studies on nitrilases at both protein and gene levels could provide information about their evolutionary implication.

SUMMARY

The 1.4-kb downstream region from a nitrilase gene (*nitA*) of *Rhodococcus rhodochrous* J1 was found to be required for the isovaleronitrile-dependent induction of nitrilase synthesis in experiments using a *Rhodococcus-Escherichia coli* shuttle vector pK4 in a *Rhodococcus* strain. Sequence analysis of the 1.4-kb region revealed the existence of an open reading frame (*nitR*) of 957 bp which would encode a protein with a *M*r of 35,100. Its deduced amino acid sequence showed similarity to a positive regulator family including XylS from *Pseudomonas putida* and AraC from *Escherichia coli*. Deletion of the central and 3' terminal portion of *nitR* resulted in the complete loss of nitrilase activity. The *nitR* protein product was required for nitrilase synthesis. These findings strongly demonstrate that *nitR* codes for a transcriptional positive regulator in *nitA* expression. By Northern blot analysis, the 1.4-kb transcripts for *nitA* were detected in *R. rhodochrous* J1 cells cultured in the presence of isovaleronitrile but not those cultured in the absence of isovaleronitrile. Almost no transcripts for *nitR* were detected even in the presence of isovaleronitrile in the medium, suggesting that its transcription was relatively poor. The transcriptional start site for *nitA* was mapped to a C residue located 26 bp upstream of its translational start site. Deletion analysis to define the *nitA* promoter region suggested the possible participation of an inverted repeat sequence, centered on bp -52, in induction of *nitA* transcription.

CONCLUSION

In this thesis, the author investigated the organization and regulation of genes involved in nitrile metabolism in *Rhodococcus rhodochrous* J1, which is used in the industrial production of useful amides. The results described in each chapter are summarized as follows:

CHAPTER I

This chapter described the gene organization of high molecular-mass nitrile hydratase (H-NHase) from *R. rhodochrous* J1.

Genes required for the expression of (H-NHase) were identified by using a host-vector system in *Rhodococcus*. Sequence analysis of the DNA region responsible for *nhhBA* expression revealed the presence of at least five open reading frames (*nhhC*, *nhhD*, *nhhE*, *nhhF* and *nhhG*) in addition to *nhhBA*. Deletion of *nhhC* or *nhhD* resulted in decrease of NHase activity, suggesting a positive regulatory role for both genes in the expression of the *nhhBA*. NhhC showed significant similarity to a regulatory protein, AmiC, which is involved in regulation of amidase expression by binding an inducer amide in *Pseudomonas aeruginosa*. *nhhF*, which has been found to be uninvolved in regulation of *nhhBA* expression by enzyme assay for its deletion transformant and by Northern blot analysis for *R. rhodochrous* J1, showed high similarity of the amino acid sequence to transposases from insertion sequences of several bacteria. Determination of H-NHase activity and *nhhBA* mRNA levels in *R. rhodochrous* J1 indicated that the expression of *nhhBA* is regulated by an amide at the transcriptional level (Section 1).

The author investigated the insertion sequence (IS*1164*) from *Rhodococcus rhodochrous* J1. In addition, the author compared the structure of IS*1164* and IS*1081*, which shows the highest similarity to IS*1164*, and found two pairs of terminal inverted repeats flanking their probable transposases. This 1430 bp-long IS has two pairs of imperfect terminal inverted repeats (IR-1 and IR-2) flanked by nine base pair direct repeats (DR), and contains an open reading frame encoding a putative transposase. Structures of the terminal region containing inverted repeats were found to be highly conserved both in IS*1164* and in IS*1081* from *Mycobacterium bovis*. Hybridization analyses against total DNA from *R. rhodochrous* J1, 16 *Rhodococcus* strains and 3 other bacteria catabolizing nitriles as well as *R. rhodochrous* J1 showed that *R. rhodochrous* J1 had three other IS*1164*-like elements, and 11 out of 16

Rhodococcus strains contained IS*1164*-like elements varying in copy number from one to at least seven (Section 2).

CHAPTER II

This chapter described the structure of flanking region of low molecular-mass nitrile hydratase (L-NHase) gene from *R. rhodochrous* J1 and its regulation.

The author presented the evidence that at least two amidases exist in *R. rhodochrous* J1. *R. rhodochrous* J1 produced at least two amidases differing in substrate specificity, judging from the effects of various amides on amidase activity in this strain. These amidases seemed to be inducible enzymes depending on amide compounds (Section 1).

The author cloned and sequenced the amidase gene, which was considered to be linked to the L-NHase gene (*nhlBA*). This amidase gene (*amdA*) was located 1.9-kb downstream of *nhlA*. Therefore, gene arrangement of the amidase and the NHase in *R. rhodochrous* J1 differed from those in *Rhodococcus* sp. N-774, *Pseudomonas chlororaphis* B23 and *Rhodococcus* sp. The nucleotide sequence indicated that the amidase consisted of 515 amino acids (M_r = 54,626 Da), and the deduced amino acid sequence of the amidase had high similarity to those of amidases from *Rhodococcus* species including N-774 and *P. chlororaphis* B23 and indole-3-acetamide hydrolase from *Pseudomonas savastanoi*. The amidase gene (*amdA*) modified in the nucleotide sequence upstream from its start codon expressed 8% of the total soluble protein in *E. coli* under the control of *lac* promoter, and the amidase was purified from extracts of the *E. coli* transformant and characterized. The relative molecular mass of the enzyme estimated by HPLC was about 110 kDa, and the enzyme consists of two subunits identical in molecular mass (55 kDa). The enzyme acted upon aliphatic amides such as propionamide and also upon aromatic amides such as benzamide. It was highly specific for the *S*-enantiomer of 2-phenylpropionamide, but could not recognize the configuration of 2-chloropropionamide. It also catalyzed the transfer of an acyl group from an amide to hydroxylamine to produce the corresponding hydroxamate (Section 2).

The author identified the genes required for the amide-dependent induction of low molecular-mass nitrile hydratase (L-NHase). The 3.5-kb of 5'-upstream region from *nhlBA* was required for the amide-dependent expression of *nhlBA* in a *Rhodococcus* host strain. Sequence analysis of the region revealed the presence of two open reading frames, *nhlD* and *nhlC*. *nhlD* had similarity to regulatory genes *merR*, *cadC* and *arsR*, which are all located upstream of the heavy metal resistance genes (*merAB*, *cadA* and *arsBC*, respectively) and are

supposed to have transcriptional regulatory functions for the resistance genes. NhlC had similarity to the regulators AmiC for the expression of an aliphatic amidase from *P. aeruginosa* and NhhC for the expression of *nhhBA* from *R. rhodochrous* J1. Assay for NHase activity of transformants carrying *nhlD* deletion or *nhlC* deletion suggested a negative regulatory role for *nhlD* and a positive regulatory role for *nhlC* in the process of the L-NHase formation. Assay for NHase and amidase activities and Western blot analysis of various *Rhodococcus* transformants carrying each deletion-plasmid, showed that *nhlBA* and *amdA* were regulated in the same manner. These findings presented the genetic evidence for a novel gene cluster of L-NHase and amidase induced by amide compounds in *R. rhodochrous* J1 (Section 3).

Cobalt is an essential component of L-NHase from *R. rhodochrous* J1. The author identified a new gene, *nhlF*, in the intervening region between *nhlBA* and *amdA*. The product of *nhlF*, NhlF, showed a significant sequence similarity with those of *hoxN* from *Alcaligenes eutrophus*, *hupN* from *Bradyrhizobium japonicum*, *nixA* from *Helicobacter pylori* and *ureH* from *Bacillus* sp., which are considered to be involved in nickel uptake into these cells. Sequence and hydropathy plot analyses showed that NhlF was a 352-amino acid protein with eight hydrophobic putative membrane-spanning domains. *nhlF* expression conferred uptake of ^{57}Co upon *R. rhodochrous* ATCC12674 and *E. coli* JM109 host cells. The studies using uncouplers suggested that proton gradients are involved in the cobalt transport. These findings suggested that NhlF located in cell membrane energy-dependently mediates the transport of cobalt ions into the cell and therefore facilitates its incorporation into the L-NHase enzyme (Section 4).

CHAPTER III

This chapter described the structure and regulation of nitrilase gene from *R. rhodochrous* J1.

The author cloned and sequenced the nitrilase gene (*nitA*) from *R. rhodochrous* J1. The predicted amino acid sequence from *nitA* showed similarity with that of the bromoxynil nitrilase from *Klebsiella ozaenae*. *nitA* modified in the sequence upstream of the presumed ATG start codon was expressed to about 50% of the total soluble protein in *E. coli*. The 5,5'-dithiobis(2-nitrobenzoic acid) modification of the nitrilase from *R. rhodochrous* J1 resulted in inactivation with the loss of one sulfhydryl group per enzyme subunit. Mutant enzymes containing Ala or Ser instead of Cys-165 which was only conserved in the *Klebsiella* nitrilase

did not exhibit nitrilase activity. These findings suggested that Cys-165 played an essential role in the function of the active site (Section 1).

The author investigated the regulation of *nitA* expression in *R. rhodochrous* J1. The 1.4-kb downstream region from *nitA* was responsible for the isovaleronitrile-dependent induction of nitrilase synthesis in a *Rhodococcus* host strain. Sequence analysis of the region revealed the existence of a new gene, *nitR*, which would encode a protein with *M*r of 35,100. Its deduced amino acid sequence showed similarity to a positive regulator family including XylS from *P. putida* and AraC from *E. coli*. Deletion of the central and 3' terminal portion of *nitR* resulted in the complete loss of nitrilase activity. These findings together with the result that *nitA* modified in the sequence upstream of the ATG start codon was highly expressed under the control of the *lac* promoter in *E. coli*, even when *nitR* was absent in the downstream region of *nitA*, strongly demonstrated that *nitR* coded for a transcriptional positive regulator in *nitA* expression. By Northern blot analysis, the 1.4-kb transcripts for *nitA* were detected in *R. rhodochrous* J1 cells cultured in the presence of isovaleronitrile but not those cultured in the absence of isovaleronitrile. The transcriptional start site for *nitA* was mapped to a C residue located 26 bp upstream of its translational start site. Deletion analysis to define the *nitA* promoter region suggested the possible participation of an inverted repeat sequence, centered on bp -52, in induction of *nitA* transcription (Section 2).

REFERENCES

1. Conn, E.E. (1981) in Cyanide in Biology, (eds. Vennesland, B., Conn, E.E., Knowles, C.J., Westley, J. & Wissing, F.), pp. 183-196, Academic Press, New York.
2. Yamada, H. & Kobayashi, M. (1996) *Biosci. Biotech. Biochem.* in press.
3. Asano, Y., Tani, Y. & Yamada, H. (1980) *Agric. Biol. Chem.* **44**, 2251-2252.
4. Kobayashi, M. & Shimizu, S. (1994) *FEMS Microbiol. Lett.* **120**, 217-224.
5. Kobayashi, M., Izui, H., Nagasawa, T. & Yamada, H. (1993) *Proc. Natl. Acad. Sci. USA* **90**, 247-251.
6. Bartling, D., Seedorf, M., Mithofer, A. & Weiler, E.W. (1992) *Eur. J. Biochem.* **205**, 417-424.
7. Bartling, D., Seedorf, M., Schmidt, R.C. & Weiler, E. W. (1994) *Proc. Natl. Acad. Sci. USA* **91**, 6021-6025.
8. Bartel, B. & Fink, G.R. (1994) *Proc. Natl. Acad. Sci. USA* **91**, 6649-6653.
9. Kobayashi, M., Suzuki, T., Fujita, T., Masuda, M. & Shimizu, S. (1995) *Proc. Natl. Acad. Sci. USA* **92**, 714-718.
10. Kobayashi, M., Nagasawa, T. & Yamada, H. (1992) *Trends in Biotechnol.* **10**, 402-408.
11. Nagasawa, T., Kobayashi, M. & Yamada, H. (1988) *Arch. Microbiol.* **150**, 89-94.
12. Nagasawa, T., Takeuchi, K. & Yamada, H. (1991) *Eur. J. Biochem.* **196**, 581-589.
13. Kobayashi, M., Nishiyama, M., Nagasawa, T., Horinouchi, S., Beppu, T. & Yamada, H. (1991) *Biochim. Biophys. Acta* **1129**, 23-33.
14. Ikehata, O., Nishiyama, M., Horinouchi, S. & Beppu, T. (1989) *Eur. J. Biochem.* **181**, 563-570.
15. Nishiyama, M., Horinouchi, S., Kobayashi, M., Nagasawa, T., Yamada, H. & Beppu, T. (1991) *J. Bacteriol.* **173**, 2465-2472.
16. Nagasawa, T. & Yamada, H. (1989) *Trends in Biotechnol.* **7**, 153-158.
17. Robinson, W.G. & Hook, R.H. (1964) *J. Biol. Chem.* **239**, 4257-4262.
18. Hook, R.H. & Robinson, W.G. (1964) *J. Biol. Chem.* **239**, 4263-4267.
19. Harper, D.B. (1985) *Int. J. Biochem.* **17**, 677-683.
20. Harper, D.B. (1977) *Biochem. J.* **165**, 309-319.
21. Harper, D.B. (1977) *Biochem. J.* **167**, 685-692.

22. Bandyopadhyay, A.K., Nagasawa, T., Asano Y., Fujishiro, K., Tani, Y. & Yamada, H. (1986) *Appl. Environ. Microbiol.* **51**, 302-306.
23. Kobayashi, M., Nagasawa, T. & Yamada, H. (1989) *Eur. J. Biochem.* **182**, 349-356.
24. Stalker, D.M., Malyj, L.D. & McBride, K.E. (1988) *J. Biol. Chem.* **263**, 6310-6314.
25. Kobayashi, M., Yanaka, N., Nagasawa, T. & Yamada, H. (1990) *J. Bacteriol.* **172**, 4807-4815.
26. Nagasawa, T., Mauger, J. & Yamada, H. (1990) *Eur. J. Biochem.* **194**, 765-772.
27. Goodfellow, M. (1986) in Sneath, P.H.A., Mair, N.S., Sharpe, M.E. & Holt, J.G. (ed.), *Bergey's Manual of Systematic Bacteriology*, vol. **II**, pp. 1472-1481, The Williams & Wilkins Co., Baltimore.
28. Finnerty, W.R. (1992) *Annu. Rev. Microbiol.* **46**, 193-218.
29. Nagasawa, T., Takeuchi, K. & Yamada, H. (1988) *Biochem. Biophys. Res. Commun.* **155**, 1008-1016.
30. Sambrook, J., Fritsch, E.F. & Maniatis, T. (1989) in *Molecular cloning: A Labolatory Manual*, 2nd edn. Cold Spring Harbor Laboratory, Cold Spring Harbor, New York.
31. Hashimoto, Y., Nishiyama, M., Yu, F., Watanabe, I., Horinouchi, S. & Beppu, T. (1992) *J. Gen. Microbiol.* **138**, 1003-1010.
32. Chomczynski, P. & Sacchi, N. (1987) *Anal. Biochem.* **162**, 156-159.
33. Wilson, S. & Drew, R. (1991) *J. Bacteriol.* **173**, 4914-4921.
34. Cohen, S.P., Hachler, H. & Levy, S.B. (1993) *J. Bacteriol.* **175**, 1484-1492.
35. Roper, D.I., Fawcett, T. & Cooper, R.A. (1993) *Mol. Gen. Genet.* **237**, 241-250.
36. Collins, D.M. & Stephens, D.M. (1991) *FEMS Microbiol. Lett.* **67**, 11-15.
37. Byrne, M.E., Rouch, D.A. & Skurray, R.A. (1989) *Gene* **81**, 361-367.
38. Wheatcroft, R. & Laberge, S. (1991) *J. Bacteriol.* **173**, 2530-2538.
39. Kelly, M. & Clarke, P.H. (1962) *J. Gen. Microbiol.* **27**, 305-316.
40. Wilson, S.A., Wachira, S.J., Drew, R.E., Jones, D. & Pearl, L.H. (1993) *EMBO J.* **12**, 3637-3642.
41. Hashimoto, Y., Nishiyama, M., Horinouchi, S. & Beppu, T. (1994) *Biosci. Biotech. Biochem.* **58**, 1859-1865.
42. Mayaux, J.-F., Cerbelaud, E., Soubrier, F., Yeh, P., Blanche, F. & Petre, D. (1991) *J. Bacteriol.* **173**, 6694-6704.
43. Duran, R., Nishiyama, M., Horinouchi, S. & Beppu, T. (1993) *Biosci. Biotech. Biochem.* **57**, 1323-1328.

44. Mayaux, J.-F., Cerbelaud, E., Soubrier, F., Faucher, D. & Petre, D. (1990) *J. Bacteriol.* **172**, 6764-6773.
45. Galas, D.J. & Chandler, M. (1989) in Berg, D. E. & Howe, M.M. (ed.), *Mobil DNA*. pp. 109-162, American Society for Microbiology, Washington, D. C.
46. Denome, S.A. & Young, K.D. (1995) *Gene* **161**, 33-38.
47. Jager, W., Schafer, A., Kalinowski, J. & Puhler, A. (1995) *FEMS Microbiol. Lett.* **126**, 1-6.
48. Asano, Y., Yasuda, T., Tani, Y. & Yamada, H. (1982) *Agric. Biol. Chem.* **46**, 1183-1189.
49. Saito, H. & Miura, K. (1963) *Biochim. Biophys. Acta* **72**, 619-629.
50. Wood, M.S., Byrne, A. & Lessie, T.G. (1991) *Gene* **105**, 101-105.
51. Tailliez, P., Ehrlich, S.D. & Chopin, M.-C. (1994) *Gene* **145**, 75-79.
52. Yates, J.R., Cunningham, R.P. & Holmes, D.S. (1988) *Proc. Natl. Acad. Sci. USA* **85**, 7284-7287.
53. Dodd, H.M., Horn, N. & Gasson, M.J. (1994) *J. Bacteriol.* **176**, 3393-3396.
54. Guilhot, C., Gicquel, B., Davis, J. & Martin, C. (1992) *Mol. Microbiol.* **6**, 107-113.
55. van der Meer, J.R., Zehnder, A.J.B. & de Vos, W.M. (1991) *J. Bacteriol.* **173**, 7077-7083.
56. Kato, K., Ohtsuki, K., Mitsuda, H., Yomo, T., Negoro, S. & Urabe, I. (1994) *J. Bacteriol.* **176**, 1197-1200.
57. Hashimoto, Y., Nishiyama, M., Ikehata, O., Horinouchi, S. & Beppu, T. (1991) *Biochim. Biophys. Acta* **1088**, 225-233.
58. Sanger, F., Nicklen, S. & Coulson, A.R. (1977) *Proc. Natl. Acad. Sci. USA* **74**, 5463-5467.
59. Bradford, M.M. (1976) *Anal. Biochem.* **72**, 248-254.
60. Laemmli, U. K. (1970) *Nature (London)* **227**, 680-685.
61. Fawcett, J. K. & Scott, J. E. (1960) *J. Clin. Pathol. (London)* **13**, 156-159.
62. Conway, E. J. & Byrne, A. (1933) *Biochem. J.* **27**, 419-429.
63. Hutt, A. T., Fournel, S. & Coldwell, J. (1986) *J. Chromatogr.* **378**, 409-418.
64. Shine, J. & Dalgarno, L. (1974) *Proc. Natl. Acad. Sci. USA* **71**, 1342-1346.
65. Rosenberg, M. & Court, D. (1979) *Annu. Rev. Genet.* **13**, 319-353.
66. Yamada, T., Palm, C.J., Brooks, B. & Kosuge, T. (1985) *Proc. Natl. Acad. Sci. USA* **82**, 6522-6526.

67. Kobayashi, M., Komeda, H., Nagasawa, Y., Yamada, H & Shimizu, S. (1993) *Biosci. Biotech. Biochem.* **57**, 1949-1950.
68. Asano, Y., Tachibana, M., Tani, Y. & Yamada, H. (1982) *Agric. Biol. Chem.* **46**, 1175-1181.
69. Thiery, A., Maestracci, M., Arnaud, A., Galzy, P. & Nicolas, M. (1986) *J. Basic Microbiol.* **26**, 299-311.
70. Yamamoto, K., Ueno, Y., Otsubo, K., Kawakami, K. & Komatsu, K. (1990) *Appl. Environ. Microbiol.* **51**, 302-306.
71. Nagasawa, T., Nanba, H., Ryuno, K. & Yamada, H. (1987) *Eur. J. Biochem.* **162**, 691-698.
72. Kobayashi, M., Komeda, H., Nagasawa, T., Nishiyama, M., Horinouchi, S., Beppu, T., Yamada, H. & Shimizu, S. (1993) *Eur. J. Biochem.* **217**, 327-336.
73. Komeda, H., Kobayashi, M. & Shimizu, S., submitted for publication.
74. Hoshino, T. & Kose, K. (1989) *J. Bacteriol.* **171**, 6300-6306.
75. Sedlmeier, R. & Altenbuchner, J. (1992) *Mol. Gen. Genet.* **236**, 76-85.
76. Nucifora, G., Chu, L., Misra, T.K. & Silver, S. (1989) *Proc. Natl. Acad. Sci. USA* **86**, 3544-3548.
77. San Francisco, M.J.D., Hope, C.L., Owolabi, J.B., Tisa, L.S. & Rosen, B.P. (1990) *Nucleic Acids Res.* **18**, 619-624.
78. Clarke, P.H. & Slater, J.H. (1986) in Sokatch, J.R. (ed.), *The Biology of Pseudomonas. The Bacteria*, vol. **10**, pp. 71-144, Academic press, Orlando.
79. Drew, R.E. & Lowe, N. (1989) *J. Gen. Microbiol.* **135**, 817-823.
80. Brammar, W.J., Charles, I.G., Matfield, M., Cheng-Pin, L., Drew, R.E. & Clarke, P.H. (1987) *FEBS Lett.* **215**, 291-294.
81. O'Halloran, T.V. (1993) *Science* **261**, 715-725.
82. Endo, G. & Silver, S. (1995) *J. Bacteriol.* **177**, 4437-4441.
83. Wu, J. & Rosen, B.P. (1993) *J. Biol. Chem.* **268**, 52-58.
84. Komeda, H., Kobayashi, M. & Shimizu, S., submitted for publication.
85. Stokes, H.W. & Hall, R.M. (1989) *Mol. Microbiol.* **3**, 1669-1683.
86. Battersby, A.R. (1993) *Acc. Chem. Res.* **26**, 15-21.
87. Arfin, S.M., Kendall, R.L., Hall, L., Weaver, L.H., Stewart, A.E., Matthews, B.W. & Bradshaw, R.A. (1995) *Proc. Natl. Acad. Sci. USA* **92**, 7714-7718.
88. Wrigley, N.G., Chio, J.P. & Wood, H.G. (1977) *J. Biol. Chem.* **252**, 1500-1504.

89. Hemker, J., Kleinschmitdt, L. & Witzel, H. (1987) *Rec. Trav. Chim.* **106**, 350.
90. Nies. D.H. & Silver, S. (1989) *J. Bacteriol.* **171**, 4073-4075.
91. Nies, D.H. (1992) *Plasmid* **27**, 17-28.
92. Silver, S. & Walderhaug, M. (1992) *Microbiol. Rev.* **56**, 195-228.
93. Eitinger, T. & Friedrich, B. (1991) *J. Biol. Chem.* **266**, 3222-3227.
94. Komeda, H., Kobayashi, M. & Shimizu, S., submitted for publication.
95. Fu, C., Javedan, S., Moshiri, F. & Maier, R.J. (1994) *Proc. Natl. Acad. Sci. USA* **91**, 5099-5103.
96. Mobley, H.L.T., Garner, R.M. & Bauerfeind, P. (1995) *Mol. Microbiol.* **16**, 97-109.
97. Maeda, M., Hidaka, M., Nakamura, A., Masaki, H. & Uozumi, T. (1994) *J. Bacteriol.* **176**, 432-442.
98. Kyte, J. & Doolittle, R.F. (1982) *J. Mol. Biol.* **157**, 105-132.
99. Nagasawa, T., Takeuchi, K., Vincenzo, N.-D. & Yamada, H. (1991) *Appl. Microbiol. Biotechnol.* **34**, 783-788.
100. Kaback, H R., Reeves, J.P., Short, S.A. & Lombardi, F.J. (1974) *Arch. Biochem. Biophys.* **160**, 215-222.
101. Terada, H. (1981) *Biochim. Biophys. Acta* **639**, 225-242.
102. Nagasawa, T. Ryuno, K. & Yamada, H. (1986) *Biochem. Biophys. Res. Commun.* **139**,1305-1312.
103. Lohmeyer, M. & Friedrich, C.G. (1987) *Arch. Microbiol.* **149**, 130-135.
104. Eitinger, T. & Friedrich, B. (1994) *Mol. Microbiol.* **12**, 1025-1032.
105. von Heijne, G. (1992) *J. Mol. Biol.* **225**, 487-494.
106. Wolfram, L., Friedrich, B. & Eitinger, T. (1995) *J. Bacteriol.* **177**, 1840-1843.
107. Conklin, D.S., Mcmaster, J.A., Culbertson, M.R. & Kung, C. (1992) *Mol. Cell. Biol.* **12**, 3678-3688.
108. Conklin, D.S., Culbertson, M.R. & Kung, C. (1994) *Mol. Gen. Genet.* **244**, 303-311.
109. Conklin, D.S., Kung, C. & Culbertson, M.R. (1993) *Mol. Cell. Biol.* **13**, 2041-2049.
110. Nies, D., Mergeay, M., Friedrich, B. & Schlegel, H.-G. (1987) *J. Bacteriol.* **169**, 4865-4868.
111. Liesegang, H., Lemke, K., Siddiqui, R.A. & Schlegel, H.-G. (1993) *J. Bacteriol.* **175**, 767-778.

112. Kobayashi, M., Yanaka, N., Nagasawa, T. & Yamada, H. (1990) *J. Antibiotics* **43**, 1316-1320.
113. Kobayashi, M., Nagasawa, T. & Yamada, H. (1988) *Appl. Microbiol. Biotechnol.* **29**, 231-233.
114. Beaucage, S.L. & Caruthers, M.H. (1981) *Tetrahedron Lett.* **22**, 1859-1862.
115. Feinberg, A.P. & Vogelstein, B. (1983) *Anal. Biochem.* **132**, 6-13.
116. Taylor, J.W., Ott, J. & Eckstein, F. (1985) *Nucleic Acids Res.* **13**, 8764-8785.
117. Gething, M.J. & Davidson, B.E. (1972) *Eur. J. Biochem.* **30**, 352-353.
118. Bibb, M.J., Findlay, P.R. & Johnson, M.W. (1984) *Gene* **30**, 157-166.
119. Kagawa, Y., Nojima, H., Nukiwa, N., Ishizuka, M., Nakajima, T., Yasuhara, T., Tanaka, T. & Oshima, T. (1984) *J. Biol. Chem.* **259**, 2956-2960.
120. George, D.G., Barker, W.C. & Hunt, L.T. (1986) *Nucleic Acids Res.* **14**, 11-15.
121. Ouchterlony, O. (1953) *Acta Pathol. Microbiol. Scand.* **32**, 231-240.
122. Yamada, T., Tsukamoto, H., Shiraishi, T., Nomura, T. & Oku, H. (1990) *Ann. Phytopathol. Soc. Jpn.* **56**, 532-540.
123. Kobayashi, M., Komeda, H., Yanaka, N., Nagasawa, T. & Yamada, H. (1992) *J. Biol. Chem.* **267**, 20746-20751.
124. Kobayashi, M., Yanaka, N., Nagasawa, T. & Yamada, H. (1992) *Biochemistry* **31**, 9000-9007.
125. Inouye, S., Nakazawa, A. & Nakazawa, T. (1986) *Gene* **44**, 235-242.
126. Wallace, R.G., Lee, N. & Fowler, A.V. (1980) *Gene* **12**, 179-190.
127. Gallegos, M.-T., Michan, C. & Ramos, J.L. (1993) *Nucleic Acids Res.* **21**, 807-810.
128. Nakai, R., Horinouchi, S. & Beppu, T. (1988) *Gene* **65**, 229-238.
129. Ramos, J.L., Rojo, F., Zhou, L. & Timmis, K.N. (1990) *Nucleic Acids Res.* **18**, 2149-2152.
130. Strohl, W. R. (1992) *Nucleic Acids Res.* **20**, 961-974.
131. Bork, P. & Koonin, E.V. (1994) *Protein Science* **3**, 1344-1346.
132. Novo, C., Tata, R., Clemente, A. & Brown, P.R. (1995) *FEBS Lett.* **367**, 275-279.

ACKNOWLEDGEMENTS

The author wishes to express his sincere thanks to Professor Sakayu Shimizu, Kyoto University, for his kind guidance and warm encouragement during the course of this work.

The author is greatly indebted to Emeritus Professor Hideaki Yamada, Kyoto University, for his kind support in carrying out this study.

The author greatly appreciates to Senior Lecturer Michihiko Kobayashi, Kyoto University, for his direction of this study, valuable discussions, critical reading of the manuscripts and continuous warm encouragement in carrying out the study.

The author also wishes to express his thanks to Professor Toru Nagasawa, Okayama University, for his helpful suggestions.

The kind suggestions and the continuous encouragements by Assistant Professor Michihiko Kataoka and Assistant Professor Jun Ogawa, Kyoto University, are greatefully acknowledged.

The author is deeply indebted to Emeritus Professor Teruhiko Beppu, Professor Sueharu Horinouchi and Associate Professor Makoto Nishiyama, The University of Tokyo, and Mr. Wataru Mizunashi, Nitto Chemical Industry, for providing the *Rhodococcus-E. coli* host-vector. The author also wishes to thank Professor Seiki Kuramitsu, Osaka University, and Dr. Kengo Akimoto, Suntory Institute for Biomedical Research, for the analysis of amino acid sequences of the nitrilase and amidase. The author also thanks Dr. Mikita Suyama, The Institute for Chemical Research, Kyoto University, for the computer search of amino acid sequences. The author is also grateful to Dr. Teruo Kawada, Kyoto University, for the preparation of antibodies. Thanks are also due to Dr. Hideto Miyoshi, Kyoto University, for providing the author with the uncoupler SF6847. The author also thanks Dr. Toru Aoki, Kyoto University Radioisotope Research Center, for his valuable advices on the experiments of ^{57}Co uptake.

Special thanks are due to Mr. Noriyuki Yanaka, Mr. Takayuki Fujita, Mr. Yuji Hori and Mr. Satoshi Sasaki for their many helpful collaborations.

The author greatly appreciates to members of the laboratory of Fermentation Physiology and Applied Microbiology, Department of Agricultural Chemistry, Kyoto University.

Finally, but not the least, the author thanks his families for their encouragement and support.

PUBLICATIONS

a) Komeda, H., Kobayashi, M. & Shimizu S. Characterization of the gene cluster of high molecular-mass nitrile hydratase (H-NHase) induced by its reaction product in *Rhodococcus rhodochrous* J1. Submitted for publication.

b) Komeda, H., Kobayashi, M. & Shimizu S. Characterization of IS*1164*, an insertion sequence isolated from *Rhodococcus rhodochrous* J1. Submitted for publication.

c) Kobayashi, M., Komeda, H., Nagasawa, T., Yamada, H. & Shimizu S. (1993) Occurrence of amidases in the industrial microbe *Rhodococcus rhodochrous* J1. *Biosci. Biotech. Biochem.* **57**, 1949-1950.

d) Kobayashi, M., Komeda, H., Nagasawa, T., Nishiyama, M., Horinouchi, S., Beppu, T., Yamada, H. & Shimizu S. (1993) Amidase coupled with low-molecular-mass nitrile hydratase from *Rhodococcus rhodochrous* J1 : Sequencing and expression of the gene and purification and characterization of the gene product. *Eur. J. Biochem.* **217**, 327-336.

e) Komeda, H., Kobayashi, M. & Shimizu S. A novel gene cluster including the *Rhodococcus rhodochrous* J1 *nhlBA* genes encoding a low molecular-mass nitrile hydratase (L-NHase) induced by its reaction product. Submitted for publication.

f) Komeda, H., Kobayashi, M. & Shimizu S. A novel transporter involved in cobalt uptake. Submitted for publication.

g) Kobayashi, M., Komeda, H., Yanaka, N., Nagasawa, T. & Yamada, T. (1992) Nitrilase from *Rhodococcus rhodochrous* J1 : Sequencing and overexpression of the gene and identification of an essential cysteine residue. *J. Biol. Chem.* **267**, 20746-20751.

h) Komeda, H., Hori, Y., Kobayashi, M. & Shimizu S. Transcriptional regulation of the *Rhodococcus rhodochrous* J1 *nitA* gene encoding a nitrilase. Submitted for publication.